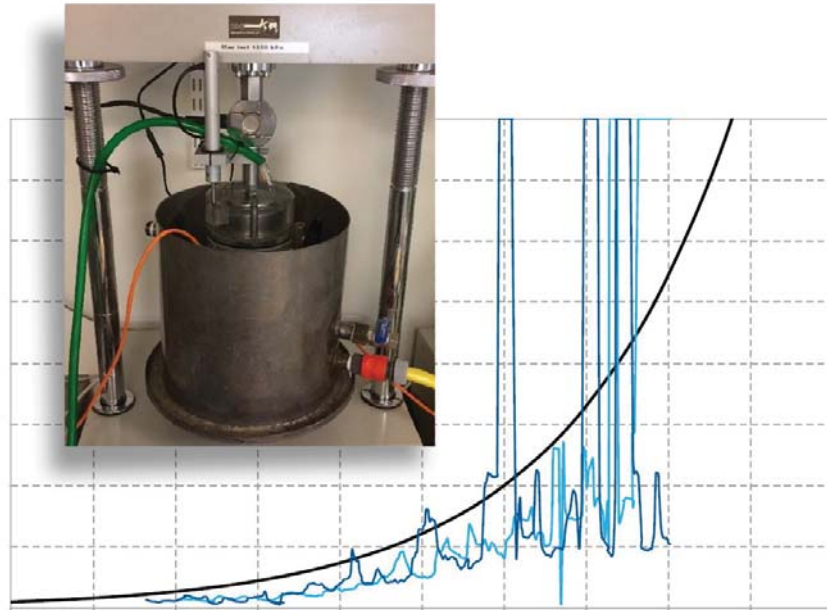




**LUND**  
UNIVERSITY



# LABORATORY TESTING RELATED TO UNLOADING MODULUS OF SOFT CLAY

SOFIA HASSELBERG

Geotechnical  
Engineering

*Master's Dissertation*



DEPARTMENT OF CONSTRUCTION SCIENCES

## GEOTECHNICAL ENGINEERING

ISRN LUTVDG/TVGT--18/5062--SE (1-104) | ISSN 0349-4977

MASTER'S DISSERTATION

# LABORATORY TESTING RELATED TO UNLOADING MODULUS OF SOFT CLAY

SOFIA HASSELBERG

Supervisors: **ERIKA TUDISCO**, PhD, Geotechnical Engineering, LTH, Lund  
and **JOHANNES TORNBORG**, Geotechnical Engineer, Skanska Sverige AB.

Examiner: Professor **OLA DAHLBLOM**, Dept. of Construction Sciences, LTH, Lund

Copyright © 2018 Geotechnical Engineering,  
Dept. of Construction Sciences, Faculty of Engineering LTH, Lund University, Sweden.

Printed by V-husets tryckeri LTH, Lund, Sweden, September 2018 (*PI*).

**For information, address:**

Geotechnical Engineering, Dept. of Construction Sciences,  
Faculty of Engineering LTH, Lund University, Box 118, SE-221 00 Lund, Sweden.

Homepage: [www.geoteknik.lth.se](http://www.geoteknik.lth.se)



## ABSTRACT

The unloading modulus, together with the permeability, are responsible for the swelling process of a soil that is subjected to unloading. Studies to examine the unloading modulus of clay has previously been performed and several relationships describing this parameter has hence been developed. The methods to study the unloading modulus has previously been both laboratory studies and field measurements. The laboratory studies has generally focused on using incremental loading (IL) oedometer tests.

This master thesis has three aims:

- Examine if the storage time of the samples will affect the obtained unloading modulus for soft clay.
- To investigate if modified CRS-tests can be used in order to determine the unloading modulus of soft clay in the same extent as IL-tests.
- Investigate if one set of model parameters, obtained from PLAXIS 2D and restricted to the *Soft soil creep* model, can describe the behaviour of the soil when exposed to both compression and unloading.

Piston sampler of the type STI was used in order to retrieve undisturbed samples of clay to performed laboratory tests on. Samples from 3 levels; 17 m, 20 m, and 25 m were obtained from one location in central Gothenburg, Sweden. Standard CRS-tests were initially perform in order to develop an understanding of the stress history of the clay and serve as the basis for determining the unloading sequences of the samples from the borehole. Two rounds of unloading tests, using modified CRS-tests, were performed on samples with 8 weeks of storage time in between.

There could not be found any tendency that suggested that the unloading modulus of soft clay is affected by storage time. The clay in these specific sample tubes however had a tendency to swell extensively which might have affected the initial tests. The result from the performed tests showed that modified CRS-test appears to work satisfactory in order to capture the unloading behaviour of soft clay in the same extent as IL-tests. The data showed that the unloading modulus, obtained with modified CRS-test, was larger for unloading sequences above the in-situ pre-consolidation pressure than below.

If the set of parameters, that was obtained for compression of the clay in the software PLAXIS 2D and the material model *Soft soil creep*, was used to also describe the behaviour of the soil during unloading, the magnitude of the expansion of the soil was underestimated.

**Keywords:** *CRS, unloading modulus, clay, Gothenburg, storage time*



# SAMMANFATTNING

Avlastningsmodulen, tillsammans med permeabiliteten, reglerar svällningen av en jord som utsätts för avlastning. Studier för att undersöka avlastningsmodulen av lera har tidigare utförts och flera samband som beskriver denna parameter har följaktligen utvecklats. Metoderna som tidigare har används för att studera avlastningsmodulen har varit både laboratorieundersökningar och fältmätningar. Laboratorieundersökningarna har generellt fokuserat på att använda stegvisa ödometer försök (förkortade till IL).

Detta examensarbete har tre delsyften:

- Undersöka om lagringstiden av proverna påverkar den erhållna avlastningsmodulen för lera.
- Undersöka om modifierade CRS-tester kan användas för att bestämma avlastningsmodulen för lera i samma utsträckning som IL-tester.
- Undersök om ett parametersett kan användas i programmet PLAXIS 2D, och material modellen *Soft soil creep*, för att beskriva jordens beteende när den utsätts för både kompression och avlastning.

Standard kolvprovtagare av typen STI användes för att erhålla ostörda lerprover att utföra laborietesterna på. Prover från 3 nivåer; 17 m, 20 m och 25 m erhöles från en plats i centrala Göteborg. Standard CRS-tester utfördes initialt på proverna för att få en förståelse för lerans spänningshistorik samtidigt som resultatet från testerna användes för att bestämma avlastningssekvenser som prover från samma borrhål skulle utsättas för. Två omgångar av avlastningstester utfördes, med modifierad CRS, på prover med en lagringstid på 8 veckors däremellan.

Någon tendens som antydde att avlastningsmodulen för leran påverkas av lagringstiden kunde inte observeras. Leran i dessa specifika prover hade emellertid en tendens att svälla i stor utsträckning, vilket kan ha påverkat de initiala testerna. Resultatet från de utförda testerna visade att modifierade CRS-tester tycks fungera för att fånga avlastningsbeteendet hos lera i ungefär samma utsträckning som IL-tester. Utifrån den erhållna datan kunde slutsatsen dras att avlastningsmodulen, erhållen med modifierade CRS-tester, är högre för avlastningssekvenser under in-situ förkonsolideringstrycket jämfört med avlastningssekvenser över in-situ förkonsolideringstrycket.

Om samma uppsättning parametrar som erhöles för kompressionsförhållanden av leran, i programmet PLAXIS 2D och material modellen *Soft soil creep*, används för att beskriva lerans beteende även under avlastning kommer storleken på expansionen av leran att underskattas.

**Nyckelord:** CRS, avlastningsmodul, lera, Göteborg, lagringstid





## **PREFACE**

This master's thesis was conducted as the last part of the five year education of Civil Engineering at Lund University. The study was performed during spring 2018 as collaboration between Lund University and Skanska Teknik in Gothenburg.

I wish to thank my supervisor at Skanska Teknik, Johannes Tornborg, for putting great effort in to helping and guiding me along this process as well as for always taking the time to answer my questions. I would like to thank my supervisor at Lund University, Erika Tudisco, for her guidance and feedback.

I would also like to thank Anders Kullingsjö, Skanska Teknik, whom with his incredible knowledge of everything related to geotechnical engineering managed to confuse me even more before explaining any possible questions with great enthusiasm; your help has been greatly appreciated. I would also like to thank David Ekstrand, Skanska Teknik, whom with great patience spent many hours helping me with PLAXIS 2D and providing valuable insight on the subject.

Furthermore, I like to express my appreciation to everyone at Skanska Teknik, Gothenburg, for showing interest in my work and always making time out of their busy schedules to help me. A special thanks to Fredhy Hansen and Lennart Hedström for help me with the sample retrieval and the laboratory work while making sure to explain the processes along the way.

Gothenburg, May 2018

*Sofia Hasselberg*



# TABLE OF CONTENTS

<b>1</b>	<b>INTRODUCTION</b> .....	<b>1</b>
1.1	BACKGROUND.....	1
1.2	AIM & OBJECTIVES .....	2
1.3	METHOD.....	2
1.4	LIMITATIONS .....	3
1.5	OUTLINE OF REPORT.....	3
<b>2</b>	<b>THEORETICAL BACKGROUND</b> .....	<b>5</b>
2.1	BREIF REVIEW OF SOIL MECHANICS .....	5
2.1.1	<i>TOTAL STRESS, EFFECTIVE STRESS AND PORE WATER</i> .....	7
2.1.2	<i>DRAINED AND UNDRAINED CONDITIONS</i> .....	7
2.1.3	<i>SENSITIVITY</i> .....	8
2.1.4	<i>ATTERBERG LIMITS</i> .....	8
2.1.5	<i>STRESS HISTORY OF SOILS</i> .....	9
2.2	CONSOLIDATION .....	9
2.3	UNLOADING .....	11
2.4	COMPRESSION MODULUS .....	12
2.5	UNLOADING MODULUS .....	13
2.6	SAMPLING AND SAMPLING QUALITY .....	16
2.6.1	<i>SAMPLE DISTURBANCE EFFECT</i> .....	17
<b>3</b>	<b>METHODOLOGY</b> .....	<b>21</b>
3.1	PISTON SAMPLING.....	21
3.2	ROUTINE TESTS .....	22
3.2.1	<i>BULK DENSITY</i> .....	22
3.2.2	<i>WATER CONTENT</i> .....	22
3.2.3	<i>FALL CONE TEST</i> .....	23
3.3	OEDOMETER TESTS.....	26
3.4	FINITE ELEMENT METHOD - PLAXIS .....	28
<b>4</b>	<b>SITE CONDITIONS AND CONDUCTED TESTS</b> .....	<b>31</b>
4.1	GEOLOGY OF THE GOTHENBURG REGION .....	31
4.2	SITE DESCRIPTION.....	31
4.3	VERTICAL IN SITU EFFECTVE STRESS .....	35
4.4	SAMPLE RETRIVAL IN BH1 .....	36
4.5	STORAGE .....	38
4.6	RESULTS FROM ROUTINE TESTS.....	38
4.7	CRS-TESTS .....	39
4.7.1	<i>LOADING TESTS WITH CRS</i> .....	40
4.7.2	<i>UNLOADING TESTS WITH CRS</i> .....	41
4.8	TESTS USING INCREMENTAL LOAD OEDOMETER .....	43
<b>5</b>	<b>SUMMARY OF RESULTS, ANALYSIS AND DISCUSSION</b> .....	<b>45</b>
5.1	GENERAL REMARKS .....	45
5.2	UNLOADING MODULUS OBTAINED USING MODIFIED CRS TESTS.....	46
5.2.1	<i>STORAGE TIME EFFECT ON UNLODING MODULUS</i> .....	50
5.2.2	<i>UNLOADING MODULUS OBTAINED WITH MODIFIED CRS COMPARED TO UNLOADING MODULUS OBTAINED FROM IL</i> .....	52

5.3	NUMERICAL MODELLING.....	53
5.4	REFLECTIONS REGARDING THE LABORATORY TESTS.....	58
<b>6</b>	<b>CONCLUSIONS AND PROPOSED FURTHER STUDIES .....</b>	<b>61</b>
6.1	CONCLUSIONS .....	61
6.2	PROPOSED FURTHER STUDIES .....	61
<b>7</b>	<b>REFERENCES.....</b>	<b>63</b>
	<b>APPENDIX A .....</b>	<b>I</b>
	<b>APPENDIX B.....</b>	<b>II</b>
	<b>APPENDIX C .....</b>	<b>IV</b>
	<b>APPENDIX D .....</b>	<b>VII</b>
	<b>APPENDIX E.....</b>	<b>VIII</b>
	<b>APPENDIX F.....</b>	<b>XX</b>
	<b>APPENDIX G .....</b>	<b>XXV</b>
	<b>APPENDIX H.....</b>	<b>XXVI</b>
	<b>APPENDIX I.....</b>	<b>XXXI</b>

## LIST OF FIGURES

Figure 2.1: The components of a soil segment, inspired by (Larsson, 2008) .....	5
Figure 2.2: Relationship between total stress, effective stress and pore water pressure when a load is applied to a fully saturated soil. Inspired by Sällfors (2013).....	10
Figure 2.3: Effective stress-strain relation for clay (Tudisco & Dahlblom, 2016) .....	13
Figure 2.4: The compressional modulus corresponding to effective stress level for clay (Tudisco & Dahlblom, 2016) .....	13
Figure 2.5 Summary of the relationships for the unloading modulus that has been presented. In the equation from TR Geo 13 (Trafikverket, 2016) $\sigma v'$ is chosen instead of $\sigma 0'$ , based on already described reasons. ....	15
Figure 2.6: Strain difference before reaching the pre-consolidation pressure in oedometer tests, inspired by (Larsson et. al., 2007).....	17
Figure 2.7: Sample quality based on natural water content and strain difference (from Figure 2.6) of sample in oedometer tests, inspired by (Larsson et. al., 2007).....	17
Figure 3.1: Fall cone apparatus .....	23
Figure 3.2: Oedometer device, inspired by (ISO, 2017) .....	26
Figure 3.3: Determination of pre-consolidation pressure, inspired by (SIS, 1991a) .....	28
Figure 3.4: Definition of stiffness parameters $\kappa^*$ and $\lambda^*$ , inspired by (PLAXIS, 2016). .....	29
Figure 3.5: Definition of stiffness parameter $\mu^*$ , inspired by (PLAXIS, 2016). ....	29
Figure 4.1: Location of site (Google, 2018).....	32
Figure 4.2: Location of BH1 and surrounding studied boreholes. ....	33
Figure 4.3: Pore pressure in C025 .....	34
Figure 4.4: Stress variation with depth for BH1 and C025.....	36
Figure 4.5: Preparation of the tubes on the piston sampler. ....	37
Figure 4.6: Separation of the tubes after sample collection. ....	37
Figure 4.7: Examination of undisturbed shear strength using the fall cone test. ....	39
Figure 4.8: One of the CRS in the laboratory at Skanska. ....	40
Figure 5.1: Evaluated sample quality. ....	45
Figure 5.2: Evaluated unloading modulus for level 20 m. ....	47
Figure 5.3: Unloading modulus for all levels below pre-consolidation pressure.....	48
Figure 5.4: Unloading modulus for all levels above the pre-consolidation pressure. ....	48
Figure 5.5: Obtained unloading modulus compared to established relationships of the same parameter. ....	50
Figure 5.6: Unloading modulus for level 17 m, first unloading series.....	51
Figure 5.7: Unloading modulus for level 17 m, second unloading series.....	51
Figure 5.8 Swelling of the sample collected from 25 m, 8 days after sampling. Similar on the other end. ....	52
Figure 5.9: Parameter optimisation by SSC for CRS curve, level 17 m. ....	56
Figure 5.10: Consistency between the reference curve for unloading sequences below the pre-consolidation pressure and the curve developed by SSC parameter optimisation for compression.....	57
Figure 5.11: Consistency between the reference curve for unloading sequences above the pre-consolidation pressure and the curve developed by SSC parameter optimisation for compression.....	58

## LIST OF TABLES

Table 2.1: Determination of soil based on particle size, inspired by Swedish Standard Institute (2002). .....	6
Table 2.2: Sensitivity classification, inspired by (Swedish Standards Institute, 2004) .....	8
Table 2.3: Classification of soil based on OCR, inspired by Sveriges Geotekniska Förening (2016). .....	9
Table 2.4: Relationship between sample quality and sampling method, inspired by (Swedish Standards Institute, 2006).....	16
Table 3.1: Cones that can be used for fall cone test in order to determine undrained shear strength, inspired by (Swedish Standards Institute, 2008a). .....	25
Table 3.2: Requirements on penetration, inspired by (Swedish Standards Institute, 2008b) ..	25
Table 4.1: Borehole and their individual filling thickness .....	33
Table 4.2: Measured groundwater level in borehole C025 .....	34
Table 4.3: Assumed conditions in BH1. ....	34
Table 4.4: Vertical effective in-situ stress for the three sample levels .....	35
Table 4.5: Classification of the obtained samples. ....	37
Table 4.6: Density of the samples .....	38
Table 4.7. Summary of results from routine tests. ....	39
Table 4.8. Parameters determined from CRS tests.....	41
Table 4.9: Stages for the unloading tests.....	42
Table 4.10: Start date, finish date and total test time for the first series of loading-unloading tests.....	43
Table 4.11: Start date, finish date and total test time for the second series of loading-unloading tests performed 8 weeks of after the first series of tests.....	43
Table 4.12: Start date, finish date and elapsed time for each unloading test using IL. ....	43
Table 5.1: Parameters obtained from the optimisation using SSC.....	56

# LIST OF NOTATIONS

Listed below are the notations and abbreviations used in this master's thesis. The notations and abbreviations are also described in the text when initially introduced.

## Roman letters

$a$	Constant (Karlsruud, 2012)
$b$	Constant (Karlsruud, 2012)
$b$	Load factor (Larsson, 1986)
$c$	Constant for tip angle (Swedish Standards Institute, 2008a)
$c_{ufc}$	Undrained undisturbed shear strength determined by fall cone test
$c_{urfc}$	Undrained disturbed shear strength determined by fall cone test
$c_v$	Coefficient of consolidation
$e$	Euler's number (constant)
$g$	Gravitational acceleration
$i$	Average penetration depth for fall cone test
$k$	Permeability
$m$	Mass
$M$	Constant for cone penetration test (SIS, 1990)
$M$	Compression modulus
$M_0$	Compression modulus for effective stresses lower than the pre-consolidation pressure
$M_L$	Compression modulus for effective stresses in an interval between pre-consolidation pressure and effective stresses where the modulus starts to increase
$M'$	Compression modulus for stresses exceeding $\sigma'_L$
$M_{ul}$	Unloading modulus
$N$	Constant for cone penetration test (SIS, 1990)
$S_t$	Sensitivity
$t$	Time
$u$	Pore water pressure
$V$	Volume
$w$	Water content
$w_L$	Liquid limit
$w_N$	Natural water content
$w_p$	Plastic limit
$w_s$	Shrinkage limit
$z$	Depth coordinate

## Greek letters

$\alpha_s$	Swelling index (Larsson, 1986)
$\gamma$	Unit weight of soil

$\gamma_w$	Unit weight of water
$\varepsilon_v$	Vertical strain
$\rho$	Bulk density
$\sigma$	Total stress
$\sigma'$	Effective stress
$\sigma_0$	Total in-situ stress
$\sigma'_0$	Effective in-situ stress
$\sigma'_L$	Effective stress level over which the oedometer modulus starts to increase
$\sigma'_c$	Pre-consolidation pressure
$\sigma_v$	Total vertical stress
$\sigma'_v$	Effective vertical stress
$\sigma_{v0}$	Total vertical in-situ stress
$\sigma'_{v0}$	Effective vertical in-situ stress

### **Abbreviations**

CRS	Constant rate of strain
FEM	Finite element method
IL	Incremental loading
OCR	Over consolidation ratio
SSC	Soft soil creep



# 1 INTRODUCTION

This initial chapter has the aim to introduce the reader to the subject of the thesis and explain the background for conducting this study. Based on the background description, the aim and the objectives of the thesis will be established as well as the limitations of the study. Furthermore, the outline of the report will be drafted in the end of this chapter to give the reader a comprehension of the disposition of the thesis.

## 1.1 BACKGROUND

When unloading of soil occurs, due to for example excavation works, the reduction of effective stresses below a certain level will cause the volume of the soil to increase. This occurs as a result of that the pores increase while they are filled with water. The process is referred to as swelling by Terzaghi (1943). If a foundation is placed on an excavated bottom where there is an on-going swelling process, this may result in a pressure on the foundation from the soil (Tornborg, 2017). According to Terzaghi (1943), the swelling process depends on the permeability and the unloading modulus of the clay.

The unloading modulus of soil has previously been studied using both laboratory and field test data and several relationships for the unloading modulus have consequently been developed (e.g. Larsson, 1986, Karlsrud, 2012 and Persson, 2004).

Previous studies by for example, NIFS (2014) and Wood (2016) have shown that the mechanical behaviour of the soil in samples can change as a result of storage time and the results obtained from laboratory tests may hence depend on the elapsed time after sample retrieval. The studies that have previously been performed on the effect of storage time have focused on e.g. the effect on the pre-consolidation pressure and shear strength of clay (e.g. Henriksson & Carlsten, 1994 and Bjerrum, 1973). No documentation regarding the storage time of the soil samples before testing has been found in the previously performed laboratory studies (Larsson, 1986 and Persson, 2004) related to the unloading modulus. Tornborg (2017) states in a recently conducted SBUF-project that also the unloading modulus of soft clay should hence be studied further to obtain a comprehension of the impact of storage time on the unloading modulus.

The laboratory test method used to study the unloading modulus has generally been incremental loaded (IL) oedometer tests (Larsson, 1986, Persson, 2004 and Karlsrud, 2012) which is a time-consuming method usually performed by manually applying loadsteps every 24 hours. Constant rate of strain (CRS) test is commonly used to obtain the compression behaviour of soil but has generally not been used for investigating the unloading behaviour of soil. This is because the CRS-test set-up was not able to keep a constant stress rate (rather than constant strain rate) during unloading. However, computer control of the CRS apparatus has improved and it is therefore now possible to control the stress rate of the test. Compared to IL-test, CRS-test is a faster method since the machine has a constant deformation rate and the pore pressure can be measured.

## 1.2 AIM & OBJECTIVES

The primary aim of this master's thesis is to evaluate if the unloading modulus of soft clay, obtained using laboratory test, may be affected by the storage time of the sample. The chosen laboratory test method is a computer controlled modified CRS-test. This method was chosen in order to investigate a second aim; if a modified execution of a CRS-test, with a constant decreasing stress rate, can be used to gain information regarding the unloading modulus in the same extent as the IL-test. The soil in the Gothenburg area, which consists mainly of clay (cohesive soil), has been chosen as test material.

Additionally, is it of interest to investigate if one set of model parameters, obtained from the FEM software PLAXIS 2D, restricted to the *Soft soil creep* model, can describe the behaviour of the soil when exposed to both compression and unloading.

The following objectives of the study have been identified:

- Conducting unloading tests, with modified CRS-test, on newly obtained samples of soft clay from a location in Gothenburg.
- Conducting unloading tests on similar samples 8 weeks after the initial tests.
- Analyse and compare the results for the unloading modulus obtained by the laboratory tests conducted with varying storage time.
- Analyse and compare the results for the unloading modulus obtained by the modified CRS-test with the established relationships for the unloading modulus e.g. by TR Geo 13 (Trafikverket, 2016).
- Compare the results of the unloading modulus obtained using modified CRS-tests and results obtained using IL-tests.
- Use the finite element software PLAXIS 2D and the material model *Soft soil creep* in order to simulate the unloading tests conducted with CRS and examine if one set of parameters can describe the soil during compression as well as unloading.

## 1.3 METHOD

Initially a literature study was conducted in order to gain sufficient knowledge about the concepts relevant for this study. Focus was on the theory and research concerning unloading modulus as well as sample disturbance due to storage time. The sampling method and laboratory tests methods used for this thesis were also studied. Laboratory tests, using modified CRS-tests, were conducted on two occasions and IL-tests were conducted on one occasion. The data sets from the initial modified CRS-tests were used to simulate tests in the software PLAXIS 2D, using the *Soft soil creep* model, in order to find a set of parameters that describes the behaviour of the soil. Finally, the results obtained from the laboratory tests and from the *Soft soil creep* study were analysed and discussed.

## 1.4 LIMITATIONS

In order to be able to complete the thesis within the time limit and limiting the scope of the study to a reasonable level, certain limitations had to be established.

- A limited number of sample levels (3) were collected and tested.
- The samples were obtained from one location in Gothenburg due to the cost that sample collection brings. This cost was funded by Skanska.
- Modified CRS-tests were performed with a time interval of 8 weeks. It would have been desirable to conduct test after longer storage time as well but this was not feasible within the time limit of the thesis.
- The geotechnical parameters determined using routine tests were only investigated in the extent that was considered to be relevant for the study.

## 1.5 OUTLINE OF REPORT

Presented below is the outline of the thesis, as well as a brief description of the content in each chapter.

### **Chapter 1: Introduction**

Chapter 1 provides an introduction to the master's thesis and contains *Background, Aim & Objective, Method, Limitations* and *Outline of report*.

### **Chapter 2: Theoretical background**

In Chapter 2 the theoretical aspects relevant for the thesis are described and focus will specifically be on unloading and sampling quality. Some relevant previous studies will be presented.

### **Chapter 3: Methodology**

In Chapter 3 the selected methods for the study are presented and described.

### **Chapter 4: Site conditions and conducted tests**

In Chapter 4 the site conditions, the sampling procedure and the conducted laboratory tests are described. The conducted tests include routine tests, standard CRS-tests, modified CRS-tests for unloading purposes as well as IL-test for unloading purposes.

### **Chapter 5: Summary of results, analysis and discussion**

The data obtained from the unloading tests performed by modified CRS and IL is presented, analysed and compared in this chapter. The finite element software PLAXIS 2D is used in order to simulate the unloading tests with the *Soft soil creep* model. In this chapter the parameters that might have influenced the obtained results are also highlighted and discussed.

### **Chapter 6: Conclusion and proposed further studies**

In Chapter 6, conclusions regarding the objectives are presented as well as suggestions for further studies within the field.



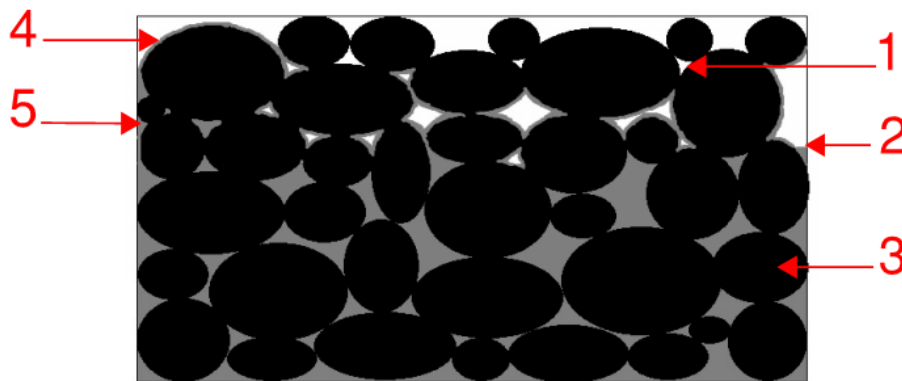
## 2 THEORETICAL BACKGROUND

The purpose of this chapter is to give the reader sufficient background knowledge to understand the descriptions, reasoning and analyses in the following chapters. Concepts and terminology of relevance for this study will be described and explained. It is assumed that the reader has a basic knowledge of geotechnical engineering.

It should be kept in mind when reading this chapter that the study was conducted on soft clay and the focus of this theoretical background will, therefore, be on the aspects relevant for this type of soil.

### 2.1 BREIF REVIEW OF SOIL MECHANICS

Soil is composed of solid particles and pores filled either with water, gas or both, see Figure 2.1. The soil can be either a two or a three phase material, depending on the degree of saturation. The degree of saturation is the ratio between the volume of water and the volume of pores. In a completely saturated soil all of the pores are filled with water while in a completely dry soil all of the pores are filled with gas. The level where the water pressure is equal to the atmospheric pressure is called the water table. It is considered that the soil is completely saturated beneath the water table even though small quantities of air can be trapped in pores below this level. Water can also be bound to the soil particle due to capillary or chemical forces.



- Legend
1. Pore filled with gas
  2. Groundwater surface
  3. Solid particle
  4. Water bound to particle surface
  5. Capillary bound water

Figure 2.1: The components of a soil segment, inspired by (Larsson, 2008)

Particle size distribution, organic content, clay content, particle shape and type of mineral dominating the particles are factors that determine the characteristics of a soil. Mineral soil are divided and named based on the particle size that the soil consist of, according to European standard ISO 14688-1:2002 (Swedish Standards Institute, 2002). Determination

corresponding to particle size ranges are given by Table 2.1. Larger particle sizes exist but are not included in Table 2.1 due to lack of relevance for this study.

*Table 2.1: Determination of soil based on particle size, inspired by Swedish Standard Institute (2002).*

<b>Fraction</b>	<b>Sub-fraction</b>	<b>Particle size [mm]</b>
Coarse soil	<b>Gravel</b>	>2.0 – 63
	Coarse gravel	>20 – 63
	Medium gravel	>6.3 – 20
	Fine gravel	>2.0 – 6.3
	<b>Sand</b>	>0.063 – 2.0
	Coarse sand	>0.63 – 2.0
	Medium sand	>0.2 – 0.63
	Fine sand	>0.063 – 0.2
Fine soil	<b>Silt</b>	> 0.002 – 0.063
	Coarse silt	> 0.02 – 0.063
	Medium silt	> 0.0063 – 0.02
	Fine silt	> 0.002 – 0.0063
	<b>Clay</b>	≤ 0.002

In Table 2.1 the soil fraction size is classified as coarse or fine. Furthermore, soils can be divided into two categories, frictional- and cohesive soil, depending on the mechanism responsible for the strength of the material. Other qualities such as deformation behaviour and permeability are also related to the specific soil type (Hansbo, 1975).

For coarser soils, friction is the main mechanism contributing to the strength of the soil and these soils are hence called frictional soils (some amount of apparent cohesion may exist). The magnitude of the frictional force depends on the position of the soil with respect to the ground water table, with water pressure reducing the inter-particle friction (Sveriges Geotekniska Institut, 2017).

Cohesion is an effect of inter-molecular forces that create an attraction between fine soil particles. In soils classified as cohesive, both cohesion and friction contributes to creating the soil's strength. Cohesive soils have some tensile strength while this is lacking for (pure) frictional soils (Hansbo, 1975). Clay is the main cohesive soil but also silt can exhibit some cohesive behaviour.

In order for a soil to be classified as clay, at least 20 weight per cent of the fine particles ≤ 0.063 mm need to be of the fraction clay. The clay particles consist of both single crystal minerals of rock and of clay minerals (Sveriges Geotekniska Förening, 2016). The most common clay mineral in Sweden is illite but chlorite, kaolinite, and montmorillonite can also be found (Hansbo, 1975). The clay particles have a negative charge that results in bounding of water, which is a dipole, to the surface of the particle. Around the clay particle there is hence a film of water that has been absorbed by the surface of the particle. The clay particles generally have a flat shape.

Generally, there are  $10^{15}$ - $10^{16}$  clay particles per  $\text{cm}^3$  due to the small size of the particles. The porosity, which is the pore volume divided by the total volume, is usually between 40 and 75

% (Hansbo, 1975) and the permeability is low,  $< 10^{-9}$  m/s (Sveriges Geotekniska Förening, 2016).

### 2.1.1 TOTAL STRESS, EFFECTIVE STRESS AND PORE WATER

In a soil with no applied load the vertical stress, which is generally the largest stress, depend on the overlaying soil. The in-situ stress in a soil, therefore, increase with depth as a function of the unit weight and the thickness of the overlaying soil:

$$\sigma_{v0} = \int \gamma(z) dz \quad (2.1)$$

where:

$\sigma_{v0}$  = Vertical in-situ stress [kPa]

$z$  = Depth below the ground surface[m]

$\gamma$  = Unit weight of the soil [kN/m<sup>3</sup>]

Compressive stress is defined as positive in soil mechanics since most stress in soil is of the compressive kind.

The total stress in a saturated soil can be divided into effective stress and pore water pressure. The effective stress is the part of the total stress that is transmitted to the solid particles and the pore water pressure is the part of the total stress that is transmitted to the water phase. The relationship between total stress, pore water pressure and effective stress for a fully saturated soil: (Terzaghi, 1943):

$$\sigma = \sigma' + u \quad (2.2)$$

where:

$\sigma$  =Total stress [kPa]

$\sigma'$  =Effective stress [kPa]

$u$  =Pore water pressure [kPa]

The pore water pressure at hydrostatic conditions i.e., when the pore water is in equilibrium, can be calculated using:

$$u = \gamma_w z_w \quad (2.3)$$

where:

$\gamma_w$  = Unit weight of the water [kN/m<sup>3</sup>], approximately 10 kN/m<sup>3</sup>

$z_w$  = Depth below the ground water table [m]

### 2.1.2 DRAINED AND UNDRAINED CONDITIONS

Undrained conditions are described as when the excess pore water pressure is not permitted to leave the soil. The pore water pressure aims to reach a static value through equalization of the

excess pore water pressure and this process is referred to as dissipation. When the static value is reached (no excess pore water pressure), drained conditions are obtained. The dissipation time is closely linked to the permeability of the soil so that highly permeable soils can reach drained conditions fast while this process can be very slow for low-permeable soils (Knappett & Craig, 2012).

In laboratory compression tests that are classified as drained, the pore water is permitted to flow out of the sample. The volume of the sample can hence change unconstricted. In the undrained compression tests, however, water flow is not allowed in or out of the sample and this will result in the soil not being able to change volume. Condition for zero volume change during undrained compressional test is that the soil is saturated and that the water and the soil skeleton are incompressible (Muir Wood, 1990).

### 2.1.3 SENSITIVITY

If clay is exposed to heavy stirring, this will cause the strength of the clay to decrease since the bonding forces between the clay particles are reduced. When the disturbance is terminated, some of the strength is often rapidly regained by the clay. Sensitivity ( $S_t$ ) is defined as the ratio between undisturbed shear strength and the remoulded (stirred) shear strength (Hansbo, 1975). In Table 2.2 the classification of clay depending on the obtained sensitivity is presented.

*Table 2.2: Sensitivity classification, inspired by (Swedish Standards Institute, 2004)*

<b>Term</b>	<b>Sensitivity</b>
Highly sensitive	> 30
Medium sensitive	8-30
Low sensitive	< 8

### 2.1.4 ATTERBERG LIMITS

Remoulded, fine soils, such as clay, has a behaviour that depend on the amount of water the soil contains. By adapting the amount of water within the soil, it can change consistency states. The consistency limits related to the water content is described by the terms liquid limit, plastic limit and shrinkage limit. These consistency limits are called Atterberg limits (Hansbo, 1975).

Liquid limit, often denoted  $w_L$ , is the water content when a soil transfers from behaving like a liquid to obtaining a plastic behaviour (Larsson, 2008). The plastic limit ( $w_p$ ) is the water content for when the plastic behaviour of a soil is replaced by a brittle behaviour. When the volume of a soil sample is not reduced further, even if more water evaporates from the sample, the shrinkage limit ( $w_s$ ) is reached (Hansbo, 1975).



There are two methods in order to determine the liquid limit, the use of fall cone test or the use Casagrande's apparatus. The method that is preferred in Sweden is the fall cone test (Swedish Standards Institute, 2010).

### 2.1.5 STRESS HISTORY OF SOILS

The slow process of sedimentation will result in an increase in effective stress in the soil due to the increase in overburden pressure. This in turn will result in consolidation of the soil, which will be further described in Section 2.2. Natural processes like erosion or man-made processes such as excavations can cause the soil to be unloaded. The consolidation history is very important for the behaviour of clay while it affects frictional soils to a limited extent (Sällfors, 2013).

A soil that has been exposed to a higher stress level than the current stress, and has been consolidated at that stress level, is referred to being over consolidated. The highest stress level that the soil has experienced is called the pre-consolidation stress and is denoted  $\sigma'_c$ . If the current stress level is the highest that the soil has been exposed to and the pore water pressure is stationary, the soil is normally consolidated. A soil can also be under-consolidated if primary consolidation (see Section 2.2) is still occurring in the soil (Sveriges Geotekniska Förening, 2016).

The over-consolidation ratio (OCR) describes the relationship between the pre-consolidation pressure and the current effective vertical stress in the soil.

$$OCR = \frac{\sigma'_c}{\sigma'_{v0}} \quad (2.4)$$

where:

$\sigma'_c$  = Pre-consolidation pressure [kPa]

$\sigma'_{v0}$  = Vertical effective in-situ stress [kPa]

The classification of the soil based on the value of the OCR is summarised in Table 2.3.

*Table 2.3: Classification of soil based on OCR, inspired by Sveriges Geotekniska Förening (2016).*

<b>Term</b>	<b>OCR</b>
Under consolidated	1
Normally consolidated or slightly over-consolidated	>1-1.15
Over consolidated	>1.5-10
Highly over consolidated	>10

## 2.2 CONSOLIDATION

When the total stress is increased instantaneously in a fully saturated soil, this will result in an excess pore water pressure as initially all stress increase is transmitted to the water phase,

owing to the fact that the water phase being virtually incompressible. The excess pore water pressure is reduced when the water dissipates and the same amount of the stress is transmitted to the soil skeleton as an effective stress increase (Terzaghi, 1943). The total stress is constant during this process, while the ratio between the effective stress and the pore water pressure is altered, illustrated in Figure 2.2. After a certain time, the pore water pressure is once again at the value that it had before the load was applied. The described process is called primary consolidation. During the consolidation process, when the water dissipates from the pores but is not replaced with pore gas, the volume of the voids in the soil will decrease and the volume of the soil will hence decrease (Terzaghi, 1943).

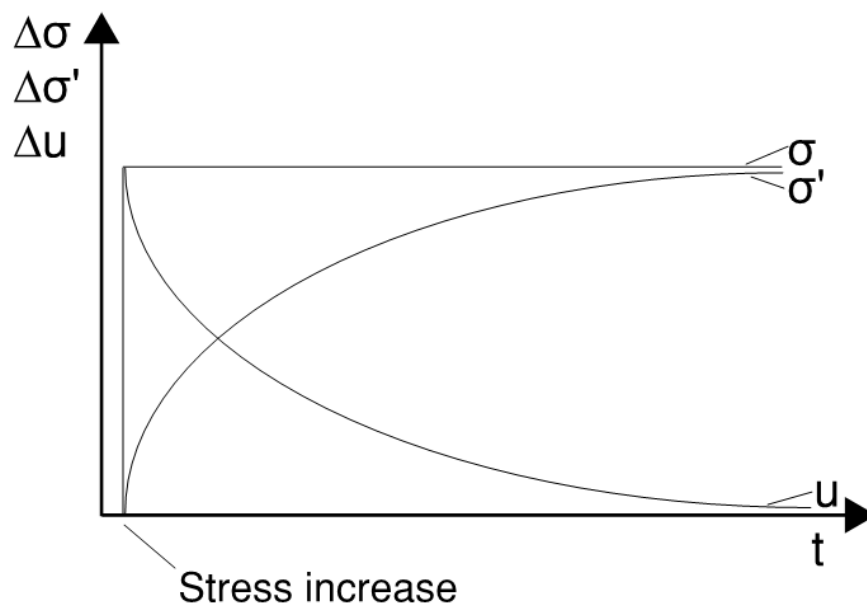


Figure 2.2: Relationship between total stress, effective stress and pore water pressure when a load is applied to a fully saturated soil. Inspired by Sällfors (2013).

The consolidation is time-dependant since excess pore water is being pressed out of the soil. The process can be very slow for soil with low permeability, like clays and silty clays, while the process can be considered almost instantaneous in courser soils.

The theory of consolidation was introduced by Terzaghi in 1923 and also described in later work by the same author (Terzaghi, 1943). Terzaghi's one-dimensional theory of consolidation is based on the following assumptions:

- The soil is fully saturated.
- The soil is homogeneous.
- Both the water and the soil particles are incompressible.
- The coefficient of permeability is constant during the consolidation process.
- The volume decrease in the soil depends entirely on the increase of the effective stress.
- Darcy's law is valid.

The equation established based on the previously described assumptions for calculating consolidation:

$$\frac{\partial u}{\partial t} = \frac{M}{\gamma_w} k \frac{\partial^2 u}{\partial z^2} \quad (2.6)$$

where:

$M$  = Compression modulus [kPa]

$k$  = Coefficient of permeability [m/s]

$t$  = Time [s]

$z$  = Depth below the ground surface [m]

Equation 2.6 describes how the excess pore water pressure, which was created due to the stress increase, varies with time and depth of the soil layer.  $c_v$  is the coefficient of consolidation and is a function of the compression modulus and the permeability:

$$c_v = \frac{M}{\gamma_w} k \quad \rightarrow \quad \frac{\partial u}{\partial t} = c_v \frac{\partial^2 u}{\partial z^2} \quad (2.7)$$

The consolidation process hence depends on the parameters permeability and compression modulus of the soil (Terzaghi, 1943).

Secondary consolidation is the deformation that occurs during constant effective stress. No hydraulic gradient occurs due to secondary consolidation since it is a slow process. Both primary and secondary deformation occurs simultaneously (Larsson, 2008). The reason for the secondary consolidation is thought to be the re-arrangement of the soil particles (Knappett & Craig, 2012). The secondary consolidation is generally limited for coarse soils while it can represent a large part of the deformation for fine soils, especially for stresses close to the pre-consolidation pressure (Larsson, 2008).

## 2.3 UNLOADING

If a saturated soil is subjected to unloading due to reduction in total stress, the reverse of the consolidation process, which was described above, is considered to occur. Terzaghi's consolidation theory is considered to be applicable for the unloading situation as well. Due to unloading, a negative excess pore water pressure is created in the soil. The negative excess pore water pressure will in time be equalised in order for the pore water pressure to reach a new static value. While this occurs, the volume of the voids increase and are filled with water. The described process is referred to as swelling (Terzaghi, 1943).

Swelling is, as consolidation, a time-dependent process. By using Terzaghi's consolidation theory the swelling due to unloading can be estimated by the coefficient of swelling which is analogue to the coefficient of consolidation. The swelling process hence depend on the permeability and the unloading modulus of the soil (Terzaghi, 1943).

A condition for the soil to swell is that the unloading is large enough to overcome potential effects of secondary consolidation processes in the soil. If a small stress reduction occurs, this may merely slow or stop the secondary consolidation process without causing swelling of the soil (Larsson, 1986).

## 2.4 COMPRESSION MODULUS

The stiffness of the soil during loading in oedometer conditions is described by the oedometer compression modulus  $M$ . An increase of the effective stress will result in an increase in the strain:

$$M = \frac{d\sigma'_v}{d\varepsilon_v} \quad (2.8)$$

where:

$\sigma'_v$  = Effective vertical stress [kPa]

$\varepsilon_v$  = Vertical strain [%]

Equation 2.8 is valid provided that no horizontal strains are allowed

The compression modulus for clays is strongly dependent on the stress history of the soil. If a load is applied to an over-consolidated clay the deformations will be small, provided that the applied load is less than the pre-consolidation pressure. The deformations that occur due to loads larger than the pre-consolidation pressure, on the other hand, will be much larger than for loads below the pre-consolidation pressure.

Figure 2.3 and Figure 2.4 show a simplified stress-strain behaviour, respectively the corresponding compression modulus for a clay. The previously described behaviours of the soil, with smaller deformations due to loads lower than the pre-consolidation pressure and larger deformations due to loads larger than this pressure, can be seen in the figures.  $M_0$  represents the stiffness for stresses below the pre-consolidation pressure,  $M_L$  represents the stiffness in the interval between the pre-consolidation pressure and  $\sigma'_L$ , and  $M'$  is the stiffness tangent for stress above  $\sigma'_L$ . As can be seen in Figure 2.4 both  $M_0$  and  $M_L$  are constant in the interval that they are valid for.

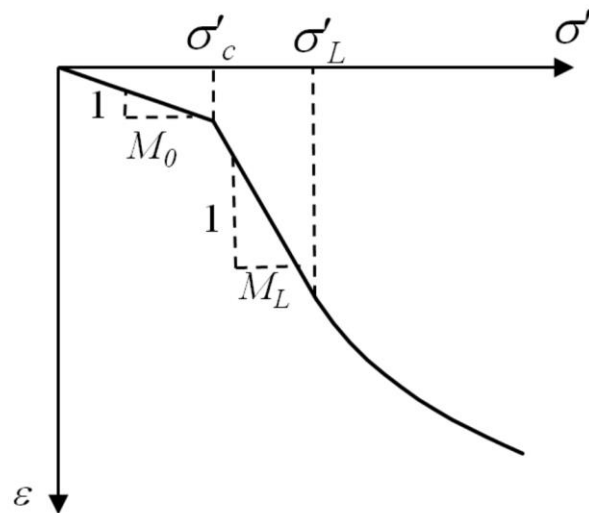


Figure 2.3: Effective stress-strain relation for clay (Tudisco & Dahlblom, 2016)

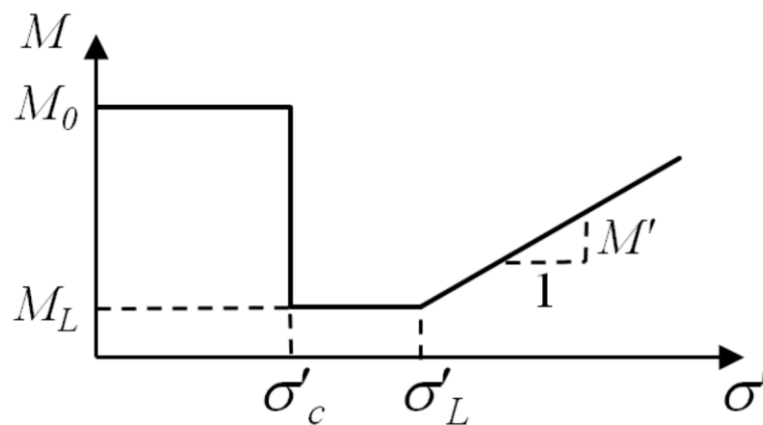


Figure 2.4: The compressional modulus corresponding to effective stress level for clay (Tudisco & Dahlblom, 2016)

## 2.5 UNLOADING MODULUS

The unloading modulus,  $M_{ul}$ , for clay has not been as widely studied as the compression modulus, although studies by, for example Larsson (1986) and Persson (2004) have been performed. Both laboratory tests and field measurements were conducted, in order to determine the unloading modulus. Based on the laboratory tests, agreement prevails regarding the fact that the unloading modulus depend on the effective stress in a non-linear way (Persson, 2004, Larsson, 1986, Karlsrud, 2012). Different relationships regarding the stress-dependency of the unloading stiffness has been established based on the previously performed researches. The results from some of the laboratory studies will be presented below in a chronological order.

Larsson (1986) used incremental load oedometer tests, with loading and unloading cycles, in order to study the unloading modulus. The conclusion from these test are that the unloading

modulus depend on the effective stress and varies from high values for small decrease in effective stress to lower values for larger decrease in effective stress. The following relationship was established for the unloading modulus based on the performed tests:

$$M_{ul} = \frac{\sigma'_v}{a_s} \quad (2.9)$$

where:

$a_s$  = Swelling index [-]

$\sigma'_v$  = Vertical effective stress [kPa]

The swelling index depends on the grain size and larger grains result in a decrease of the swelling index. The swelling index was found to be between 0.007-0.012 for soft clays and around 0.001 for sand and gravel.

As mentioned above, the unloading has to be large enough to overcome potential effects of secondary consolidation in order for swelling to occur. The stress level for which this occurs was described as  $b \cdot \sigma'_c$  by Larsson (1986), where  $b$  is the load factor and  $\sigma'_c$  is the pre-consolidation pressure. The load factor depends on particle size with increasing grain size resulting in increasing loading factor. For clays  $b$  was found to be about 0.8. The limitation for the relationship in Equation 2.9 to be valid is therefore  $\sigma'_v < b \cdot \sigma'_c$  (Larsson, 1986).

In 2003, Karlsrud studied the unloading and re-loading modulus of clay from Björsvika in Oslo, Norway by using incremental load oedometer tests. A summary of the obtained results were later presented (Karlsrud, 2012). The clay was loaded and re-loaded for various stress levels and the following relationship for the unloading modulus was found:

$$M_{ul} = a \sigma'_v (\sigma'_v / (\sigma'_c - \sigma'_v))^b \quad (2.10)$$

where:

$M_{ul}$  = Unloading modulus [kPa]

$a$  = Constant which was 250 for the clay at Björsvika [-]

$b$  = Exponent which was 0.3 for the clay at Björsvika [-]

Persson (2004) performed laboratory tests and field measurements during excavation work for a part of the Götatunnel when studying the unloading behaviour of soft clay in Gothenburg, Sweden. For the laboratory tests, incremental load oedometer tests and triaxial tests were conducted and in the field measurements of swelling, pore water pressure and earth pressure were performed during a two year period.

The same trend was observed for both the field measurements and the laboratory tests, with an initial stiffer behaviour that becomes less stiff with lower effective stress. The relationship presented by Persson for the unloading modulus was based primarily on the field measurement data since the results from the laboratory tests indicated a lower modulus than what could be concluded from the field measurements (Persson, 2004). The relationship for

the unloading modulus was reviewed from the form presented in 2004 and the final relationship is: (Persson, 2007).

$$M_{ul} = 35 \sigma'_c e^{3.5/OCR} \quad (2.11)$$

The relationship for the unloading modulus presented in the Swedish framework for geotechnical calculations, TR Geo 13 (Trafikverket, 2016) is based on the results from the study conducted by Persson (2004):

$$M_{ul} = 10 \sigma'_c e^{5(\sigma'_v/\sigma'_c)} \quad (2.12)$$

This expression is valid for slightly over-consolidated clay (Trafikverket, 2016).

The relationships for the unloading modulus that has been described in this section are summarised in Figure 2.5. The swelling index is chosen to  $a_s = 0.01$  for the presented relationship but this parameter varies in the way that was previously described. It should also be noted that Larsson's relationship is only valid for  $\sigma'_v < b \cdot \sigma'_c$  and that  $b$  in this case is 0.8, hence the straight line after  $\frac{\sigma'_v}{\sigma'_c} = 0.8$ . In the relationship presented by Karlsrud (2012), the constants are set to the values for the clay studied by Karlsrud (that is Björvika clay).

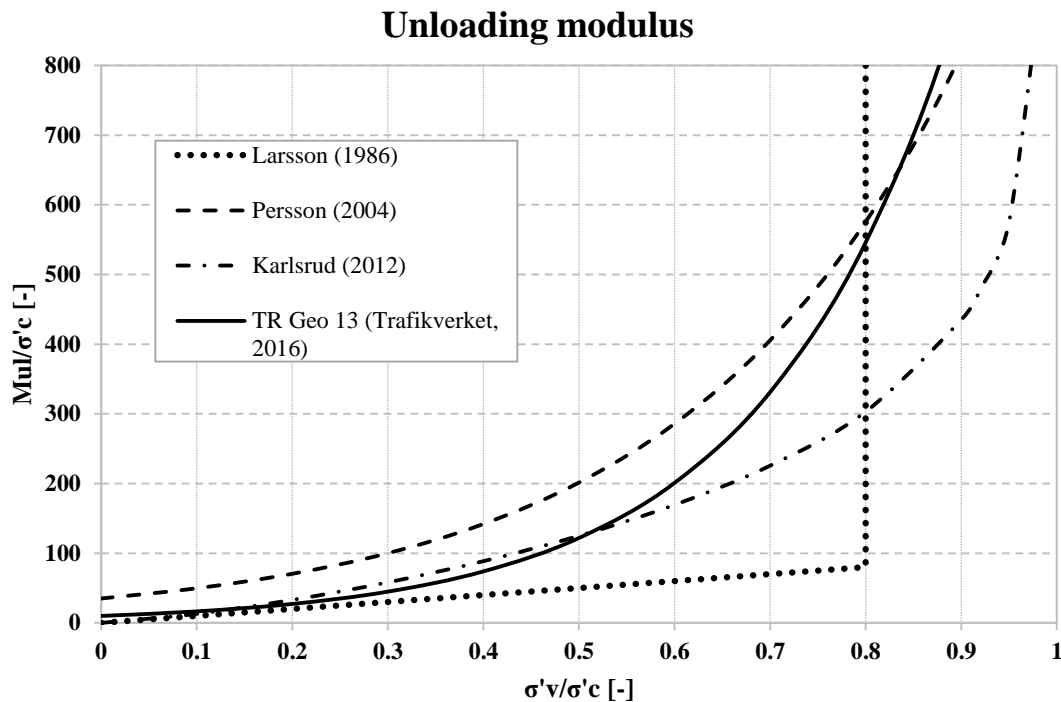


Figure 2.5 Summary of the relationships for the unloading modulus that has been presented. In the equation from TR Geo 13 (Trafikverket, 2016)  $\sigma'_v$  is chosen instead of  $\sigma'_0$ , based on already described reasons.

Since Terzaghi's consolidation theory requires a constant modulus in order to perform the calculations but the unloading modulus according to the described relationships are effective

stress dependent, the tangent unloading modulus should be used for calculation purposes. For a simplified estimation of the swelling process after unloading, a simplification can be made by using a secant unloading modulus for the relevant stress interval, see example in Tornborg (2017).

## 2.6 SAMPLING AND SAMPLING QUALITY

In Sweden, soil sampling is regulated by the standard SS-EN 1997-2:2007 (Eurocode 7) (Swedish Standards Institute, 2010) as well as ISO 22475-1:2006 (Swedish Standards Institute, 2006) .

Samples retrieved from a site can be either undisturbed or disturbed. For a sample to be classified as undisturbed, both the stratigraphy and the mechanical characteristics need to be preserved. For disturbed samples, the stratigraphy still needs to be intact while the mechanical characteristics are altered. If samples have been subjected to change of both stratigraphy as well as the mechanical characteristics, the samples are classified as stirred (Sveriges Geotekniska Förening, 2013). Undisturbed samples are required in order to perform advanced laboratory test, e.g., oedometer, direct simple shear and triaxial tests and the obtain results can be used for design purposes (Sveriges Geotekniska Förening, 2009).

Undisturbed samples can be obtained from cohesive soil as well as from mixed soils. It is also sometimes possible to obtain undisturbed samples from sand as well, if it contains organic or cohesive material that keeps the soil together (Hansbo, 1975).

The sampling methods that can be used for collection of samples that will be used for laboratory testing are divided into three categories A, B and C, according to Swedish standard Institute (2006). Depending on what sampling method is used, samples of certain qualities can be obtained, see Table 2.4. The best sample qualities are 1 and 2, and they can only be obtained by using a sampling method of category A. However, the quality of the samples obtained from sampling method A can be of the quality class 1-5. According to Sveriges Geotekniska Förening (2013), the quality class of the sample that has in fact been obtained is determined by the laboratory technician when the sample is being examined.

*Table 2.4: Relationship between sample quality and sampling method, inspired by (Swedish Standards Institute, 2006)*

Quality class of sample	1	2	3	4	5
Category of sampling methods	A	A	A B	A B	A B C

The quality of a soil sample can be classified in different ways. One way to evaluate the sample quality of a fine soil sample is to use the results obtained from oedometer test (see Section 3.3). The relative compression of the sample, at the pre-consolidation pressure, excluding initial compression due to mounting of the sample, see Figure 2.6, is measured and is then related to the natural water content,  $w_N$ , (see Section 3.2.2) in the sample (Larsson, et.



al., 2007). The procedure to evaluate the sample quality using oedometer test is illustrated in Figure 2.6 and Figure 2.7.

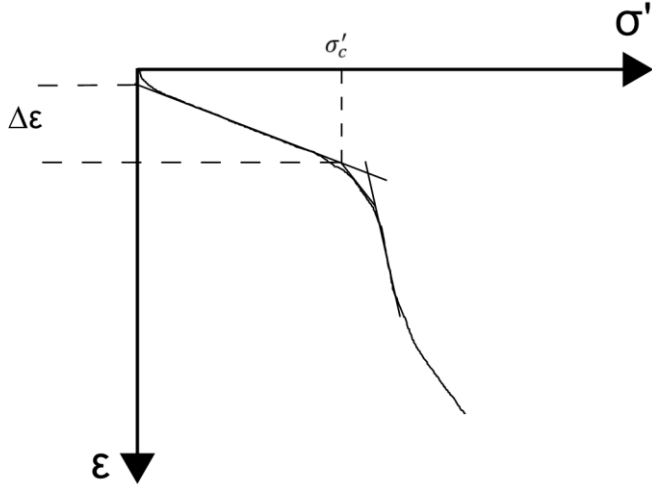


Figure 2.6: Strain difference before reaching the pre-consolidation pressure in oedometer tests, inspired by (Larsson et. al., 2007)

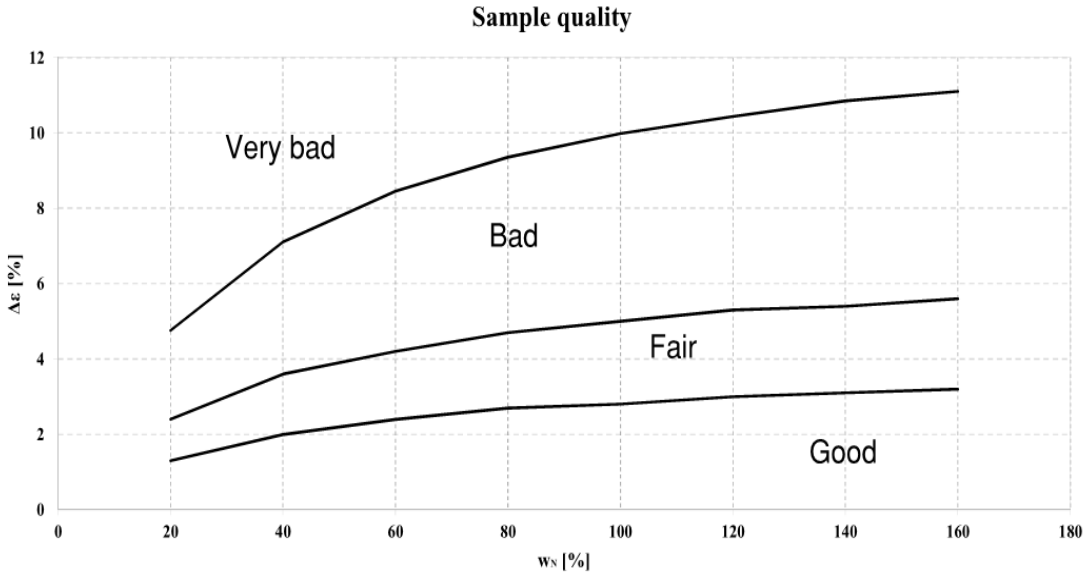


Figure 2.7: Sample quality based on natural water content and strain difference (from Figure 2.6) of sample in oedometer tests, inspired by (Larsson et. al., 2007).

**2.6.1 SAMPLE DISTURBANCE EFFECT**

According to Rabbås Holsdal (2012), samples can never be obtained fully undisturbed and the soil in the samples will always be partly altered compared to the in-situ conditions.

Disturbances occurs in all of the steps before testing the sample; sample collection, transportation, storage and preparation for laboratory tests. NIFS (2014) published a report regarding the effects of storage time on clay sample quality. The report summarises results

from many laboratory studies conducted on the subject. The report shows that, due to storage time, the clay samples are affected by, for example, decreased moisture content and drying, chemical changes (e.g., changes in pore water chemistry and aging due to oxidation) and movement of the pore water within the sample which consequently results in change in the stress distribution. These effects on the clay samples, in turn, were concluded to affect, for instance, parameters such as sensitivity, shear strength and pre-consolidation pressure of the clay.

A non-extensive collection of the laboratory studies considered in the report by NIFS is described below. Results from a study by Wood (2016) on clay from the Gothenburg area, which was published after the report by NIFS will also be presented.

Hvorslev (1949) recommended that the samples should be sealed in order to minimize moisture loss and change in chemical composition. The study by Hvorslev showed that, if the samples are properly sealed, the moisture loss is delayed substantially. The samples should be stored in a room with high humidity (close to 100%) in case proper sealing cannot be ensured.

Torrance (1976) published a study performed on soil samples of clay from Quebec, Canada that were stored during 3 months. Several different storage procedures were employed and for all samples, regardless of storage method, the pore water chemistry changed. Two different storage temperatures were examined by Torrance (1976), +20°C and +7°C. Based on the research, the preferred temperature was +7°C since less biological activity occurs at that temperature. It is mentioned, though, that even lower storage temperatures than +7°C may be preferred but this was not studied.

Bjerrum (1973) showed that a time-dependent redistribution of water takes place within clay samples after retrieval with piston sampler. This occurs due to the fact that the soil in the core of the sample tube is less disturbed than the soil next to the wall of the tube and near the ends of the tube. The negative pore pressure in the centre of the sample, which is created when obtaining the samples, will hence retrieve water from the more disturbed parts that are more compressible. This will cause the core of the sample to swell while the outer parts consolidate. Bjerrum (1973) performed the study of water distribution within samples obtained from clay from Drammen, Norway. This study demonstrated that on those clay samples, which had a natural water content of around 50 %, the water content of the outer 5 mm of the sample was on average 3-4% lower than in the sample core. When the pore water is re-distributed this will consequently affect the effective stress in the sample. This redistribution of the water within the sample will cause the undrained shear strength of the sample to decrease. This was demonstrated by Bjerrum (1973) by bringing a triaxial cell to the field and immediately placing samples of clay in the triaxial cells. Samples were also taken from the tubes 3 days later and the result demonstrated that the undrained shear strength of the samples taken from the tubes after 3 days was 15% lower than the one of the samples placed immediately in the triaxial cells.

Another study showing the effects of storage time on sample quality was performed by Lessard and Mitchell (1985). The study was conducted on quick clay from Quebec, Canada

and the samples were tested throughout a year. Lessard and Mitchell used different types of storage methods which showed that all samples were exposed to aging when stored. Ageing of the soil samples occurred mainly through oxidation which is a chemical process that occurs when oxygen is present. The authors concluded that the most important oxidation processes that occurs in samples is oxidation of organic matter and oxidation of iron sulphide. Ageing was more profound in samples that were stored in +20°C than in samples stored in +4°C. After storage, it was observed in the study by Lessard and Mitchell (1985) that the liquid limit increased and the sensitivity decreased while the undisturbed shear strength and water content was virtually the same for the samples.

Henriksson and Carlsten (1994) conducted a study on the effect of storage on samples collected with Swedish standard piston sampler. In the study, the authors investigated the pre-consolidation pressure by conducting CRS-tests on samples on two occasions, with 18 months storage time in between. The results from the study was irregular and inconclusive since some of the samples had a higher pre-consolidation pressure after the storage time while for other samples the opposite occurred after storage. Although, the trend was that the pre-consolidation pressure decreased during the storage time but as already mentioned, this result was not unanimous for all the tests.

A more recent study that has investigated the effect of storage time and sample quality on soil parameters was conducted by Wood (2016). Wood conducted laboratory tests on clay samples, which were stored in +7°C and 100% humidity, over a period of 30 days. The result demonstrated a change in natural water content and liquid limit during the laps of the storage time. Wood also observed that the shear strength of the samples as well as the sensitivity varied for the samples during the laps of the storage time. The author, therefore, recommends that samples should be tested close after sampling, preferably within two days of collection, since the results obtained from the laboratory test can otherwise be affected by the storage time. According to Wood (2016), the soil in the middle tube of the standard piston sampler is generally least disturbed and it could hence be concluded that the clay sample from this part should be best suited for laboratory tests.



### 3 METHODOLOGY

The methodology selected for this study will be presented in this chapter. The sampling technique as well as the laboratory tests methods that were performed are described.

#### 3.1 PISTON SAMPLING

Undisturbed samples of clay are in Sweden often retrieved using a Ø50 mm piston sampler. The European standard used for piston sampling is EN ISO 22475-1:2006 (Swedish Standards Institute, 2006), which is a document that describes the general guidelines for geotechnical investigation methods. In the report “Metodbeskrivning för provtagning med standardprovtagare” (Sveriges Geotekniska Förening, 2009), piston sampling method is described more thoroughly than in the previously mentioned regulation and should therefore be used as a complement to the standard in order to obtain the sufficient sample quality required in Sweden.

The piston sampler consists of a piston that is placed inside an outer pipe. At the bottom of the pipe a sharp cutting edge is situated and tubes, that will collect the soil specimens, are placed inside the pipe, above the piston. The sample collection is performed by initially pushing down the sampler into the ground. The piston is blocking the pipe while the sampler is pushed into the ground in order plug it and prevent soil and water from entering. When the desired level is reached, the piston is locked in position while the pipe with the sharp edge is pushed further into the ground. Three tubes with soil samples are collected in a row at that certain level. Above and below the three sample tubes, two shorter tubes are placed, one at each end. (Sveriges Geotekniska Förening, 2009).

Each of the three sample tubes has an inner diameter of 50 mm and a length of 170 mm. The shorter tubes are 85 mm in length. The samples remain in the sampler during withdrawal as a result of the friction between the sample and the tube and due to the negative pressure that forms below the piston. After the sample tubes are collected, a rubber lid is placed at each end of the tubes. But in order to prevent the soil from sticking to the lid, a plastic foil is placed on top of the soil prior to the lid (Sveriges Geotekniska Förening, 2009).

In Sweden two types of piston sampler are used, either STI or STII. Which type of piston sampler that is used depends on the soil conditions as well as where the sampling is taking place. ST1 was used for sample collection for this study. For ST1, the locking device for the piston consist of a chain, or similar, that descends trough the hollow bars, that are connected to the sampler, and catches into a hook. The piston is then fixed to the upper position and the sampling can be performed by pushing down the pipe with the cutting edge on. The piston is kept in place by a brake when the sampler is brought up to the ground (Sveriges Geotekniska Förening, 2009).

In order to obtain samples with good quality, the tubes need to be handled carefully. It is, for example, important that the tubes are not exposed to vibrations or shock and that they are stored in a place without large temperature variations. It is also vital to prevent the samples from freezing since the samples are then unusable for laboratory purposes. Piston sampling is

classified as a sampling method of category A and can provide samples of quality 1 and 2, see Table 2.4 (Sveriges Geotekniska Förening, 2009).

The soil in the middle and the lower tube is classified as undisturbed. The best sample quality is obtained from the middle sample tube according to Wood (2016) and from the middle tube and the top part of the lower tube according to Sällfors (2013). The soil in the top tube is classified as disturbed but routine testing, for example determination of water content can be performed using soil from this tube (Sällfors, 2013).

The piston samples collected need to be stored in a room which can be controlled regarding moisture content and temperature. However, the exact storage temperature is not specified (Sveriges Geotekniska Förening, 2009).

## **3.2 ROUTINE TESTS**

A soil can be characterised using a variety of soil parameters (Swedish Standards Institute, 2010) and geotechnical routine tests can be used to determine some of these. The parameters that were determined by routine testing of the soil samples in this study was bulk density, natural water content, undrained undisturbed shear strength, sensitivity and liquid limit. The methods for determining these parameters, according to the standards, are briefly presented below.

### **3.2.1 BULK DENSITY**

The bulk density of a soil is defined as the mass of the soil divided with the volume of the soil:

$$\rho = \frac{m}{V} \quad (3.1)$$

Where:

$\rho$  = Bulk density [kg/m<sup>3</sup>]

$m$  = Mass of the soil sample [kg]

$V$  = Volume of the soil sample [m<sup>3</sup>]

Both parameters are measured for naturally moist conditions.

The volume of the sample used to determine the bulk density should be at least 50 cm<sup>3</sup> but it is preferred with larger sample volumes since small samples may not give representative results. In order to determine the density of a soil sample obtained from a piston sampler, the tube can be weighted with the soil inside, provided that the weight of the tube is known and can be subtracted from the total weight of the sample (Swedish Standards Institute, 2014a).

### **3.2.2 WATER CONTENT**

The water content is defined as the weight of the free water divided by the weight of the dry soil:

$$w = \frac{m_w}{m_s} 100 \quad (3.2)$$

where:

$w$  =Water content [%]

$m_w$ =The mass of the water in the soil [kg]

$m_d$  =The mass of the sample after drying [kg]

The natural water content of a soil, denoted  $w_N$ , is determined for soil when naturally moist conditions prevail.

In order to determine the water content of the soil, a container with a soil sample is initially weighted and thereafter placed in an oven with the temperature of 105°C-110°C (Swedish Standards Institute, 2014b). The sample is considered to be dried when the sample does not change in mass anymore. The dried sample is weighted and the water content can then be determined. The container that the sample is placed in should have a weight that is constant during drying.

### 3.2.3 FALL CONE TEST

A fall cone is an apparatus consisting of a base plate and an adjustable cone holder on a fixed bar. Next to the cone holder is a scale and a magnifier glass in order to be able to estimate the imprint from the cone into the soil sample. A photo of a fall cone apparatus can be seen in Figure 3.1.



Figure 3.1: Fall cone apparatus

By using the fall cone test, the undrained undisturbed shear strength for undisturbed samples as well as the undrained shear strength for remoulded samples can be determined for fine grained soils (Swedish Standards Institute, 2008a). The sensitivity can be determined as a

ratio between the undisturbed and the remoulded shear strengths. The liquid limit can also be estimated by using the fall cone apparatus (Swedish Standards Institute, 2008b).

The undrained shear strength, determined by fall cone test, is performed by placing the tip of the cone at the surface of the soil sample. The cone is then released and the penetration depth is measured by examining the scale on the apparatus (Swedish Standards Institute, 2008a). The penetration depth can be converted into undrained shear strength by using the following relationship:

$$c_{ufc}(\text{or } c_{urfc}) = c g \frac{m}{i^2} \quad (3.3)$$

where:

$c_{ufc}$  or  $c_{urfc}$  = The undrained undisturbed shear strength or the undrained remoulded shear strength [kPa]

$c$  = Tip angle-dependent constant.[-]

0.8 for 30° tips

0.27 for 60° tips

$g$  = The gravitational acceleration [m/s<sup>2</sup>]

$m$  = The mass of the used cone [kg]

$i$  = The average penetration depth [m]

To obtain the undrained undisturbed shear strength, the obtained value is multiplied with a correction factor, which is based on empirical knowledge (Swedish Standards Institute, 2008a):

$$\mu = \left(\frac{0.43}{w_L}\right)^{0.45} \quad (3.4)$$

Within the span of  $1.2 \geq \mu \geq 0.5$

Where:

$\mu$  = Correction factor

$w_L$  = Fall cone liquid limit (presented in fractions), see further down in this section

The undisturbed shear strength will hence be determined by:

$$c_{u\text{corrected}} = \mu c_u \quad (3.5)$$

Which cone should be used depends on the soil that is examined. The choice of cone should be adapted in order for the penetration depth to be between 5 mm and 20 mm. The cones that can be chosen according to the standard can be seen in Table 3.1. The average penetration depth of at least 3 testpoints should be used for undisturbed samples. For remoulded samples, two consecutive cone penetration depths should be the same and this value should be used (Swedish Standards Institute, 2008a).



Table 3.1: Cones that can be used for fall cone test in order to determine undrained shear strength, inspired by (Swedish Standards Institute, 2008a).

Mass [g]	Tip angle [°]
10	60
60	60
80	30
100	30
400	30

In order to determine the liquid limit by fall cone, the cone penetration is measured using the same approach as for the undrained shear strength. The sample should be remoulded. Either the 60g/60° cone or the 80g/30° cone can be used. The course of action to determine the fall cone liquid limit is to measure the cone penetration for different water contents. The cone penetration depth should be between the values presented in Table 3.2. In order to obtain these values, distilled water can be added or the sample can be dried. For each penetration of the cone, the water content should be measured according to the approach earlier described. At least four tests at different water content should be performed. The results from the tests are plotted in a graph with water content on the y-axis and cone penetration in mm on the x-axis. A best fit linear relationship should afterwards be added to the graph. The fall cone liquid limit is the water content when the penetration is either 10 mm or 20 mm, depending on which cone is used (Swedish Standards Institute, 2008b).

Table 3.2: Requirements on penetration, inspired by (Swedish Standards Institute, 2008b)

Requirements for penetration depth	80g/30°	60g/60°
Penetration interval [mm]	15-25	7-15
$w_L$ determined based on cone penetration depth [mm]	20	10

According to the Swedish standard SS 02 71 20 (SIS, 1990) the fall cone liquid limit could also be determined using an average cone penetration depth and the corresponding water content. The water content is then corrected using table values based on the penetration depth in order to obtain the fall cone liquid limit.

$$w_L = M \cdot w_i + N \quad (3.6)$$

where:

$w_L$  = Fall cone liquid limit [%]

$M$  and  $N$  = Constants obtained from Table 1 in SS 02 71 20 (SIS, 1990) [-]

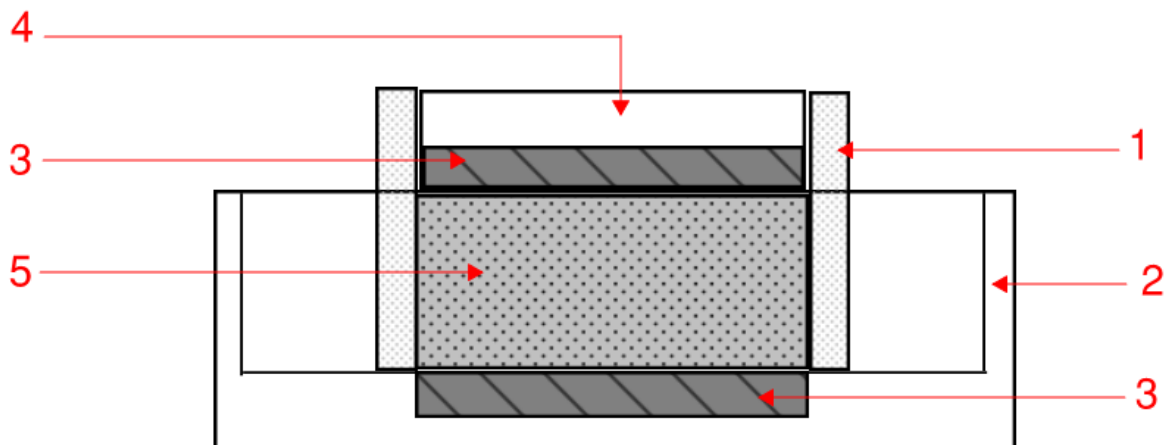
$w_i$  = Water content [%]

The cone 60g/60° is used for this method and the penetration should be between 7 mm and 14.9 mm. This method was used when determining the fall cone liquid limit for the samples in this study.

### 3.3 OEDOMETER TESTS

The most common laboratory test methods used to obtain the deformation characteristics of fine soils are oedometer tests and triaxial test (Larsson, 2008). Undisturbed samples of quality 1 are required for these types of laboratory tests. The basic principles of how the laboratory tests should be performed are regulated in Eurocode 7 (SS-EN 1997-2:2007) as well as complimentary standards (Swedish Standards Institute, 2010).

In oedometer tests, load is applied vertically to the specimen and the vertical deformation is measured. The specimen has the shape of a disk and is enclosed on the sides by a ring that inhibit horizontal deformation (Swedish Standards Institute, 2010). The ring should be smooth in order to reduce the friction along the sides. Porous stones are placed on top and on the bottom of the specimen to allow for drainage and water is surrounding the installation. For CRS, which will be described below in this section, drainage from the bottom is prevented and the excess pore water pressure is instead measured. The stone on the top is fixed to a metal device which can move inside the ring when pressure is applied to the specimen. In Figure 3.2 a sketch of an oedometer can be seen.



- Legend
- 1. Restraining ring
  - 2. Body of the cell
  - 3. Porous stone
  - 4. Loading cap
  - 5. Soil specimen

Figure 3.2: Oedometer device, inspired by (ISO, 2017)

For an oedometer test, the stress on the specimen can either be applied by incrementally increasing the load or by obtaining a constant deformation rate. The design for both the tests are basically the same with the difference that incrementally loaded oedometers uses dead weights for stress increase while a compression machine regulates the deformation for the CRS.

For the incremental loaded (IL) oedometer tests, the load is typically doubled every 24 hour. The deformation after each loading stage is recorded and plotted as points in a load-deformation graph. The oedometer modulus, the pre-consolidation pressure and the coefficient of vertical consolidation are parameters that can be determined from the test data (ISO, 2017).

CRS (constant rate of strain) is an oedometer test where the load is applied via a press at a constant deformation rate. For this test, the valve for the pore water drainage at the bottom is closed so that the specimen cannot drain from the porous stone at the bottom. A computer continuously conducts measurements of time, deformation, pore pressure and load and the data is used in order to plot graphs of the change (SIS, 1991a).

Due to the restriction of no drainage from the bottom of the specimen, the pore water distribution within the specimen is assumed to have a parabolic shape (Sällfors, 1975). The excess pore water pressure at the bottom of the specimen, that is measured, can hence be used to calculate the effective vertical stress in the middle of the sample: (Sällfors, 1975)

$$\sigma'_v = \sigma_v - \frac{2}{3}u_b \quad (3.7)$$

where:

$u_b$  = Pore water pressure in bottom of the specimen, where no drainage occurs [kPa]

In this master's thesis, the effective vertical stress for the CRS tests will be calculated using this equation.

The Swedish standard for CRS-test is SS 02 71 26 and this framework regulates equipment, test procedure and presentation of results (SIS, 1991a). The rate with which the specimen should be loaded is 0.0025 mm/min but a lower rate could be used for very soft clays, clays that contain organic particles and for heavily over-consolidated clays. The restriction for choosing lower deformation rates is that the pore water pressure should be less than 10% of the total stress (SIS, 1991a). Some recent additions to the standard have been presented by Sveriges Geotekniska Förening (2017). For instance, the loading rate should be 0.0012 mm/min for samples with pre-consolidation pressure exceeding 250 kPa as well as for some gyttja-bearing clays [Swedish: gyttjiga leror]. Sällfors (1975) performed an extensive study using different loading rates and concluded that the optimal rate was 0.0024 mm/min in order to obtain CRS-test results for the pre-consolidation pressure that corresponded to the results obtained from field tests.

The data from the CRS-test is collected by a computer program and can then be processed. The stiffness as well as the pre-consolidation pressure can be determined when the obtained data is plotted in a graph with strain versus effective stress on the axes with linear scales. In order to determine the pre-consolidation pressure both the linear parts of the graph should be extended and an isosceles triangle, with the base touching the graph, should be constructed from the extended lines. The methodology is visually explained in Figure 3.3. The rate of

loading that the specimen is exposed to affects the appearance of the graph due to viscous effects of the clay. In order to compensate for this rate-dependency, the second part of the graph is parallel moved to go through the pre-consolidation pressure (SIS, 1991a). This is also demonstrated in Figure 3.3.  $M_0$ ,  $M_L$ , and  $\sigma'_L$  can then be determined in the way that was described in Section 2.4.

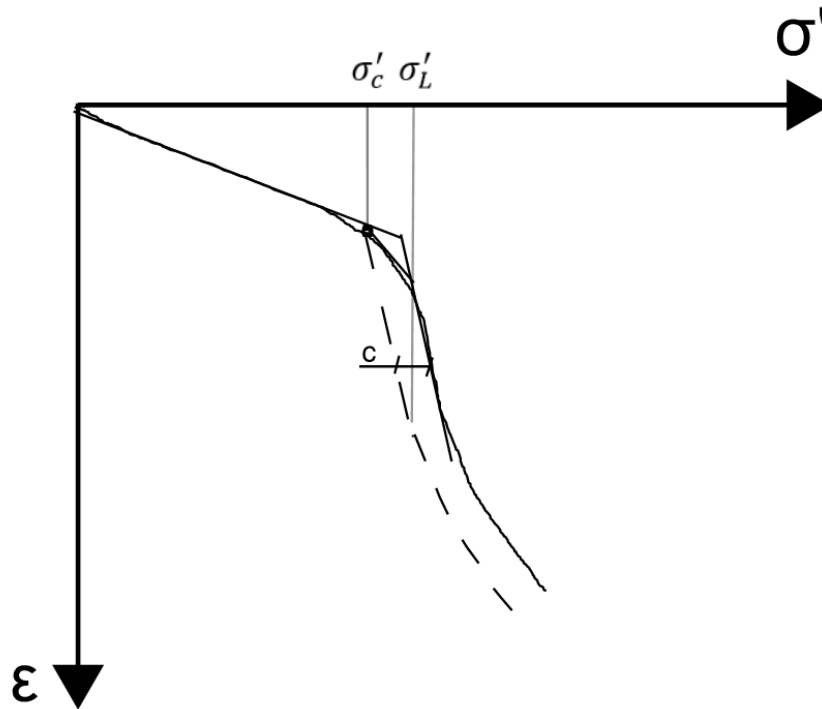


Figure 3.3: Determination of pre-consolidation pressure, inspired by (SIS, 1991a)

### 3.4 FINITE ELEMENT METHOD - PLAXIS

Differential equations are often used when modelling physical phenomena that are found in engineering problems. When these differential equations are too complex to be solved analytically, finite element method (FEM) can be used. FEM is a numerical method that gives an approximate solution of the problem by dividing the problem into smaller parts, finite elements, and then determine an approximation for each of these elements. The entire problem is solved by solving the easier approximations for each element and then merging these elements together (Ottosen & Petersson, 1992).

The accuracy of the solution depends on the amount of elements that the problem is divided into, with more elements giving a more accurate solution than fewer elements. The accuracy of the solution also depends on the assumed approximation within each finite element. The approximation is generally assumed to be polynomial of different degrees (Ottosen & Petersson, 1992).

The FEM software used for this master's thesis in order to simulate the loading-unloading CRS-tests was the geotechnical engineering software PLAXIS 2D version 2017.1 and the

material model *Soft Soil creep* (SSC). Material models are used in order to model the behaviour of the soil and different models can be used depending on, e.g., the purpose of the study and the soil material that is studied. SSC is a material model developed for the purpose of studying compression of soft soils while also taking into account the effect of secondary consolidation. In SSC, the stiffness of the soil is stress-dependent and the model distinguishes between initial loading of the soil and unloading-reloading (PLAXIS, 2016).

Initially, the soil material is defined; e.g. density and friction angle. The conducted test (which for this study is a CRS-test) is used as input in SSC for optimisation of parameters in order to match the test. Input needed for the optimisation is also the evaluated pre-consolidation pressure from the CRS-test as well as time and corresponding strain for the test. The stiffness parameters, e.g.  $\lambda^*$  (modified compression index),  $\mu^*$  (modified creep index) and  $\kappa^*$  (modified swelling index) can then be optimised to fit the test. The definition of the three parameters can be seen in

These stiffness parameters describe the general shape of the performed CRS-test and thus the stiffness of the soil depending on the effective stress.

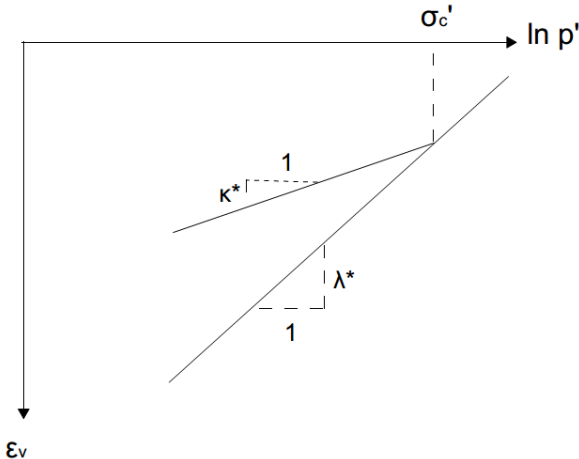


Figure 3.4: Definition of stiffness parameters  $\kappa^*$  and  $\lambda^*$ , inspired by (PLAXIS, 2016).

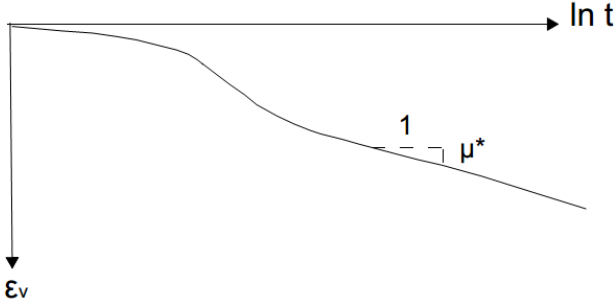


Figure 3.5: Definition of stiffness parameter  $\mu^*$ , inspired by (PLAXIS, 2016).



## **4 SITE CONDITIONS AND CONDUCTED TESTS**

In this chapter, a description of the geology and the ground conditions for the chosen site, where the samples were retrieved, will be presented. This is followed by a description of the conducted laboratory tests.

Routine and standard CRS-tests were conducted in order to obtain knowledge about the stress history of the soil. CRS-tests with unloading stages were based on the obtained knowledge of the stress history as well as the in-situ stresses, this will be described further in this chapter.

All tests, except the IL-tests, were conducted by the author with assistance from the geotechnical engineers at Skanska. The results of the tests are presented and analysed in the Chapter 5.

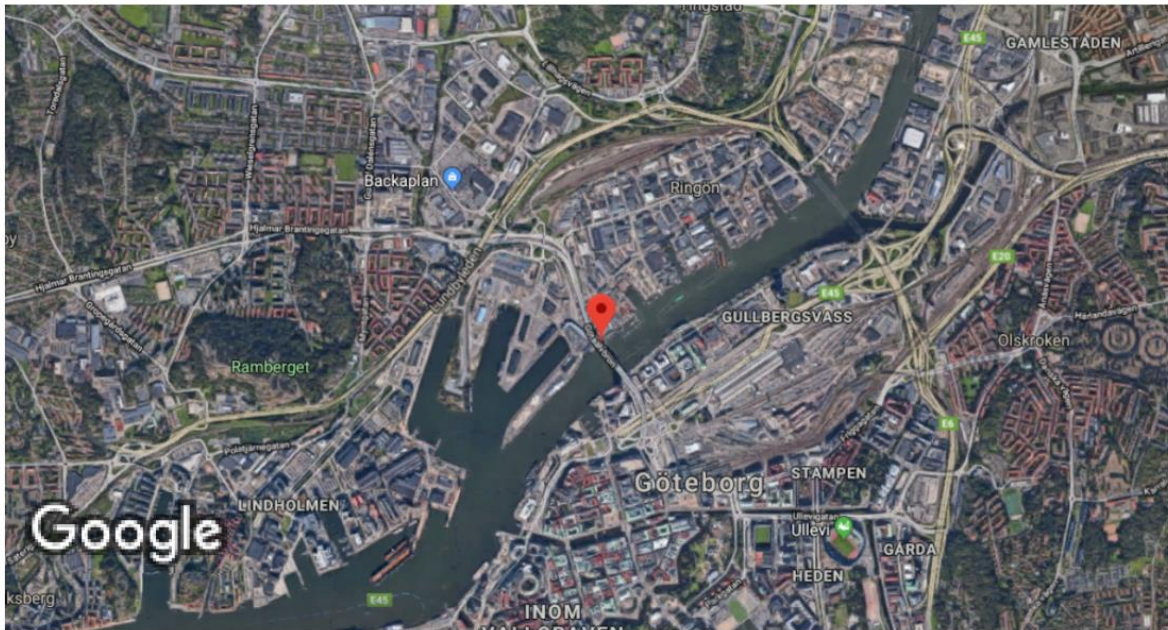
### **4.1 GEOLOGY OF THE GOTHENBURG REGION**

In order to describe the soil that can be found in the region around Gothenburg the last ice age that North of Europe had to endure needs to be studied. The ice-sheet, which was 2000-3000 m thick, weighted down the crust of the Earth and when the ice melted the crust started to rise in order to regain its initial position. The land rise is a time delayed process and is therefore still taking place but at a significantly reduced rate. Due to the large quantity of melting water from the ice, the sea level also increased. Initially the land rise was larger than the sea level rise but this eventually changed when the rate of the crust-increase slowed down. For a period of time the sea level rise was larger than the land rise and part of what is today Gothenburg was flooded. When the land rise became larger than the sea level rise yet again, the shoreline was moved forward. This means that large parts what is today land in Gothenburg used to be sea bottom (Samuelsson, 1997).

Three clay layers can be distinguished in the Gothenburg area. The two lower layers consist of glacial clay while the upper layer is post-glacial clay. The main part of the clay belongs to the category glacial clay and this type of soil sedimented during, and a while after, the melting of the ice in an Arctic sea that was created. The lower part of the lowest of the three layers contains stratum of sand and silt. The glacial clay is generally grey and homogeneous (Engdahl & Pässe, 2014).

### **4.2 SITE DESCRIPTION**

The site where the soil samples for this study were retrieved is located in central Gothenburg on the island Hisingen. Skanska is currently constructing a new bridge in the area, between Hisingen and central Gothenburg, next to the already existing Göta Älv-bridge. As a result, this site was accessible for sample retrieval. A map of Gothenburg with the location of the site marked can be seen in Figure 4.1



Bilder ©2018 Google, Kartdata ©2018 Google 500 m

*Figure 4.1: Location of site (Google, 2018)*

Samples were collected from three levels in one bore hole, denoted BH1. A drawing of the construction site, established by the project, with BH1 marked, can be seen in Appendix A. A close up of the drawing can be seen in Figure 4.2. The coordinates for BH1 is X: 6 399 865,091, Y: 147 877,300 and Z: 1,836 in the coordinate system SWEREF 991200 RH 2000.



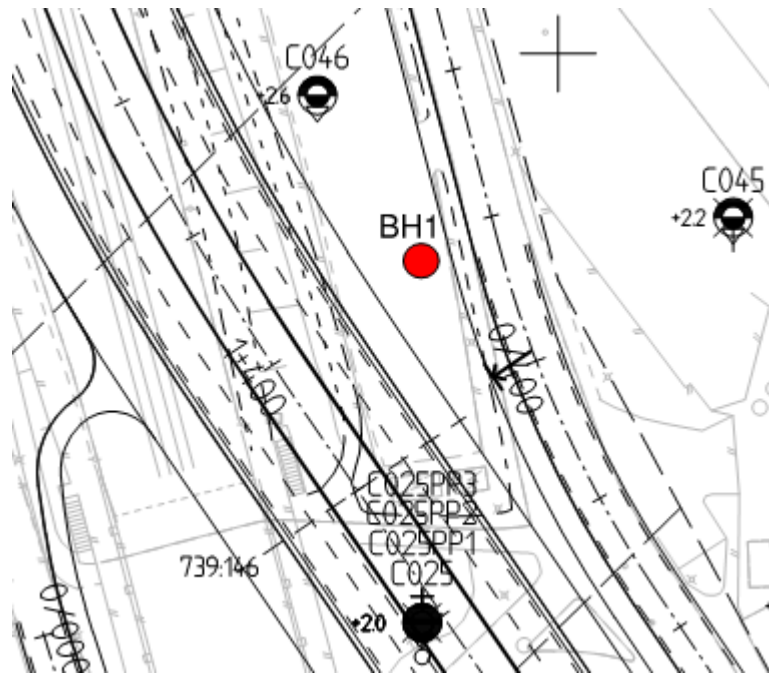


Figure 4.2: Location of BH1 and surrounding studied boreholes.

Skanska has already initiated the construction of the new bridge at the site, therefore substantial ground investigations has already been conducted in the area. As can be seen in Figure 4.2, several borings have been performed close to BH1. The collected information from these boreholes has been presented in a ground investigation report, from The City of Gothenburg (Göteborgs Stad, Trafikkontoret, 2016). Essential information about the site area could hence be obtained from the ground investigation report and incorporated into this study. The three bore holes closest to BH1 (C025, C045 and C046) were studied for the purpose of collecting information about thickness of the fill material, pore water pressure and soil density variation with depth, since this type of investigations were not conducted in BH1.

Helical auger was used in order to determine the thickness of the fill material in the boreholes C025, C045, and C046. The thickness of the fill material in the individual boreholes is presented in Table 4.1.

Table 4.1: Borehole and their individual filling thickness

Borehole	Thickness of fill [m]
C025	2 m
C045	3.2 m
C046	3.5 m

Pore pressure gauges had been placed at three levels in the borehole C025. The pore pressures that were measured can be seen in Table 4.2 and Figure 4.3. The interpreted ground water level can also be seen in Figure 4.3. The ground water level is, based on the measurements, assumed to be situated at the ground surface with pore pressure increasing hydrostatically with depth.

Table 4.2: Measured groundwater level in borehole C025

Name	Depth below ground surface [m]	Pore water pressure [kPa]	Equivalent groundwater level below ground surface [m]	Measurement date
C025PP1	10 m	99 kPa	0.1 m	2013-11-26
		99 kPa	0.1 m	2014-01-31
C025PP2	20 m	198 kPa	0.2 m	2013-11-26
		197 kPa	0.3 m	2014-01-31
C025PP3	30 m	299 kPa	0.1 m	2013-11-26
		299 kPa	0.1 m	2017-01-31

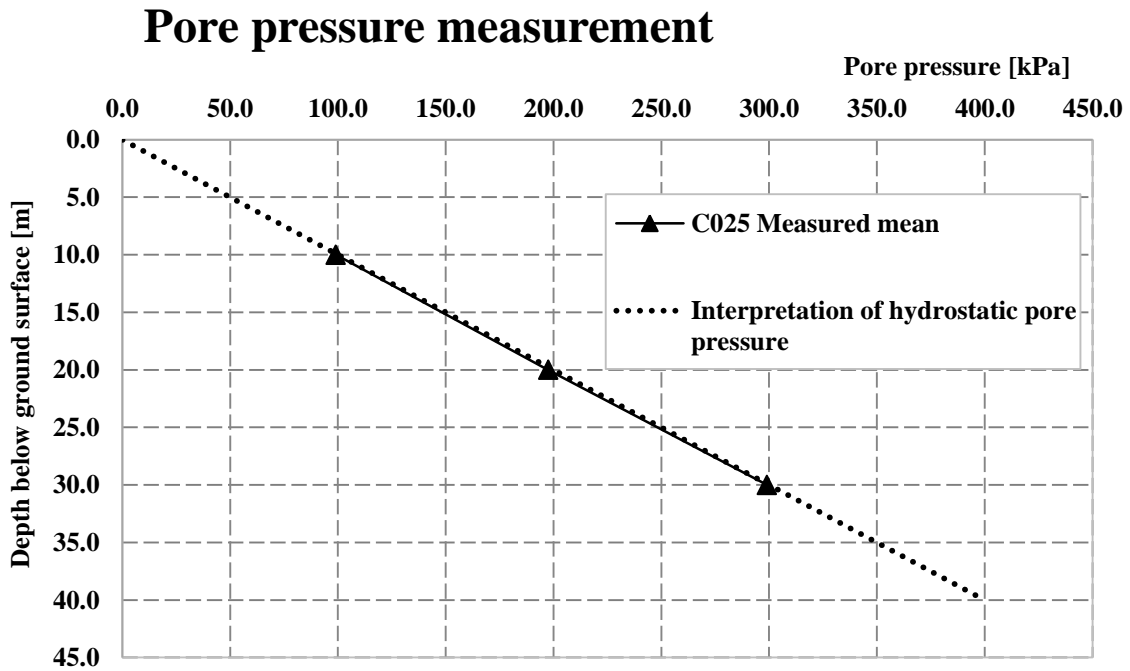


Figure 4.3: Pore pressure in C025

A summary of the soil conditions that is assumed to prevail in BH1, based on the described data, is presented in Table 4.3. The filling thickness, pore pressure and unit weight of the soil at BH1 is based on the data obtained from the surrounding boreholes.

Table 4.3: Assumed conditions in BH1.

Material	Thickness [m]	Starting level	Unit weight [kN/m <sup>3</sup> ]
Filling	2.5 m	+1.8 m	19 kN/m <sup>3</sup>
Clay	>40 m	-0.7 m	Varies, see Table 4.6
Groundwater	-	+1.8	10 kN/m <sup>3</sup>

The gravity acceleration was approximated to 10 m/s<sup>2</sup> for calculation purposes in this thesis.

### 4.3 VERTICAL IN SITU EFFECTIVE STRESS

The vertical effective in-situ stress for the three levels at BH1 was calculated using the interpreted conditions for the site, presented in Section 4.2 as well as the determined mean density of the samples tubes from the obtained levels, see Table 4.6. The unit weight of the soil above the level 17 m was assumed to be  $16.2 \text{ kN/m}^3$ , based on data from C025. The in-situ stresses calculated for BH1 are only approximate since the interpreted soil conditions for BH1, based on the nearby boreholes, may differ from the conditions that actually prevail in BH1. Despite the mentioned uncertainty, the calculated values give a good approximation of the in-situ stresses and will be used when determining the set-up for the unloading sequences using CRS, presented in Section 4.7.2. The calculated values of the effective vertical in-situ stress for the three sample levels can be seen in Table 4.4. In this table, the OCR of the samples is also presented. The OCR is calculated using the values of vertical in-situ effective stress and the values of the pre-consolidation pressure presented in Table 4.8.

*Table 4.4: Vertical effective in-situ stress for the three sample levels*

<b>Depth</b>	<b>Estimated vertical in-situ effective stress (<math>\sigma'_{v0}</math>)[kPa]</b>	<b>OCR (<math>\sigma'_c/\sigma'_{v0}</math>)</b>
17 m	114 kPa	1.5
20 m	135 kPa	1.5
25 m	168 kPa	1.3

In Figure 4.4 in-situ stresses for borehole BH1 as well as for borehole C025 are plotted. The calculated in-situ stresses for borehole C025 is based on the values obtained from the site investigation report (Göteborgs Stad, Trafikkontoret, 2016).

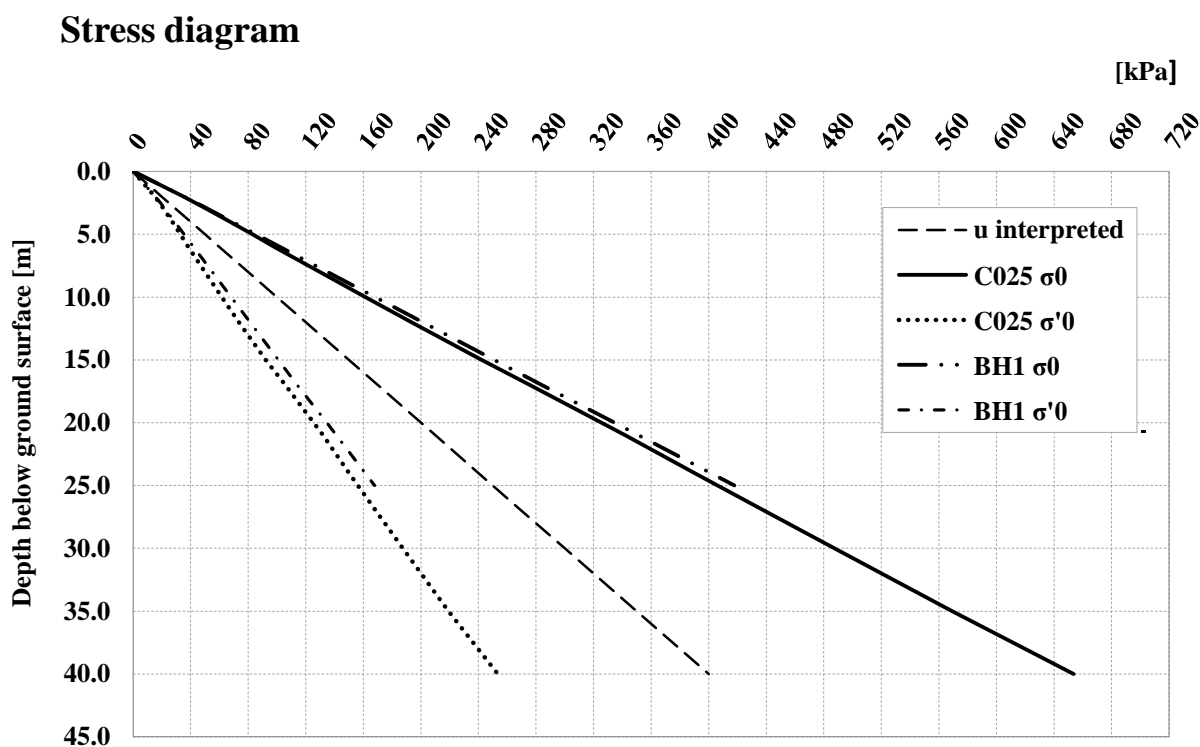


Figure 4.4: Stress variation with depth for BH1 and C025.

#### 4.4 SAMPLE RETRIVAL IN BH1

The sampling was conducted 2018-02-21 by Skanska’s field technicians Fredhy Hansen and Lennart Hedström, who both have over 30 years of working experience as field technician. The author of the thesis was present at this occasion. Photos from the sampling can be seen in Figure 4.5 - Figure 4.7.

The sampling method chosen for obtaining the specimens was piston sampling with ST1. The reason for choosing this method was that undisturbed samples were needed in order to perform CRS-tests and ST1 was the piston sampling equipment that Skanska had to their disposal in this project.

A helical auger was initially pushed through the first approximately 2.5 m of filling material before clay was reached and the soil material was soft enough to use the piston sampler to proceed.

Instead of having two shorter tubes, one below and one above the three sampling tubes in the piston sampler, as was described in Section 3.1, one extra full length tube was placed above the three sampling tubes. The reason for this being that the risk for the clay to fall out from the piston sampler is minimised, according to field technician Fredhy Hansen.



Figure 4.5: Preparation of the tubes on the piston sampler.



Figure 4.6: Separation of the tubes after sample collection.

Samples from 17 m, 20 m and 25 m were obtained. The soil was visually observed and classified in the field. The tube numbers and classification of the soil can be seen in Table 4.5.

Table 4.5: Classification of the obtained samples.

Depth [m]	Tube number		Material
17 m	o	619	Clay (with shells)
	m	314	Clay (with shells)
	u	161	Clay (with shells)
20 m	o	2969	Clay
	m	2013	Clay
	u	1509	Clay (with shells)
25 m	o	2005	Clay
	m	707	Clay
	u	119	Clay

Immediately after the sample piston reached the surface, plastic films and lids were placed on each end of the tubes and the samples were placed in a storage box. The temperature was below 0°C during the time of sampling. However, the storage box is insulated and the samples were thus protected from freezing during the field work.

## 4.5 STORAGE

The samples were transported to Skanska’s laboratory in Gothenburg where the laboratory tests were performed. The storage space used for the samples was a fridge within the laboratory, which had a constant temperature of +8°C. The samples were only removed from the storage space when subjected to testing.

## 4.6 RESULTS FROM ROUTINE TESTS

Routine test were performed using the procedures described in Chapter 3. The tests were performed at Skanska Teknik’s laboratory at Gårda in Gothenburg by the author and Lennart Hedström.

The parameters that were evaluated during the routine tests were:

- Bulk density
- Water content
- Sensitivity
- Liquid limit (using fall cone test)

Determination of the bulk density of all the sample tubes was performed the day after sample collection, 2018-02-22, and the results are presented in Table 4.6.

*Table 4.6: Density of the samples*

Depth [m]	Tube number		Bulk density[t/m <sup>3</sup> ]	Mean bulk density [t/m <sup>3</sup> ]
17 m	o	619	1.71	1.69
	m	314	1.71	
	u	161	1.65	
20 m	o	2969	1.84	1.69
	m	2013	1.62	
	u	1509	1.61	
25 m	o	2005	1.63	1.63
	m	707	1.64	
	u	119	1.63	

The remaining routine tests were performed 2018-02-28. The soil samples used for the routine tests was initially visually examined in order to choose a part of the sample that was representative for the soil material at that level and did not appear to contain any local anomalies that could influence the test results. The top part of the lower tube was used for the routine tests since undisturbed samples were required in order to determine the undisturbed shear strength. The results from the routine tests can be seen in Table 4.7.

Additionally, the water content was also determined before each of the CRS-test with unloading stages in order to determine the sample quality, which will be presented in Section 5.1.

Table 4.7. Summary of results from routine tests.

Depth	Undisturbed undrained shear stress (uncorrected) [kPa]	Undisturbed undrained shear stress (corrected) [kPa]	Sensitivity [-]	Water content [%]	Fall cone liquid limit [%]
17 m	23	19	8	62	70
20 m	24	18	9	75	78
25 m	31	24	10	69	77

In Appendix B, the results from the routine test for BH1 are plotted together with the results from the routine tests for C025. It should be noted that the values for undrained shear strength as well as for the sensitivity for C025 has been determined using the old Swedish standard, SS027125 (SIS, 1991b), while the values for BH1 were obtained using the earlier described standard SIS-CEN ISO/TS 17892-6:2007 (Swedish Standards Institute, 2008a). This affects the obtained values to some extent since the c-values in Equation 3.3 differs slightly between the two standards. In the old Swedish standard SS027125 the c-value for 30° cones is 1.0 (0.8 in SIS-CEN ISO/TS 17892-6:2007) and the c-value for 60° cones is 0.25 (0.27 in SIS-CEN ISO/TS 17892-6:2007 (SIS, 1991b)). The values for the two boreholes are still considered to be in the same range and comparable.

Figure 4.7 shows a photo taken while the undisturbed undrained shear strength was tested for BH1.



Figure 4.7: Examination of undisturbed shear strength using the fall cone test.

## 4.7 CRS-TESTS

All CRS-tests were also performed at Skanska Teknik's laboratory at Gårda in Gothenburg. The loading tests using CRS were performed in accordance with the procedure described in

Section 3.3. The Swedish standard SS 02 71 26 (SIS, 1991a) was followed if not stated otherwise. The temperature of the water surrounding the set-up, used to cool the CRS installation, had a relatively constant temperature of +11°C. In order to reduce the friction between the ring and the specimens, the ring was lubricated using Molykote, which is a silicone grease. The tests were performed by the author, with help to set up the loading-unloading sequences (for the CRS tests with unloading stages) from Skanska's geotechnical engineers Anders Kullingsjö and Johannes Tornborg. The loading-unloading sequences were programmed using the software GDSLab.

Skanska Teknik in Gothenburg has two CRS machines from GDS instruments, a photo of one of the apparatus can be seen in Figure 4.8.



Figure 4.8: One of the CRS in the laboratory at Skanska.

#### 4.7.1 LOADING TESTS WITH CRS

In order to develop an understanding of the stress history of the clay collected from BH1, standard compressional CRS-tests were initially performed. The results can be seen in Appendix C and were used to evaluate  $\sigma'_c$ ,  $\sigma'_L$ ,  $M_0$  and  $M_L$  for each level, according to the procedure earlier described. The evaluated parameters are presented in Table 4.8. These parameters are also presented together with the same parameters obtained from C025 in Appendix D.



Table 4.8. Parameters determined from CRS tests.

Depth	$\sigma'_c$ [kPa]	$\sigma'_L$ [kPa]	$M_0$ [kPa]	$M_L$ [kPa]
17 m	176	225	5411	653
20 m	196	258	3765	672
25 m	221	270	3953	790

The deformation rate employed for the CRS-tests was 0.0024 mm/min, based on the study performed by Sällfors (1975). The loading tests were executed for approximately 24 hours until a full loading curve was obtained.

#### 4.7.2 UNLOADING TESTS WITH CRS

Based on values presented in Section 4.7.1, the set-up for the loading-unloading tests was established. For the loading sequences a deformation rate of 0.0024 mm/min was used. For the unloading sequences a stress controlled condition of -0.3 kPa/min was chosen, this was based on unpublished unloading tests performed by Anders Kullingsjö around year 2003. The unloading tests were performed on clay obtained from the Göta tunnel project (Gothenburg) as a part of Kullingsjö's PhD dissertation. The loading-unloading tests are hence a modified CRS test since the loading sequences are performed with constant rate of strain while the unloading sequences are performed with a constant rate of stress. The reason for using a constant stress-rate during unloading is to make sure that the sample always has contact with the load press.

The approach for the loading-unloading sequences can be seen in Table 4.9. Stages described as relaxation stops means that the deformation rate is set to zero during a specified time while the change in axial load and pore-pressure are logged (stop by the loading press). The reason for including stop-stages was in order to try to avoid secondary consolidation during unloading close to the pre-consolidation pressure, as was described by Larsson (1986) and presented in Section 2.5. As a result of the stops, the pore pressure will decrease and the soil will consolidate.

The first series of tests were performed as soon as feasible (with respect to on-going projects at Skanska) after sample retrieval and the second test series were performed after 8 weeks of storage.

Table 4.9: Stages for the unloading tests.

Stage number	Description of stage
Stage 1	Loading until vertical in-situ effective stress ( $\sigma'_{v0}$ ). Loading rate 0.0024 mm/min
Stage 2	Relaxation stop 2 hours. Zero def.rate.
Stage 3	Unloading until $0.4 \cdot \sigma'_{v0}$ . Unloading rate 0.3 kPa/min
Stage 4	Relaxation stop 2 hours. Zero def.rate.
Stage 5	Loading until $0.8 \cdot \sigma'_c$ . Loading rate 0.0024 mm/min
Stage 6	Relaxation stop 2 hours.
Stage 7	Unloading until $0.4 \cdot \sigma'_{v0}$ . Unloading rate 0.3 kPa/min
Stage 8	Relaxation stop 2 hours. Zero def.rate.
Stage 9	Loading until a stress level in the middle of the $M_L$ spann. Loading rate 0.0024 mm/min
Stage 10	Relaxation stop 6 hours
Stage 11	Unloading until $0.4 \cdot \sigma'_{v0}$ . Unloading rate 0.3 kPa/min
Stage 12	Relaxation stop 2 hours. Zero def.rate.
Stage 13	Load until a stress level on the $M'$ spann. Loading rate 0.0024 mm/min
Stage 14	Relaxation stop 6 hours. Zero def.rate.
Stage 15	Unloading until $0.4 \cdot \sigma'_{v0}$ . Unloading rate 0.3 kPa/min
Stage 16	Relaxation stop 2 hours. Zero def.rate.
Stage 17	Loading to maximum 27% strain. Loading rate 0.0024 mm/min
Stage 18	Relaxation stop. Zero def.rate. Only for level 20 m and 25 m

The samples used for the two series of unloading tests were obtained from the undisturbed sample tubes, either the middle tube or the upper part of the lower tube. The sample-tube used for each test is specified in Table 4.10 and

Table 4.11. The reason for not using the same tubes for level 20 m and level 25 m was due to lack of clay left in the middle tubes. Since both the middle tube and the upper part of the lower tube are classified as undisturbed and of good quality this is considered to not significantly affect the test results. This is discussed further in Chapter 0. In order to test specimens that had not be subjected to air and other impact from the environment, approximately 1-2 cm were removed above the sample.

The test stages described in Table 4.9 were used for both the first series of loading-unloading tests and the second series of loading-unloading tests, performed 8 weeks after the first test series. Initiation and completion date for each test as well as the total test time for the tests are presented in Table 4.10 and

Table 4.11. The curves obtained from the two test series can be seen in Appendix E. Presented in Appendix E is also graphs showing the following:

- The pore water pressure, total axial stress and effective axial stress versus time.
- Rate of axial stress change.
- Rate of axial displacement change.

*Table 4.10: Start date, finish date and total test time for the first series of loading-unloading tests.*

Depth [m]	Tube number		Start date	Finish date	Time of test
17 m	m	314	2018-02-26	2018-03-02	91 hours
20 m	m	2013	2018-03-05	2018-03-10	117 hours
25 m	m	707	2018-03-05	2018-03-10	117 hours

*Table 4.11: Start date, finish date and total test time for the second series of loading-unloading tests performed 8 weeks of after the first series of tests.*

Depth [m]	Tube number		Start date	Finish date	Time of test
17 m	m	314	2018-04-23	2018-04-27	106 hours
20 m	u	1509	2018-04-30	2018-05-05	113 hours
25 m	u	119	2018-04-30	2018-05-05	112 hours

## 4.8 TESTS USING INCREMENTAL LOAD OEDOMETER

As was described in the Section 1.1, relatively time-consuming IL-tests have previously been used when studying the unloading modulus of soft clay. It is of interest to examine if similar results can be obtained using computer controlled (and slightly modified) CRS-tests. Both modified CRS and IL-tests were therefore performed on similar samples and then compared.

The IL-tests were performed by Johannes Tornborg at Chalmers University of Technology laboratory in Gothenburg. The load increments for the IL-tests were adapted in order to load, unload and reload the samples to approximately the same stress levels as the modified CRS.

As it can be seen in Table 4.10 and Table 4.12, the starting date for the two methods on similar samples differ slightly which is due to unforeseen events with the CRS machine that will be described in the Chapter 5. The starting dates are still close in time and the results for the IL-tests are therefore considered to be comparable with the modified CRS-tests, conducted in the first test series.

Initiation date, completion date and total test time for the test is presented in Table 4.12. The loading stages for each IL-test, as well as the obtained data are presented in Appendix F. The data is analysed in Chapter 5.

Table 4.12: Start date, finish date and elapsed time for each unloading test using IL.

<b>Depth [m]</b>	<b>Tube number</b>		<b>Start date</b>	<b>Finish date</b>	<b>Time of test</b>
17 m	m	314	2018-02-23	2018-04-07	42 days
20 m	u	1509	2018-03-02	2018-04-18	46 days
25 m	u	119	2018-03-02	2018-04-16	44 days

## 5 SUMMARY OF RESULTS, ANALYSIS AND DISCUSSION

This chapter contains the results and analysis of the conducted laboratory tests and the study with the material model *Soft soil creep*. Some discussion of how the result relates to previous studies is included as well as remarks concerning the performed laboratory tests.

### 5.1 GENERAL REMARKS

Evaluation of sample quality was performed according to the procedure described in Section 2.6. The evaluated sample quality of the specimens that were subjected to testing for this study can be seen in Figure 5.1. The water content used to establish the sample quality for the standard CRS-tests are based on the water content determined as part of the routine analysis while the water content for the unloading tests were determined in association with the initiation of each modified CRS-test.  $\Delta\varepsilon$  was determined for all the tests according to Figure 2.6.

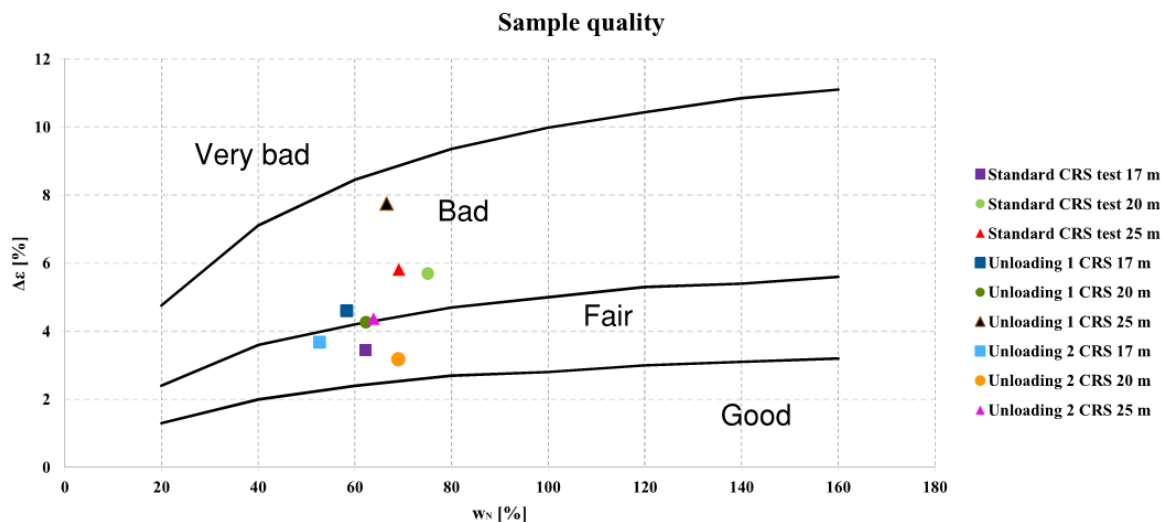


Figure 5.1: Evaluated sample quality.

As can be seen from Figure 5.1, all of the samples are evaluated to a quality between fair and bad. The sample quality for each level nevertheless, is fairly consistent in quality, with level 25 m having the poorest sample quality. This poor sample quality could indicate that the samples could have been disturbed, some levels more than others, despite caution during sample retrieval and handling. Another reason could be that the negative pore water pressures, which forms during retrieval of the samples, had time to dissipate a bit before the CRS-tests were initiated, thus resulting the samples to swell. This could be the case since the samples were taken from rather large depths, and some swelling of the samples in the tubes was observed already during the first days of storage in the laboratory, see Figure 5.8. Yet another reason for the evaluated poor quality of the samples might be the lack of previous experience that the author has on conducting CRS-tests which hence could cause a larger  $\Delta\varepsilon$ .

What should be focused on is that all samples for this study were fairly consistent regarding sample quality, especially for each sample level, and the results from the different tests are therefore considered comparable regarding the study of storage time effect. That the sample quality is low should still be kept in mind when examining the test data.

The evaluated sensitivity ( $S_t$ ) for the samples can be seen in Table 4.7. The sensitivity was between 8-10 for the three samples and the clay samples are hence classified as medium sensitive according to Table 2.2. The higher sensitivity values that the samples have, the more sensitive they are to disturbances and consequently to be managed and placed in the CRS equipment.

## **5.2 UNLOADING MODULUS OBTAINED USING MODIFIED CRS TESTS**

To compare the results obtained from this study with the results presented from previous studies, the stress level and unloading modulus for the tests in this study were normalised using the pre-consolidation pressures. However, when the stress level in the tests exceeds the initial (in-situ) pre-consolidation pressure,  $\sigma'_c$ , the sample experiences a new maximum stress level. The “new” pre-consolidation pressure denoted  $\sigma_c'^*$ , is evaluated using the same procedure as described in Section 3.3. This approach is demonstrated in Appendix G. Consequently, for evaluation of unloading sequences named ul 1 or ul 2 (unloading sequences starting from stress-level below  $\sigma'_c$ ) normalisation is made with respect to  $\sigma'_c$  while for unloading sequences named ul 3 and ul 4 (unloading sequences starting from stress-level exceeding  $\sigma'_c$ ) normalisation is made with respect to  $\sigma_c'^*$ . For the IL-tests  $\sigma_c'^*$  is assumed to be the highest stress level that the samples have been subjected to since the samples have time to consolidate (no excess pore pressures assumed) for that stress level before the next load increment is applied. This approach to present the highest stress level for IL-tests and to evaluate the pre-consolidation pressure for CRS-tests using the method described in the standard for the CRS, is considered to be comparable.

After the pre-consolidation pressures had been determined, the normalised unloading modulus could be plotted versus the normalised stress level. The CRS machine had problems keeping a constant rate of stress decrease during unloading (see Appendix E, Figure E.13- E.18) and the rate therefore varied within a span  $-0,3\pm 0,2$  kPa/min. The measured strain increments between two data recordings (2 minutes apart) during unloading were also very little or even none between some stress-intervals, since the resolution of the displacement gauge was not high enough (1/1000 mm). The consequence of these difficulties was that it was challenging to plot the unloading modulus obtained using the modified CRS-test in a representative way. The chosen approach to graphically plot the unloading modulus is described in the following paragraph.

The unloading modulus was determined using linear regression for stress intervals of  $\sim 5$  kPa. In the graphs, the unloading modulus is plotted as infinitive if the strain change was zero/negative in a stress interval. This, since when the strain difference is very small for the studied stress interval the unloading modulus is very high. The plotted modulus for the

different levels can be seen in Appendix H. An example of evaluated unloading modulus for lever 20 m (first unloading series) can be seen in Figure 5.2.

### 20 m - first unloading test series

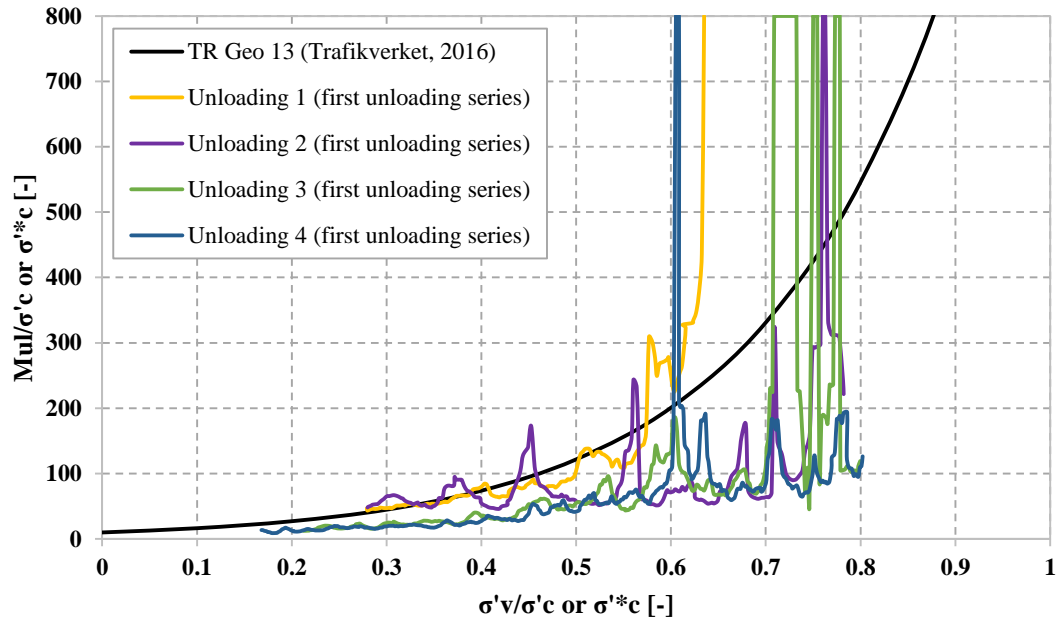


Figure 5.2: Evaluated unloading modulus for level 20 m.

Plotted in the graphs in Appendix H are only stress levels of  $\sigma'_v/\sigma'_c \leq 0.8$  or  $\sigma'_v/\sigma'^*_c \leq 0.8$ . This is since according to Larsson (1986) secondary compression will occur in the soil for higher stress levels and the modulus will hence be negative/infinite.

In Figure 5.3 and 5.4 it can be seen that the unloading modulus generally appears to be greater for load-reversal (unloading sequences) starting from stress-levels below the in-situ pre-consolidation pressure compared to those unloading sequences starting from stress levels exceeding the in-situ pre-consolidation pressure. This difference in the value of the unloading modulus for unloading sequences below and above the pre-consolidation pressure was not noted by Persson (2004). Persson concluded that no difference could be distinguished between the unloading modulus, determined studying IL-test, with unloading sequences starting from above the in-situ pre-consolidation pressure and unloading sequences starting from below the in-situ pre-consolidation pressure.

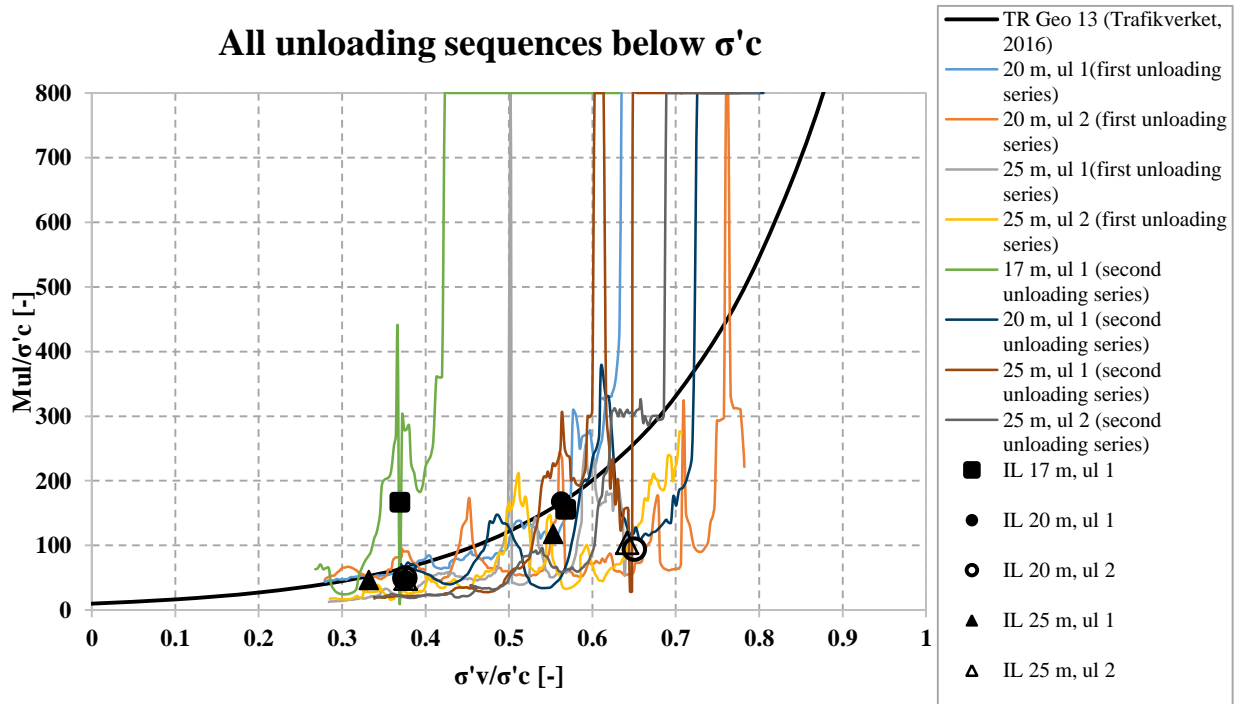


Figure 5.3: Unloading modulus for all levels below pre-consolidation pressure.

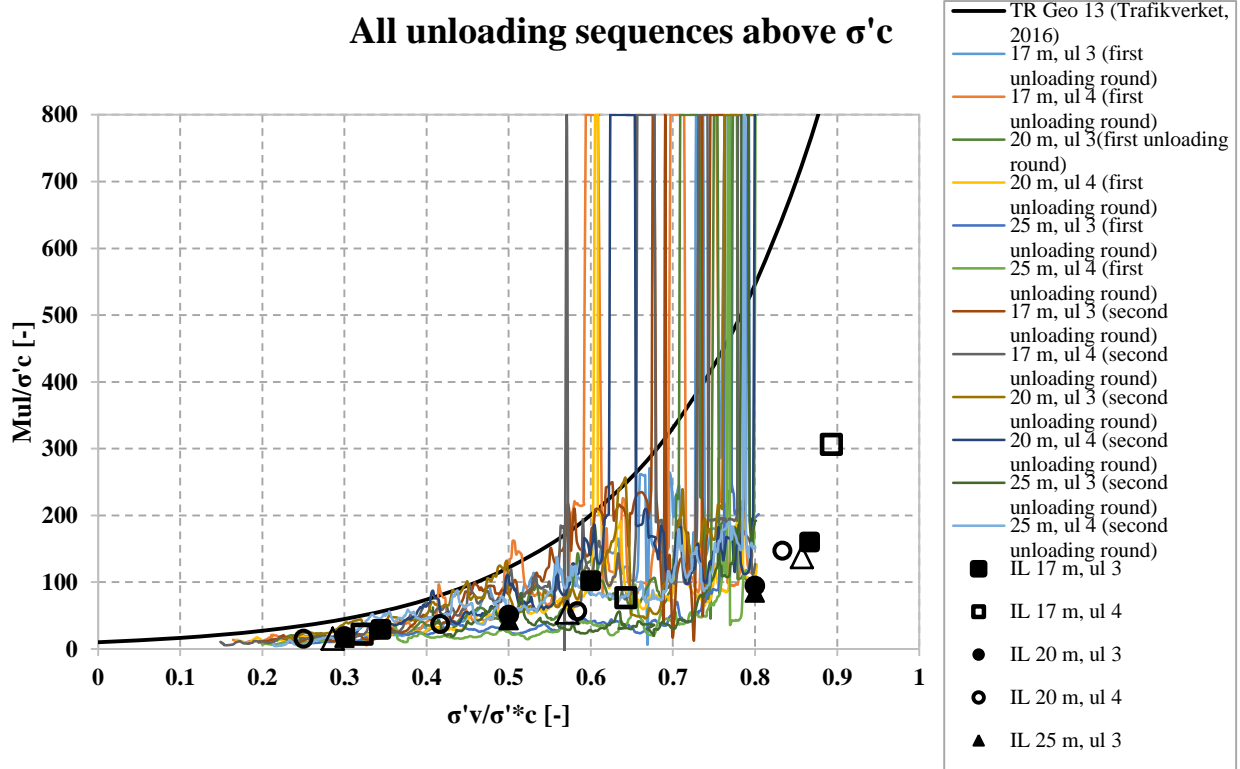


Figure 5.4: Unloading modulus for all levels above the pre-consolidation pressure.

The unloading modulus obtained using modified CRS-tests for the level 25 m is lower than for the other two levels. The reason for this can possibly be the lower sample quality for this level. What should also be noted about level 25 is that one of the CRS machines, which was



used only for level 25 m, did not register negative pore pressure. This affected the obtained unloading modulus for level 25 m since the effective stress was underestimated during unloading. The pore water pressure for 17 m and 20 m, was studied and for these levels, where negative pore water pressure was measured, the pore water pressure barely became negative for the unloading sequences below the pre-consolidation pressure. The estimated unloading modulus below the pre-consolidation pressure for 25 m is therefore not considered to be affected significantly by this error with the machine. The unloading modulus obtained from the unloading sequences above the pre-consolidation pressure on the other hand is affected. However, as it can be seen in the other CRS-tests, the excess pore-pressures are in the range of max -12 kPa excess pore pressure during unloading and thus do not affect the results to such a large extent, especially for higher stress levels. The pore water pressure for the loading-unloading CRS tests can be seen in Appendix E, Figure E.7-E.12.

The unloading modulus obtained from the laboratory tests in this study is generally lower than the already established relationships presented by Persson (2004) and Trafikverket (2016) which can be seen in Figure 5.5. This was however expected since the values for the unloading modulus presented by Persson, obtained from triaxial tests and IL-tests, were lower than the values obtained from the field measurements by the same author. Persson constructed the relationship for the unloading modulus based on results from field measurements and concluded that the laboratory tests resulted in lower unloading modulus. The relationships presented by Larsson (1986) and Karlsrud (2012) were based on laboratory tests and these relationships are in better agreement with the results from the tests conducted in this thesis.

## All unloading sequences above $\sigma'c$

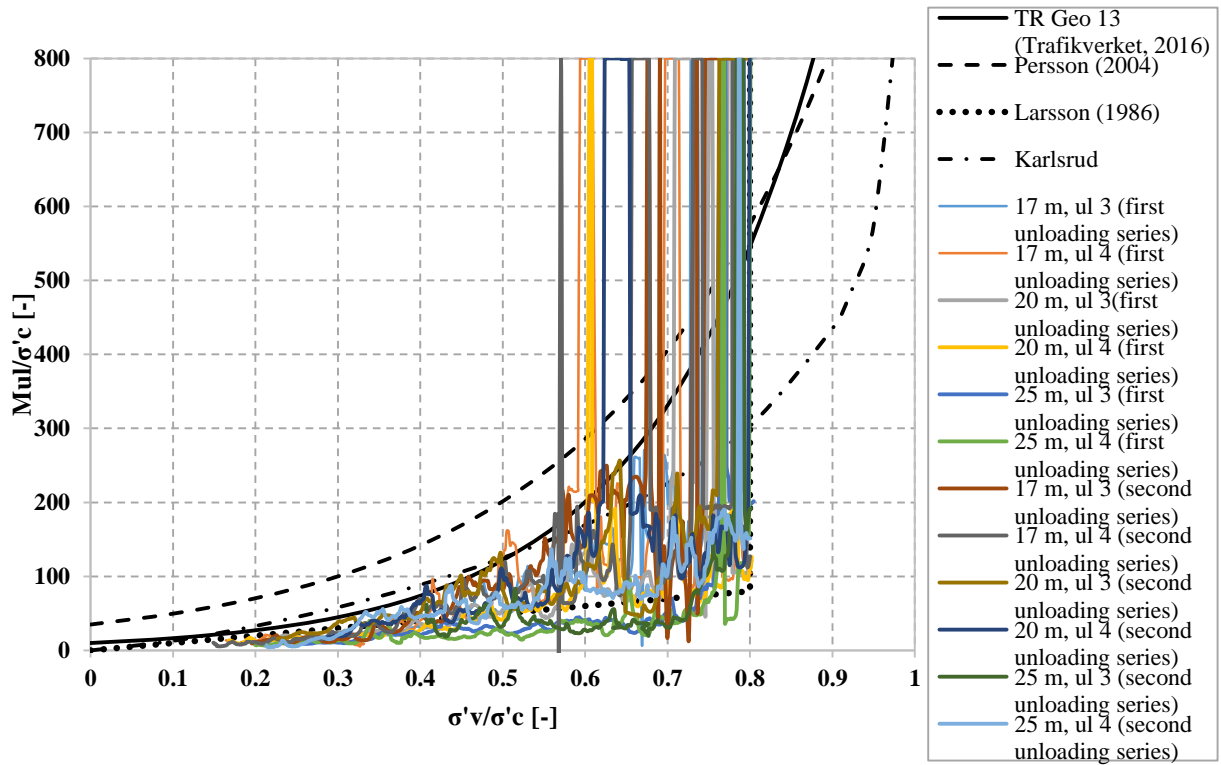


Figure 5.5: Obtained unloading modulus compared to established relationships of the same parameter.

### 5.2.1 STORAGE TIME EFFECT ON UNLOADING MODULUS

No influence regarding the storage time on the obtained unloading modulus could be noted, see Appendix H and example for level 17 m in Figure 5.6 and Figure 5.7.

### 17 m - first unloading test series

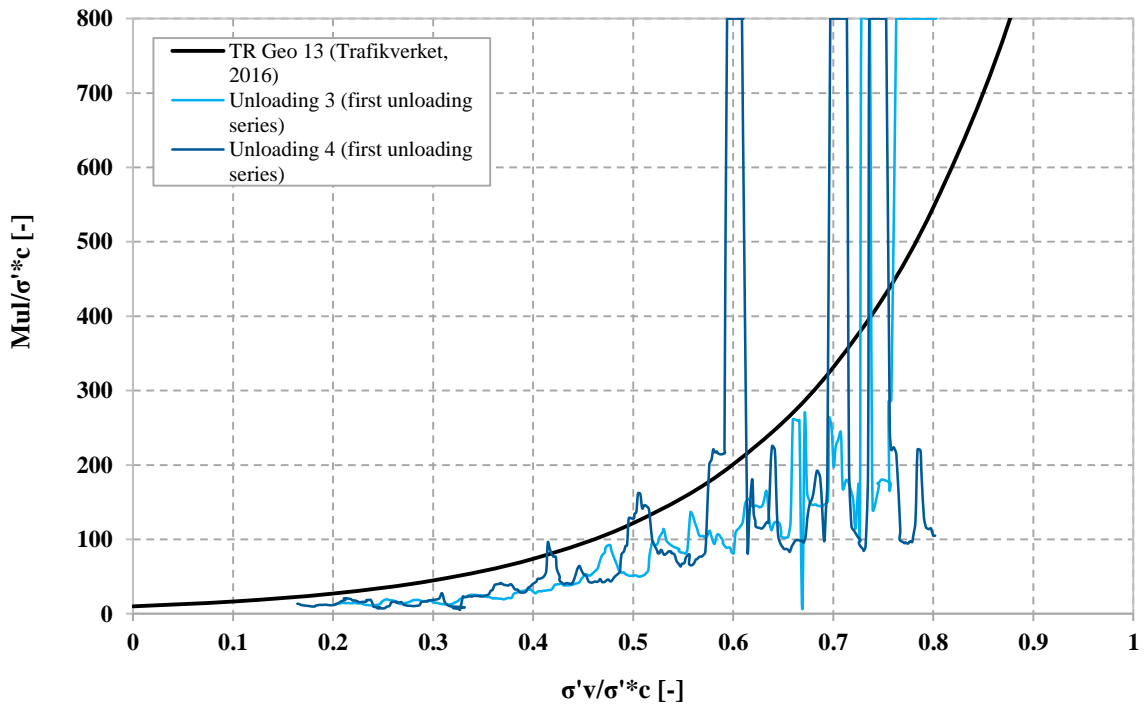


Figure 5.6: Unloading modulus for level 17 m, first unloading series.

### 17 m - second unloading test series

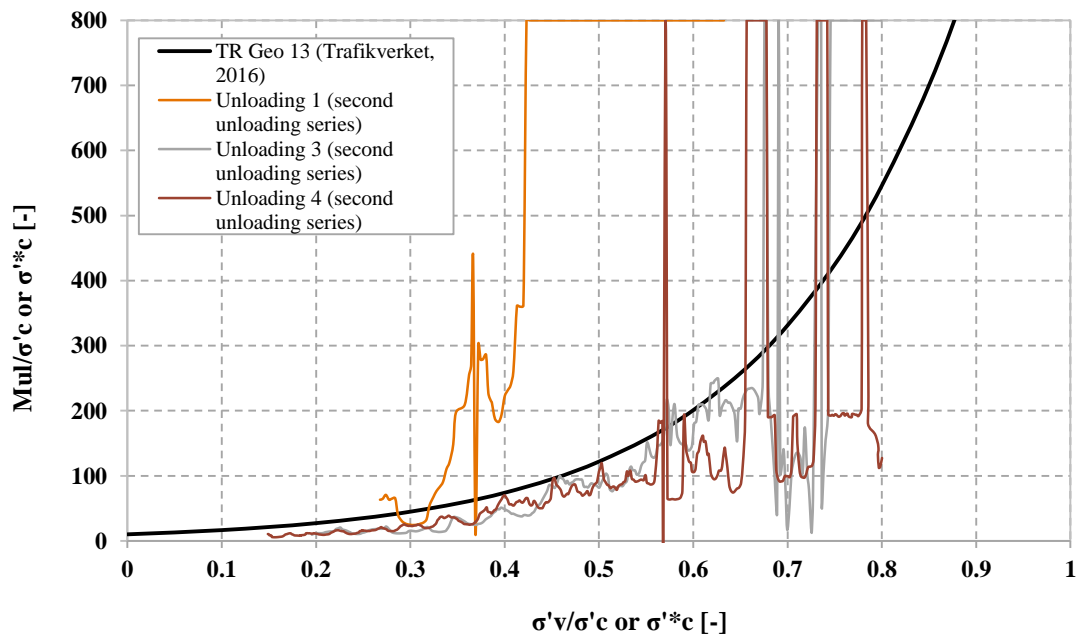


Figure 5.7: Unloading modulus for level 17 m, second unloading series.

The values obtained for all the levels were very similar for both unloading test series. That no storage effect was observed can be due to the fact that the unloading modulus is not affected to any significant extent by the effects, that were described in Section 2.6.1, that can occur in the soil samples during storage. Another explanation can be that the samples obtained for this study had a tendency to swell rapidly, see Figure 5.8, and before the first series of unloading test was initiated, negative excess pore pressures in the samples may have dissipated resulting in swelling. In order to prevent swelling, the samples would have to be stored in a way that prevented swelling before the tests could be initiated or the samples would have to be obtained at separate occasions followed by immediate mounting of the laboratory tests. If the samples used for the compressional CRS-tests had been obtained at one occasion and the samples used for the unloading tests had been obtained at a later occasion, when the stress history, and hence the “set-up” for the unloading tests was already established, the unloading test could have been initiated immediately after sample retrieval without first performing standard CRS-tests. The initial swelling of the samples, which occurred before the tests were initiated, could then perhaps have been avoided. Also, it would be possible to place steel plates and clamps at the ends of the sampling tubes thus preventing the samples to swell during storage. However, since the aim of the thesis was to investigate storage time effect for normal storage procedures, this was not done.



*Figure 5.8 Swelling of the sample collected from 25 m, 8 days after sampling. Similar on the other end.*

## **5.2.2 UNLOADING MODULUS OBTAINED WITH MODIFIED CRS COMPARED TO UNLOADING MODULUS OBTAINED FROM IL**

The unloading modulus obtained from the modified CRS-tests and the unloading modulus obtained from the IL-tests are presented together in Figure 5.3 and Figure 5.4. The unloading modulus for IL-tests is calculated using the difference between two consecutive load stages and the corresponding strain increment. The unloading modulus for IL-tests is hence a secant modulus.

The tendency that can be interpreted from Figure 5.3 and Figure 5.4 is that the modified CRS-test provides similar results as the IL-test when studying the unloading behaviour of soft clay. However, both test methods provide lower unloading modulus than the relationship in TR Geo (Trafikverket, 2016). That laboratory tests provides lower unloading modulus than the relationships established based on field measurements were discussed in the previous section.

The IL -tests performed as part of this study had a total test time of around 40 days. This was longer than required for the tests since the loads had to be applied manually and this was not feasible (with respect to weekends) to do every 24 hour. Still, this kind of test, with around 20 test stages, would ideally take a minimum of approximately 20 days to perform. This can be compared with the modified CRS-test that took around 4-5 days to perform. The modified CRS-test is also automatic so the loads do not have to be manually applied, the computer can simply be left to carry out the test. If modified CRS-tests can be used in order to obtain the unloading modulus of clay it would be beneficial, both with respect to time and in some cases, effort.

However, the computer control for the execution of the modified CRS-tests carried out in this thesis was somewhat unreliable. The problems encountered during execution of the modified CRS-test were:

- The computer acquisition of measurement values from the apparatus failed at several occasions.
- Some of the unloading sequences were not completed (see Appendix E, Figure E.5 - Figure E6). The reason for this has not been determined.
- The strain rate and unloading rate were specified but the computer control system had problems keeping these rates constant (see Appendix E, Figure E.13 – Figure E.24).
- Although the apparatus was specified to do relaxation stops (stages with specified zero strain rate) some strain was recorded during these stages (see Appendix E, Figure E.1- Figure E.6).
- The displacement transducer did not record the small strain increments with sufficient accuracy.
- Negative pore pressures could not be measured in one of the CRS machines.

### 5.3 NUMERICAL MODELLING

The main focus for this master's thesis was to perform a laboratory study in order to investigate the unloading modulus of soft clay. The analysis of the results, using the software PLAXIS 2D and the material model *Soft soil creep*, was secondary and is hence not as extensively described as the other sections. The reason for performing this analysis was in order to investigate the applicability of the obtained data for geotechnical design.

The attempt to find a set of parameters that describes the soils behaviour was divided into three sub-problems:

- Compression during loading
- Unloading below the in-situ pre-consolidation pressure
- Unloading above the in-situ pre-consolidation pressure

Initially it had to be established if the soil at the three sampling levels could be assumed to be of the same type. If this assumption was satisfied, the three sampling levels could be modelled using one set of parameters for  $\kappa^*$ ,  $\lambda^*$  and  $\mu^*$  in the *Soft soil creep* model. The assumption

was examined by plotting the result of the CRS-tests for the three sampling levels in the same graphs with the stress normalised with respect to either  $\sigma'_c$  or  $\sigma'_c^*$ . This was performed for the standard CRS-tests as well as for the unloading sequences in the modified CRS-test, which can be seen in Appendix I, Figure I.1 and Figure I.3. For the standard tests, the initial sample disturbance effect that was recorded on level 20 m and level 25 m was removed. The unloading sequences in Figure I.2 and Figure I.3 are plotted to start at the same strain in order to be comparable. The conclusion from the figures is that the soil at the three sampling levels is relatively similar. For the standard CRS-tests the most reliability is entrusted in level 17 m since the other two levels showed a CRS curve that is uncharacteristic of CRS-tests with relatively large sample disturbance effect. The variation of the unloading sequences are considered to be within the natural variation. Based on these figures, as well as the routine tests, which showed similar values for the studied parameters for the three levels, the soil at the three levels are considered to be of the same type and should hence be able to be described using the same parameter set-up.

Initially a set of parameters that described the behaviour of the soil during compression was determined using the “Optimize” function in the PLAXIS 2D soil test facility. Afterwards it was investigated how well this parameter set-up could describe the unloading sequences.

The following was established for the performed study:

- The material model used for the study was *Soft soil creep* in the FEM software PLAXIS version 2017.1.
- Only the data from the first test series of modified CRS-tests with were studied.
- An initial stress (due to for example excess negative pore water pressure) of -5 kPa was added for the compression test. This suction decreased the initial sample disturbance effect and hence created an optimisation more similar to the performed CRS-test.
- The optimisation of the parameters were limited by upper and lower limits for each parameter, corresponding to empirical values of soils from Gothenburg. The limits for the parameters were:

$$\lambda^* = 0.1 - 0.3$$

$$\mu^* = 0.0033 - 0.01$$

$$\kappa^* = 0.01 - 0.03$$

- The scope was only to try to match the test using the stiffness parameters described above and other parameters was set by default during the optimisation.
- A friction angle of  $30^\circ$  was assumed.
- The curve 17 m was chosen to represents all compression curves since this was the curve considered to be the one with least initial sample disturbance effects out of the three.
- Unloading sequence number 2 for 20 m was chosen to represents all unloading sequences below the in-situ pre-consolidation pressure and unloading sequence number 3 for 20 m was chosen to represents all unloading sequences above the in-situ

pre-consolidation pressure. The reason for choosing these sequences, was that the unloading sequence below the in-situ pre-consolidation pressure for level 17 was unsuccessful and could hence not be used.

The result from the conducted optimisation for the standard CRS-tests can be seen in Figure 5.9. The parameters describing this curve can be seen in Table 5.1.

## CRS curves

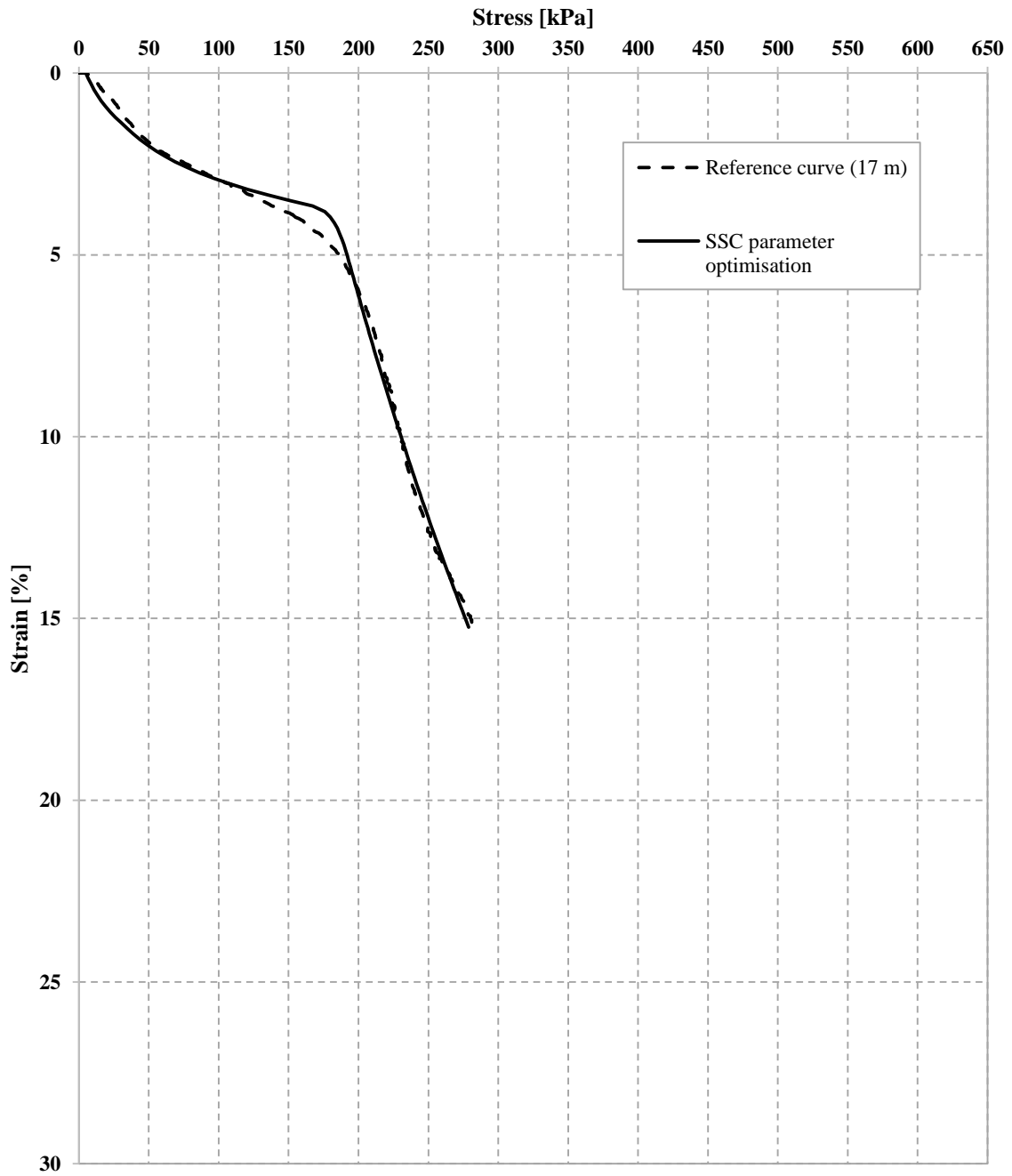


Figure 5.9: Parameter optimisation by SSC for CRS curve, level 17 m.

Table 5.1: Parameters obtained from the optimisation using SSC.

Parameter	Value
$\lambda^*$	0.28
$\mu^*$	0.0039
$\kappa^*$	0.013



How well these parameters describe the behaviour of soil during unloading in *Soft soil creep* can be seen in Figure 5.10 and Figure 5.11. It can be concluded that the magnitude of the expansion of the clay is under-estimated but if these parameters are sufficient in order to evaluate the behaviour of the soil during unloading or not should be determined by the geotechnical engineer and the design situation at hand.

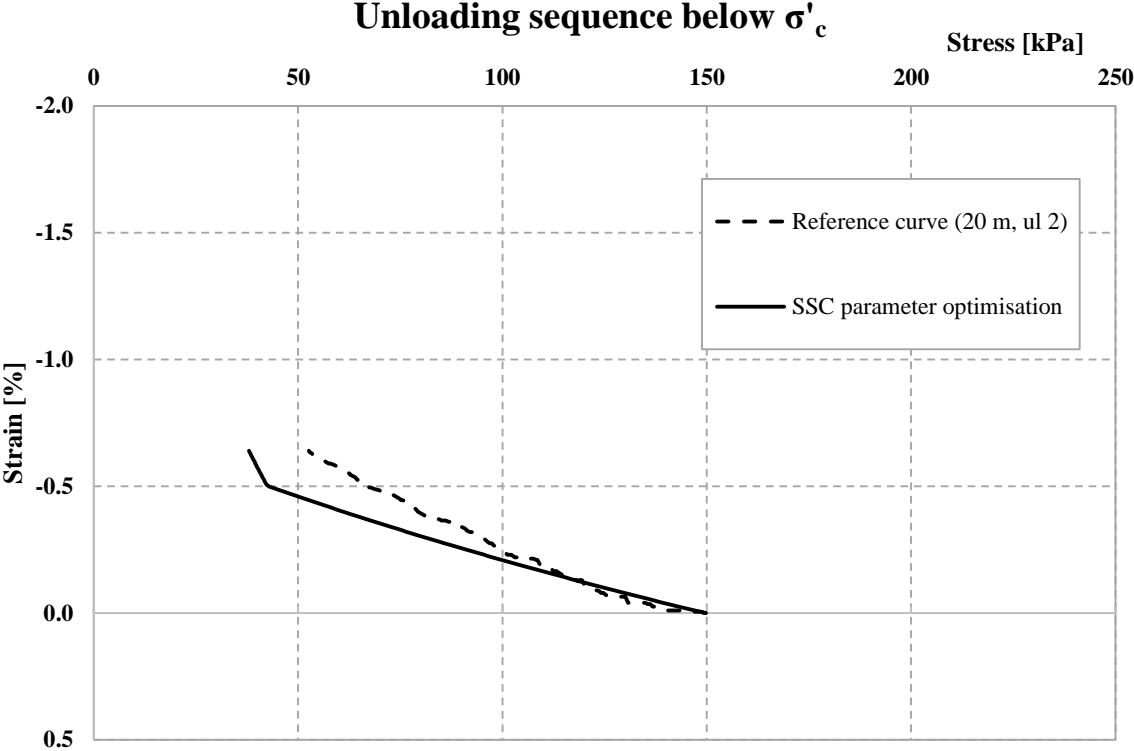


Figure 5.10: Consistency between the reference curve for unloading sequences below the pre-consolidation pressure and the curve developed by SSC parameter optimisation for compression.

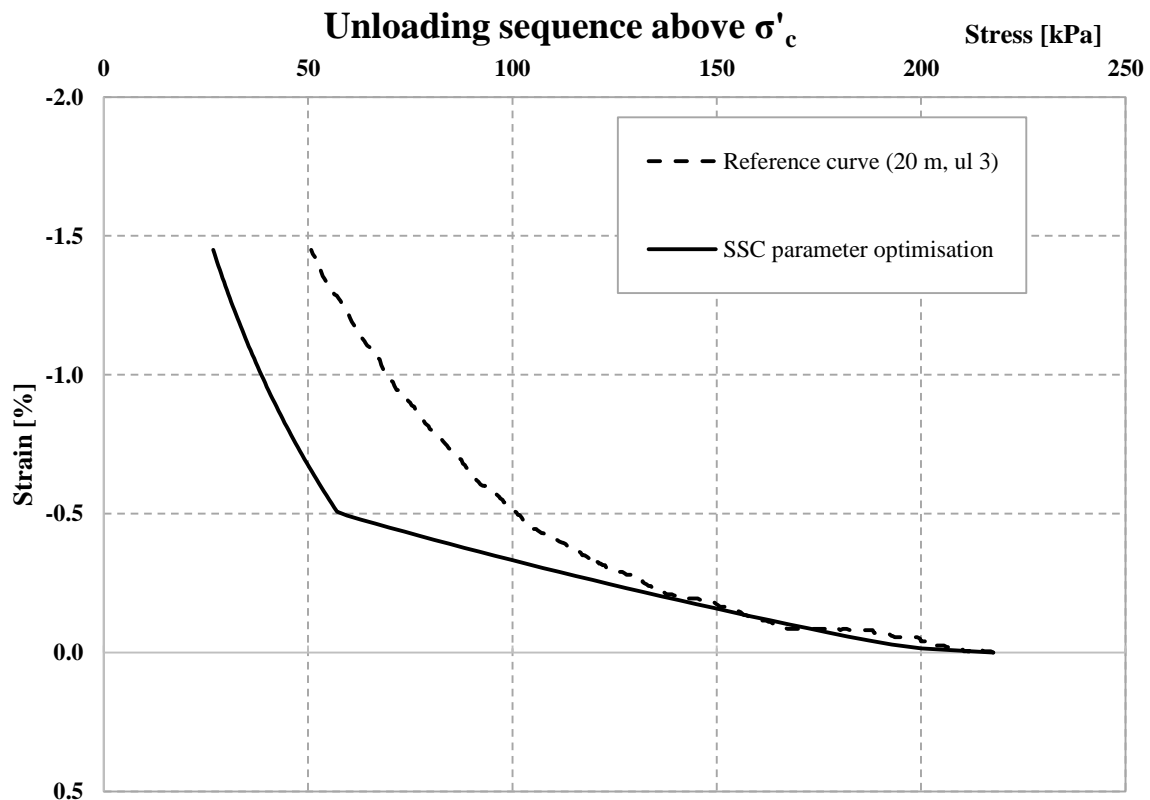


Figure 5.11: Consistency between the reference curve for unloading sequences above the pre-consolidation pressure and the curve developed by SSC parameter optimisation for compression.

## 5.4 REFLECTIONS REGARDING THE LABORATORY TESTS

When performing laboratory tests many factors can influence the results. Factors that may have been of importance for this study are listed below.

- Due to the fact that standard CRS-test had to be conducted for the three levels, in order to obtain the stress history of the sample, the samples had to be stored for some time before the first test series of unloading tests could be initiated. For level 17 m the first series of unloading tests was initiated 5 days after sample retrieval and for level 20 m and 25 m the first unloading test series was initiated 12 days after sample retrieval. Preferably the first series unloading tests would have been initiated sooner after sample retrieval but this was not feasible.
- Due to only having 2 CRS machines but 3 sample levels, the test for level 17 m was performed sooner than the tests for level 20 m and level 25 m. The samples for level 20 m and 25 m hence swelled more during the storage time before the unloading tests could be initiated.
- The laboratory computer, that collected the data from the performed CRS-test, was unexplainably re-started at several occasions while the tests were running. This resulted in loss of data and those tests had to be discarded and be re-started with a new piece of sample. Since this occurred twice, both for the first test round on 17 m and the

first test round on 20 m and 25 m, the tests were delayed. This was the reason why the modified CRS-tests and the IL-test were not started the same date.

- As a result of the complications with the computer, some of the tests had to be re-started with new piece of samples. This resulted in that more clay than anticipated was used for the first series of unloading tests. Enough clay was hence lacking in the middle tube in order to perform the second series of unloading tests for level 20 m and level 25 m. Clay from the upper part of the lower tube was instead used for the second unloading series for those levels. Since both the middle tube and the upper part of the lower tube are considered to be undisturbed this should not affect the result significantly but should still be noted.
- The evaluated sample quality was poorer than desirable, which has been discussed in Section 5.1.
- The disturbance at the beginning of many of the CRS-tests can be due to many reasons. The force transducer might not completely have touched the small ball that works as a power distributor, the permeable stone might not be completely pressed down and touching the clay, the sample might not have a completely flat surface or the shells found in some of the samples might have caused this effect. This sample disturbance effect often occurs when performing CRS-test but the relatively large disturbance effect on the performed tests for this study can also be due to the lack of experience of the operator.
- As it has been discussed, one of the CRS machines, which were used to perform both unloading tests for 25 m did not register negative pore water pressure. This was noticed after the first loading-unloading test. In order to obtain comparable results for the two tests at 25 m, the same machine was used for the second loading-unloading test as well. The fact that the machine did not register negative pore water pressure affects the results for 25 m since the effective stress is under estimated. Since both loading-unloading tests for 25 m were performed using the same machine the results are comparable from the storage time aspect.
- The temperature in the laboratory room at Chalmers University of Technology during the IL-tests varied between 5 to 15°C due to on-going parallel research at Chalmers. This may have affected the results, potentially causing a lower stiffness compared to a constant temperature of ca 7°C.
- The laboratory tests were performed almost entirely by the author, who has no previous experience in conducting these kind of tests.



## 6 CONCLUSIONS AND PROPOSED FURTHER STUDIES

In this chapter the conclusions based on the aims of the thesis will be presented. Suggestions for further studies are also included.

### 6.1 CONCLUSIONS

From the laboratory tests conducted in this study it can be concluded that the modified CRS-test and the IL-tests show the same trend regarding the unloading modulus of soft clay. To use the modified CRS is hence showing to be a possible method to, by a computer controlled and automated test, obtain the unloading behaviour of clay. The unloading in the modified CRS-tests was carried out using a constant rate of (un)loading of -0,3 kPa/min. Since the results of the evaluated unloading modulus seems to correspond approximately to the IL-test results the unloading rate seems to have been reasonable. The advantage of using a constant rate of stress decrease during unloading is that the load cap always will keep in contact with the sample. If the unloading is instead regulated using a constant rate of strain, the rate might be too fast and the load cell could hence loose contact with the sample for high unloading stiffnesses.

According to Persson (2004), the unloading moduli obtained from IL-tests did not differ depending on if the in-situ pre-consolidation pressure was exceeded or not before unloading stages were initiated. The contrary was found for this study. A trend for the unloading modulus to be larger for unloading sequences starting from stress levels below the in-situ pre-consolidation pressure than above was distinguished. This is important to note since most field situations in engineering practice, such as excavations, starts unloading from in-situ effective stress that are below the pre-consolidation pressure ( $OCR > 1$ ). Focus in laboratory tests analysing the unloading modulus should hence be to study unloading behaviour starting from a stress level similar to the in-situ soil conditions.

In this study no tendency of the unloading modulus to be affected by the storage time was found. The result might however have been affected by the initial swelling of the clay, which occurred before the first test series was initiated. If the initial unloading series was initiated closer in time to sample retrieval another result might have been obtained. The storage time for this study was also short, merely 8 weeks, since the time for this master's thesis was limited. This might also have affected the obtained result regarding storage time effect.

When using the parameter set-up in the material model *Soft soil creep* that was obtained for compression in order to describe the behaviour of clay during unloading the magnitude of the expansion of the clay was underestimated.

### 6.2 PROPOSED FURTHER STUDIES

Below are listed some future research studies that could be of interest in order to develop a deeper understanding of the unloading modulus in soft clay:

- Perform laboratory tests examining the storage effect of the unloading modulus for clay with already known stress history ( $OCR$ ) in order to initiate the unloading tests

immediately after sample retrieval. By using this approach, the swelling of the samples before initiating the unloading tests could be avoided.

- Conduct parallel IL-tests and modified CRS-tests in order to determine with certainty if the modified CRS-test can be used instead of the IL-test to determine the unloading modulus of soft clay.
- Study the effect on the obtained unloading modulus by employing different unloading rates (strain- or stress rate controlled) in the modified CRS-test.
- To analyse the unloading behaviour of soft clay starting from a stress level similar to the in-situ soil conditions triaxial testing is recommended. In the triaxial test the sample can be consolidated to in-situ vertical and horizontal stress and from there on unloading can be performed.

## 7 REFERENCES

- Bjerrum, L. (1973). *Problems of soil mechanics and construction on soft clays and structurally unstable soils (collapsible, expansive and others)*. State-of-the-Art report Session 4, pp. 111-159.
- Engdahl, M., & Påsse, T. (2014). *Geologisk beskrivning av Sävveåns dalgång (SGU-rapport 2014:37)*. Sveriges Geologiska Undersökningar.
- Google. (2018). *GoogleMaps*.  
<https://www.google.se/maps/place/G%C3%B6ta%C3%A4lvbron,+G%C3%B6teborg/@57.7320484,11.9237733,6716m/data=!3m1!1e3!4m5!3m4!1s0x464ff49e2c>  
[Accessed: 2018-05-20]
- Göteborgs Stad, Trafikkontoret. (2016). *Hisingsbron Murundersökningsrapport Geoteknik (MUR/GEO) Norra Älvstranden (Dnr:625/10)*. Göteborg: Göteborgs Stad, Trafikkontoret.
- Hansbo, S. (1975). *Jordmateriallära*. Stockholm: Almqvist & Wiksell Förlag AB.
- Henriksson, M., & Carlsten, P. (1994). *Lagringstidens inverkan på prover tagna med standardprovtagare*. Statens Geotekniska Insitut. (Varia 430)
- Hvorslev, M. J. (1949). *Subsurface exploration and sampling of soils for civil engineering purposes*. The waterways experiment station corps of engineering, U.S. Army. Vicksburg: Waterways experiment station.
- ISO. (2017). ISO 17892-5:2017. *Geotechnical investigation and testing - Laboratory testing of soil- Part 5: Incremental loading oedometer test*.
- Karlsruud, K. (2012). *Prediction of load-displacement behaviour and capacity of axially loaded piles in clay based on analyses and interpretation of pile load test results*. Thesis for the degree of Doctor of Philosophy. Trondheim: Norwegian University of Science and Technology.
- Knappett, J., & Craig, R. (2012). *Craig's Soil Mechanics*. Eighth edition. New York: Spoon Press.
- Larsson, R. (1986). *Consolidation of soft soils*. Linköping: Statens Geotekniska Insitut, Linköping. (Report 29)
- Larsson, R. (2008). *Jordens egenskaper*. Fifth edition- rev. Linköping: Statens Geotekniska Insitut.
- Larsson, R., Sällfors, G., Bengtsson, P.-E., Alén, C., Bergdahl, U., & Eriksson, L. (2007). *Skjuvhållfasthet - utvärdering i kohesionsjord*. Second edition -rev. Linköping: Statens Geotekniska Institut.

- Lessard, G., & Mitchell, J. K. (1985). The causes and effects of aging in quick clay. *Canadian Geotechnical Journal* Vol. 22, pp. 335-346.
- Muir Wood, D. (1990). *Soil behaviour and critical state soil mechanics*. New York: Cambridge University Press.
- NIFS. (2014). *Effect of storage time on sample quality*. Norges vassdrags- og energidirektorat, Statens vegvesen, Jernbaneverket. (Rapport 68/2014).
- Ottosen, N., & Petersson, H. (1992). *Introduction to the Finite Element Method*. Harlow, England : Pearson Education Limited.
- Persson, J. (2004). *The Unloading Modulus of Soft Clay: A field and Laboratory Study*. Licentiate thesis. Göteborg: Chalmers University of Technology.
- Persson, J. (2007). *Hydrogeological Methods in Geotechnical Engineering: Applied to settlement caused by underground construction*. Thesis for the degree of Doctor of Philosophy. Göteborg: Chalmers University of Technology.
- PLAXIS. (2016). *PLAXIS: Material Models Manual*. Delft, The Neatherlands: PLAXIS.
- Rabbås Holsdal, I. (2012). *Prøveforstyrrelser ved bruk av NGI 54 - en studie av prosedyreeffekter*. Norges teknisk-naturvitenskapelige universitet: Institutt for bygg, anlegg og transport.
- Samuelsson, L. (1997). Göteborgstraktens berg och jord - En översikt. In *Göteborgs Geotekniska Historia - Några sonderingar*. Uddevalla: MediaPrint, Uddevalla, pp. 17-24.
- SIS (1990). Svensk Standard SS 02 71 20. *Geotechnical tests - Cone liquid limit*. Stockholm: SIS.
- SIS (1991a). Svensk Standard SS 02 71 26. *Geotechnical tests- Compression properties- Oedometer test, CRS test - cohesive soil*. Stockholm: SIS.
- SIS (1991b). Svensk Standard SS 02 71 25. *Geotechnical tests - Shear strength- Fall-cone test- Cohesive soil*. Stockholm: SIS.
- Statens Geotekniska Institut. *Jordens hållfasthet* . Uppdated 2017-10-24.  
<http://www.swedgeo.se/sv/kunskapscentrum/om-geoteknik-och-miljogeoteknik/geoteknik-och-markmiljo/jordmateriallara/skjuvhallfasthet/>. [Accessed 2017-01-25]
- Sveriges Geotekniska Förening. (2009). *Metodbeskrivning för provtagning med standard kolvprovtagare: Ostörd provtagning i finkornig jord*. Linköping: Sveriges Geotekniska Förening. (Report 1:2009).



- Sveriges Geotekniska Förening. (2013). *Geoteknisk fälthandbok*. First edition. Göteborg: Sveriges Geotekniska Förening. (SGF Rapport 1:2013)
- Sveriges Geotekniska Förening. (2016). *Jordarters indelning och benämning*. Luleå: Sveriges Geotekniska Förening. (Rapport 1:2016).
- Sveriges Geotekniska Förening. (2017). *Metodik för bestämning av skjuvhållfasthet i lera: En vägledning*. Linköping: Sveriges Geotekniska Förening. (Rapport 1:2017).
- Swedish Standards Institute. (2002). SS-EN ISO 14688-1. *Geotechnical investigation and testing- Identification and classification of soil- Part 1: Identification and description (ISO 14688-1:2002)*. First edition. Stockholm: SIS Förlag AB.
- Swedish Standards Institute. (2006 ). SS-EN ISO 22475-1:2006. *Geotechnical investigation and testing- Sampling methods and groundwater measurements- Part 1: Technical principles for execution (ISO 22475-1:2006)*. First edition, corrected April 2014. Stockholm: SIS Förlag AB.
- Swedish Standards Institute. (2008a). Teknisk specifikation SIS-CEN ISO/TS 17892-6:2007. *Geotechnical investigation and testing - Laboratory testing of soil - Part 6: Fall cone test (ISO/TS 17892-6:2004)*. First edition. Stockholm: SIS Förlag AB.
- Swedish Standards Institute. (2008b). SIS-CEN ISO/TS 17892-12:2007. *Geotechnical investigation and testing - Laboratory testing of soils - Part 12: Determination of Atterberg limits (ISO/TS 17892-12:2004)*. First edition. Stockholm: SIS Förlag AB.
- Swedish Standards Institute. (2010). SS-EN 1997-2:2007. *Eurocode 7: Geotechnical design- Part 2: Ground investigation and testing (SS-EN 1997-2:2007)*. First edition. Stockholm: SIS Förlag AB.
- Swedish Standards Institute. (2014a). SS-EN 17892-2:2014. *Geotechnical investigation and testing - Laboratory testing of soil - Part 2: Determination of bulk density (ISO 17892-2:2014)*. First edition. Stockholm: SIS Förlag AB.
- Swedish Standards Institute (2014b). SS-EN ISO 17892-1:2014. *Geotechnical investigation and testing - Laboratory testing of soil- Part 1: Determination of water content (ISO 17892-1:2014)*. First edition. Stockholm: SIS Förlag AB.
- Sällfors, G. (1975). *Preconsolidation pressure of soft, high-plastic clays*, Thesis for the degree of Doctor of Philosophy. Göteborg: Chalmers University of Technology.
- Sällfors, G. (2013). *Geoteknik: Jordmateriallära - Jordmekanik*. Fifth Edition. Göteborg: Cremona Förlag.
- Terzaghi, K. (1943). *Theoretical soil mechanics*. New York: John Wiley & Sons, Inc.

- Tornborg, J. (2017). *Swälltryck på grund av avlastning i lös lera: Studie av hävningsförlopp och potentiella följd effekter*. Göteborg: Skanska. (SBUF ID 13303).
- Torrance, J.K. (1976). Pore water extraction and the effect of sample storage on the pore water chemistry of Leda clay. In *Soil Specimen Preparation for Laboratory Testing*, ASTM STP 599, American Society for Testing and materials, pp. 147-157.
- Trafikverket. (2016). *Trafikverkets tekniska råd för geokonstruktioner - TR Geo 13*. Trafikverket, dokument-ID TDOK 2013:0668, version 2.0, date: 2016-02-29.
- Tudisco, E., & Dahlblom, O. (2016). *Course literature in Foundation Engineering, VGTF01*. Lund: LTH, Lund University.
- Wood, T. (2016). *On the Small Strain Stiffness of Some Scandinavian Soft Clays and Impact on Deep Excavation*. Thesis for the degree of Doctor of Philosophy. Göteborg: Chalmers University of Technology.



# APPENDIX B

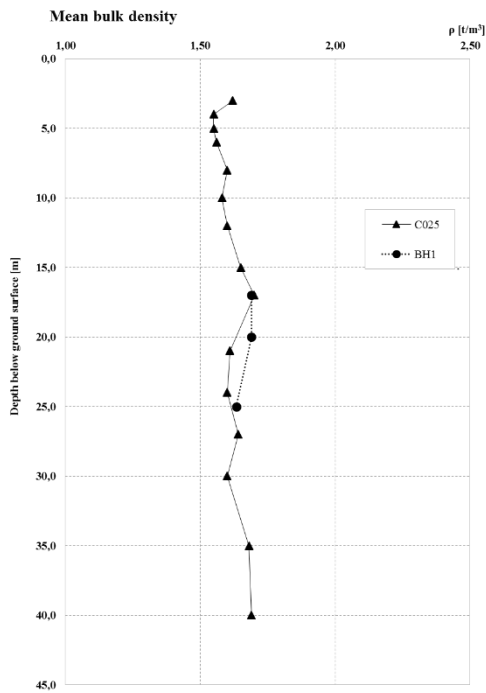


Figure B.1: Mean bulk density.

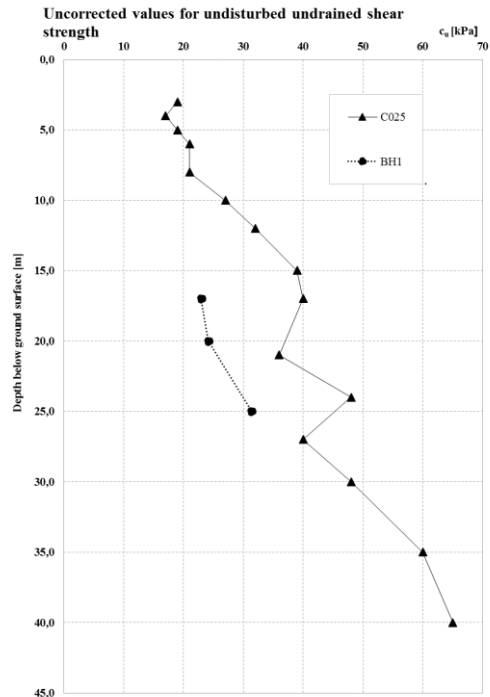


Figure B.2: Uncorrected undisturbed undrained shear strength (determined by fall cone test).

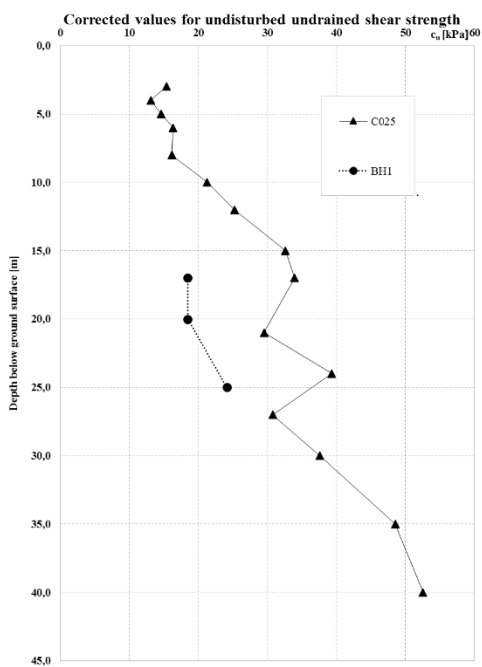


Figure B.3: Corrected undisturbed undrained shear strength (determined by fall cone test).

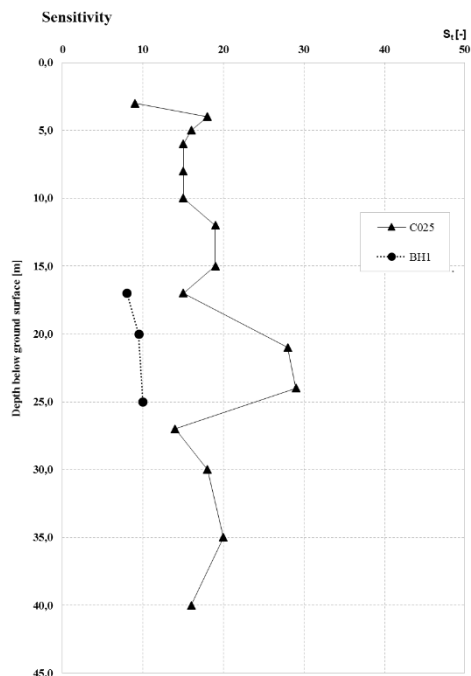


Figure B.4: Sensitivity (determined by fall cone test).

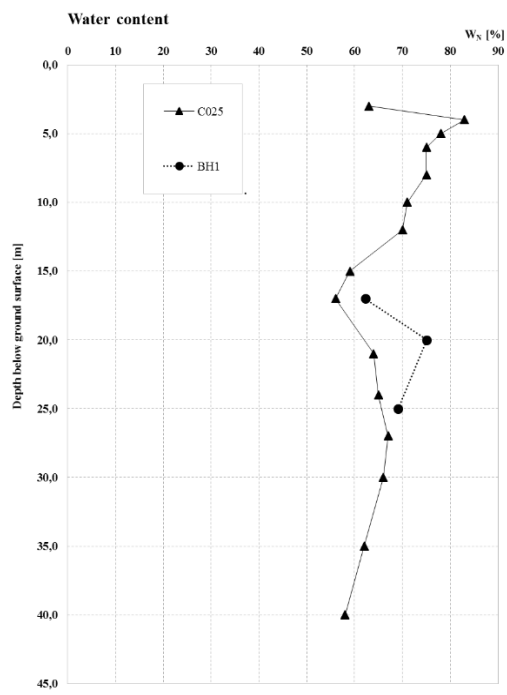


Figure B.5: Water content

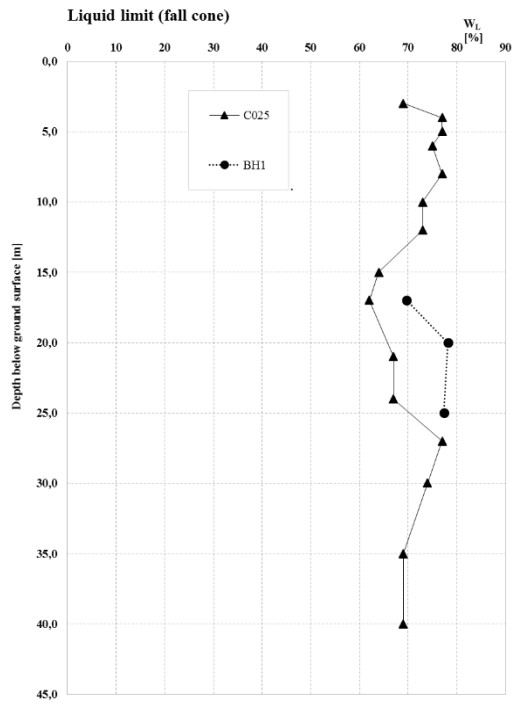


Figure B.6; Liquid limit (determined by fall cone test).

**APPENDIX C**

Conducted: 2018-02-22

**CRS 17 m**

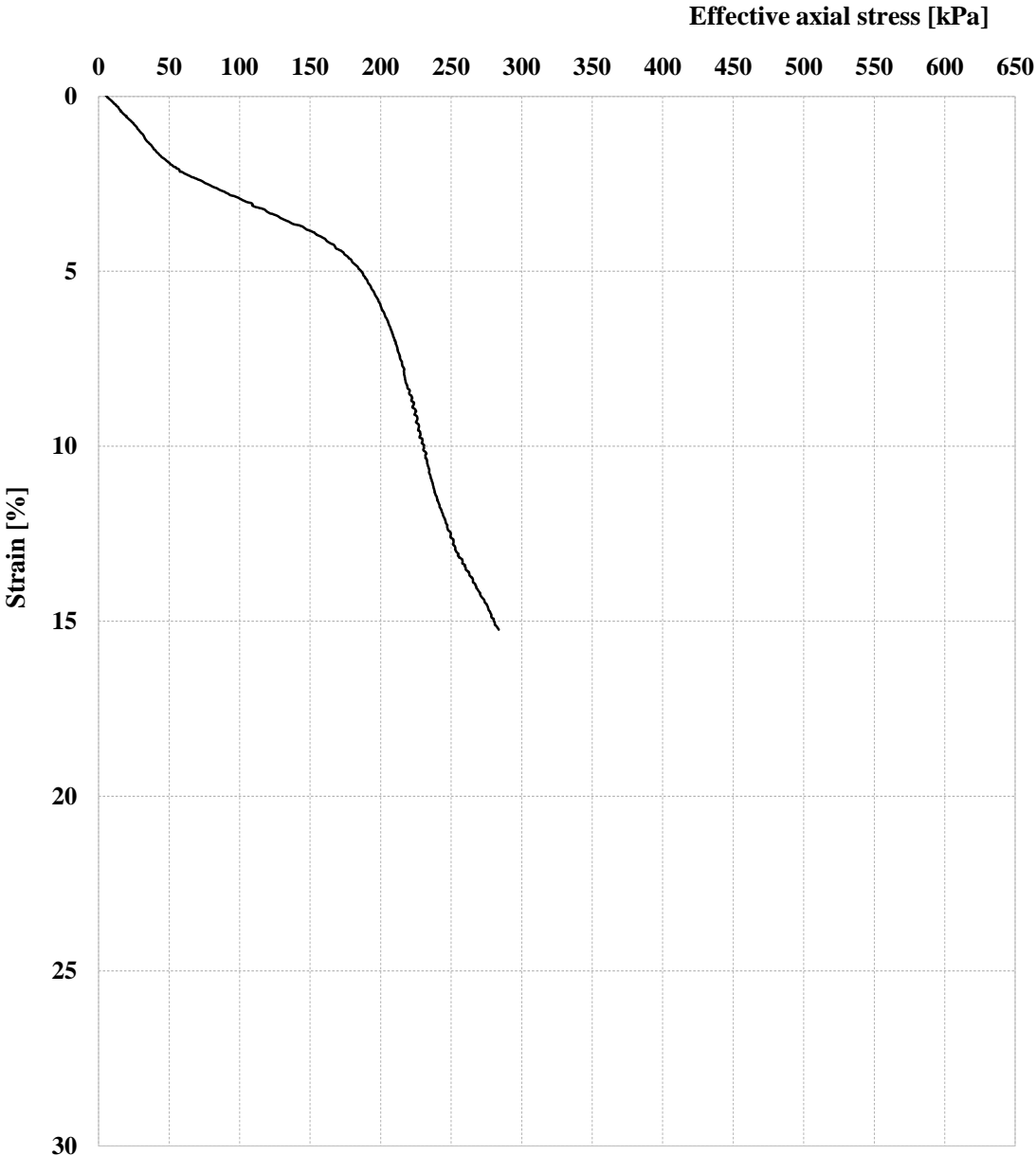


Figure C.1: Standard CRS test (0.0024 mm/min) for level 17 m.

### CRS 20 m

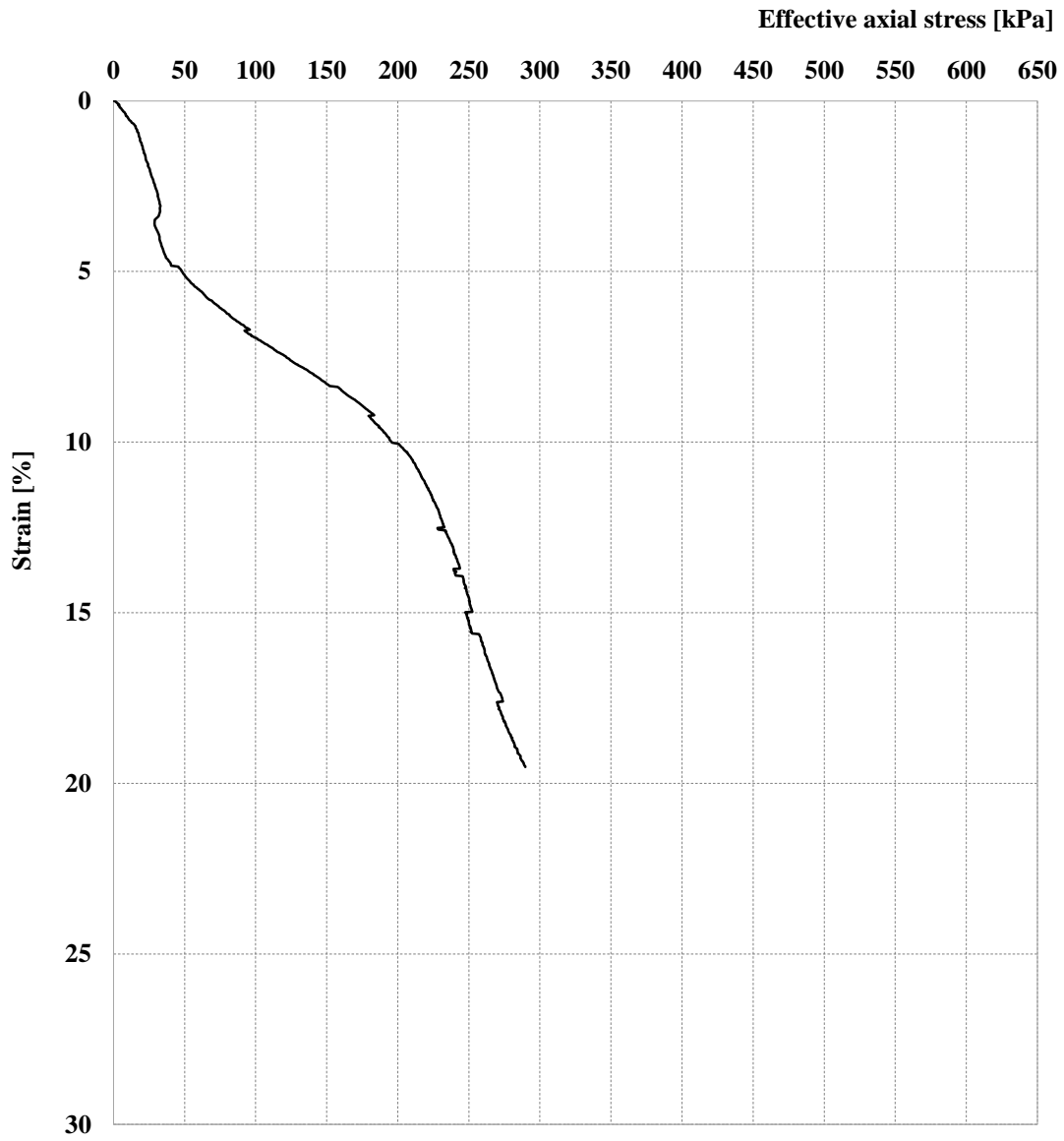


Figure C.2: Standard CRS test (0.0024 mm/min) for level 20 m.

### CRS 25 m

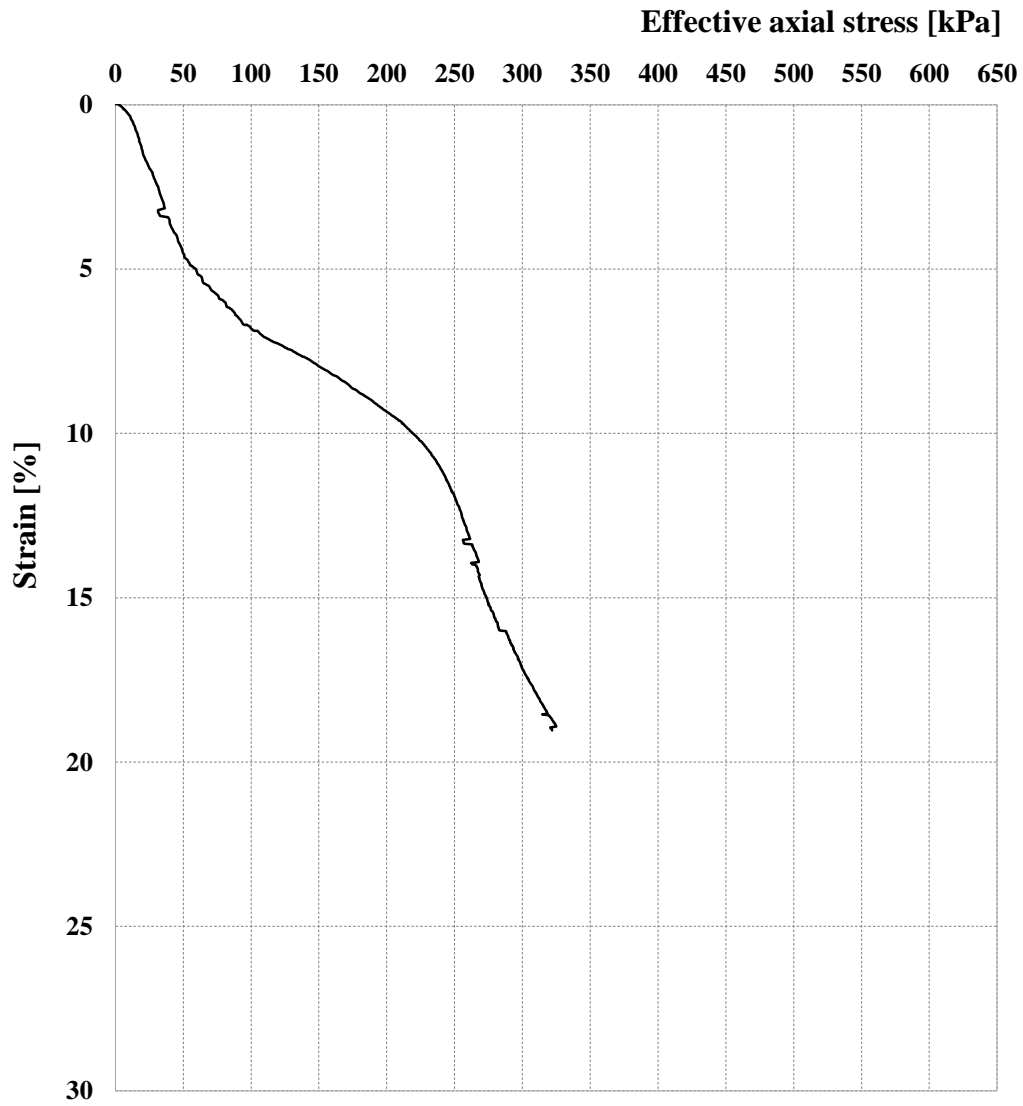


Figure C.3: Standard CRS test (0.0024 mm/min) for level 25 m.



# APPENDIX D

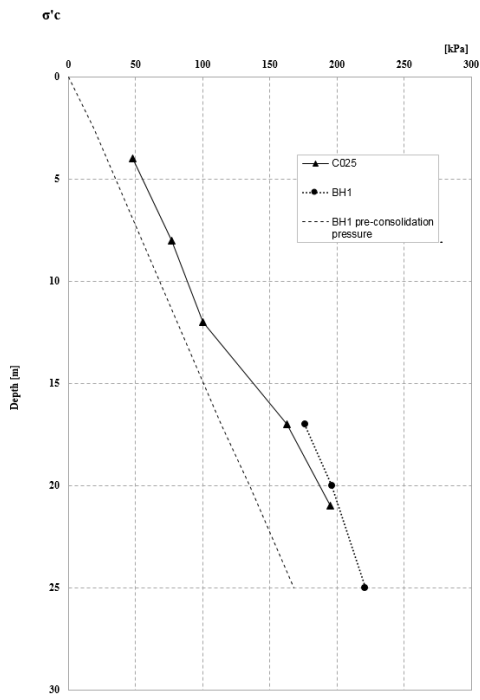


Figure D.1: Evaluated pre-consolidation pressure.

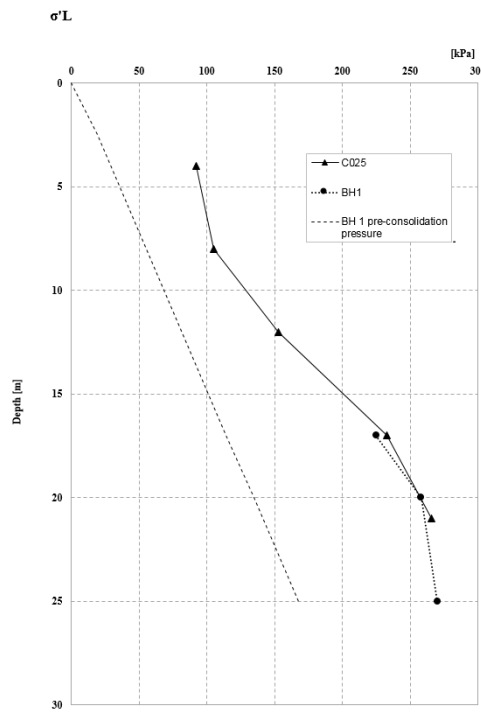


Figure D.2: Evaluated  $\sigma'_L$ .

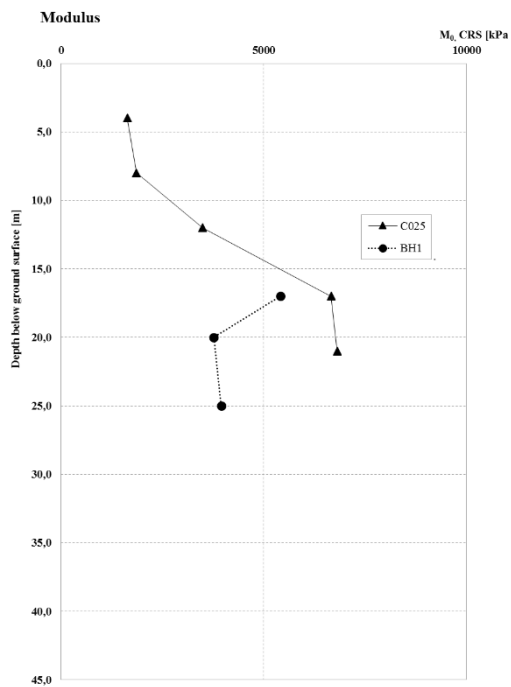


Figure D.3: Evaluated  $M_0$ .

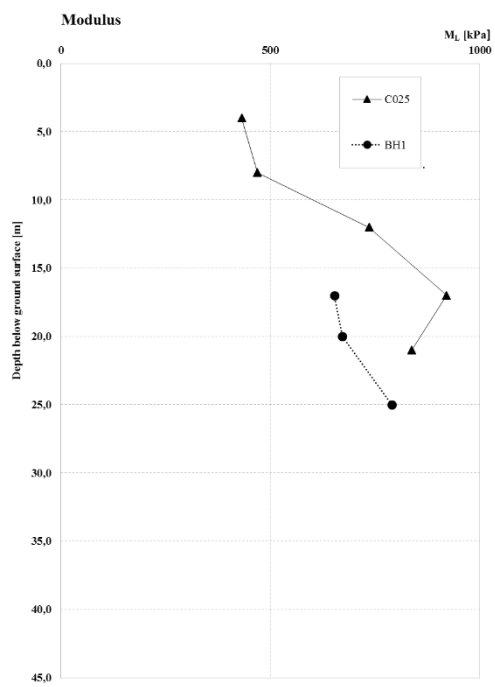


Figure D.4: Evaluated  $M_L$ .

# APPENDIX E

## CRS 17 m first unloading series

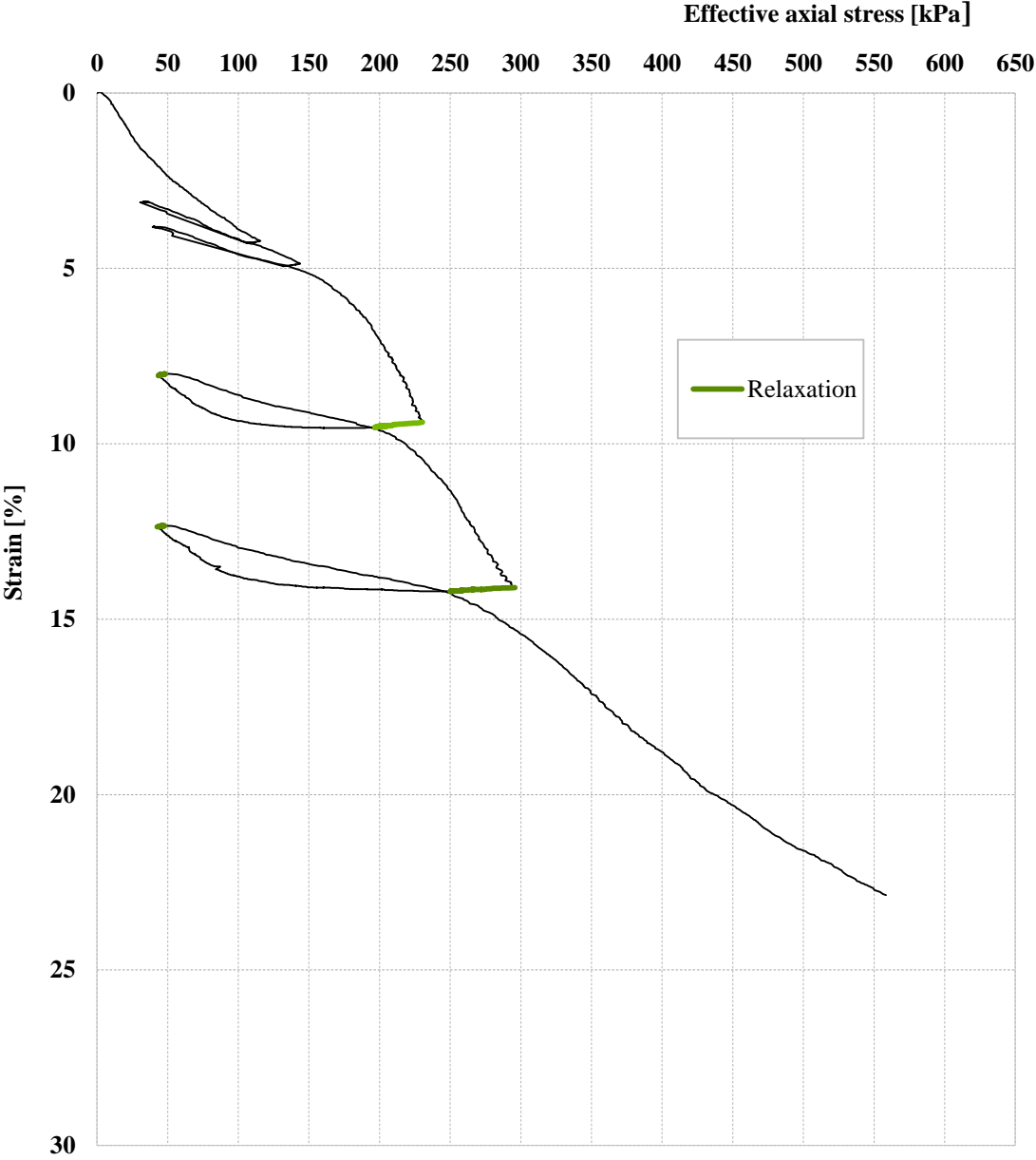


Figure E.1: First unloading series for level 17 m.

# CRS 17 m second unloading series

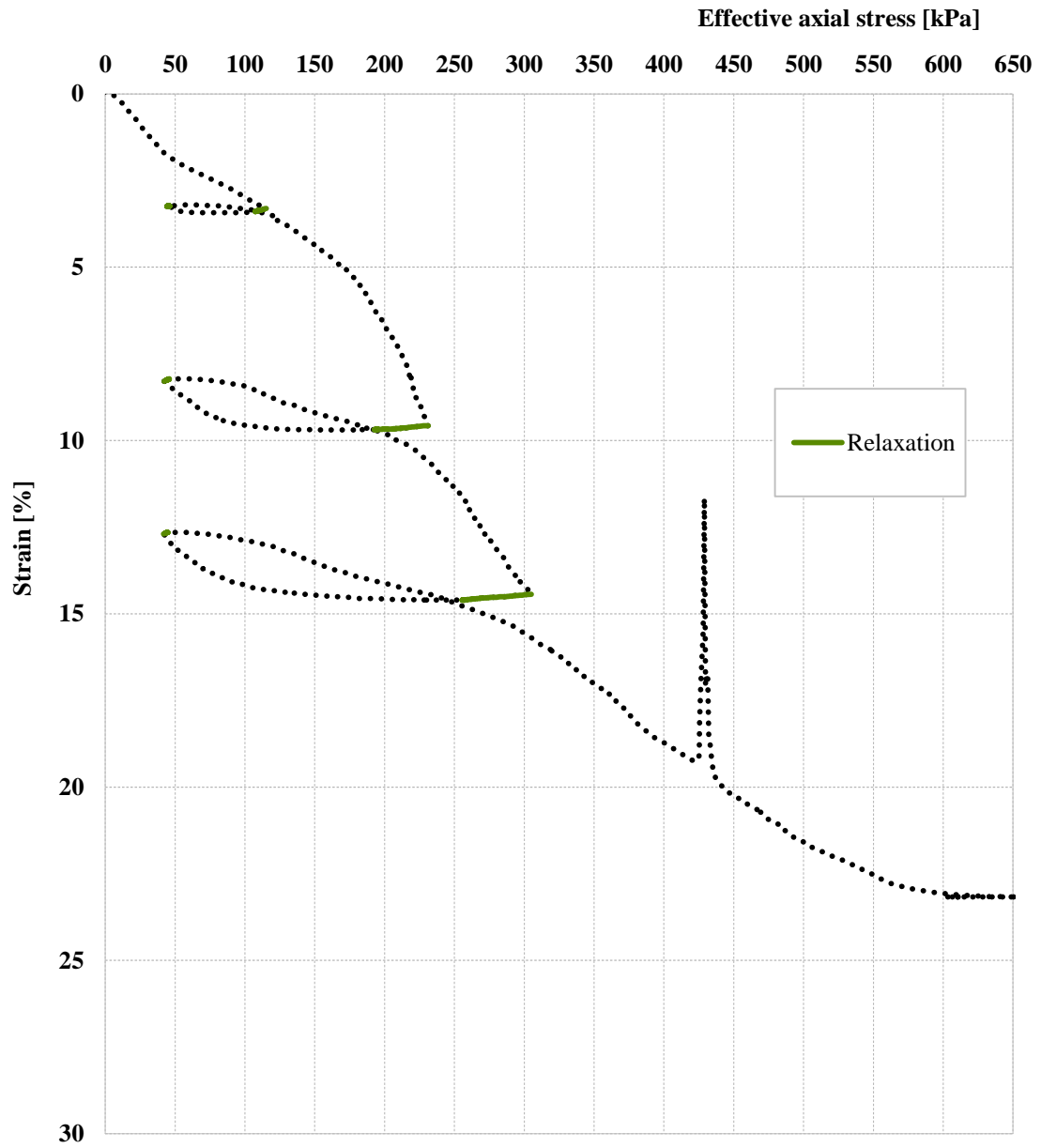


Figure E.2: Second unloading series for level 17 m.

# CRS 20 m first unloading series

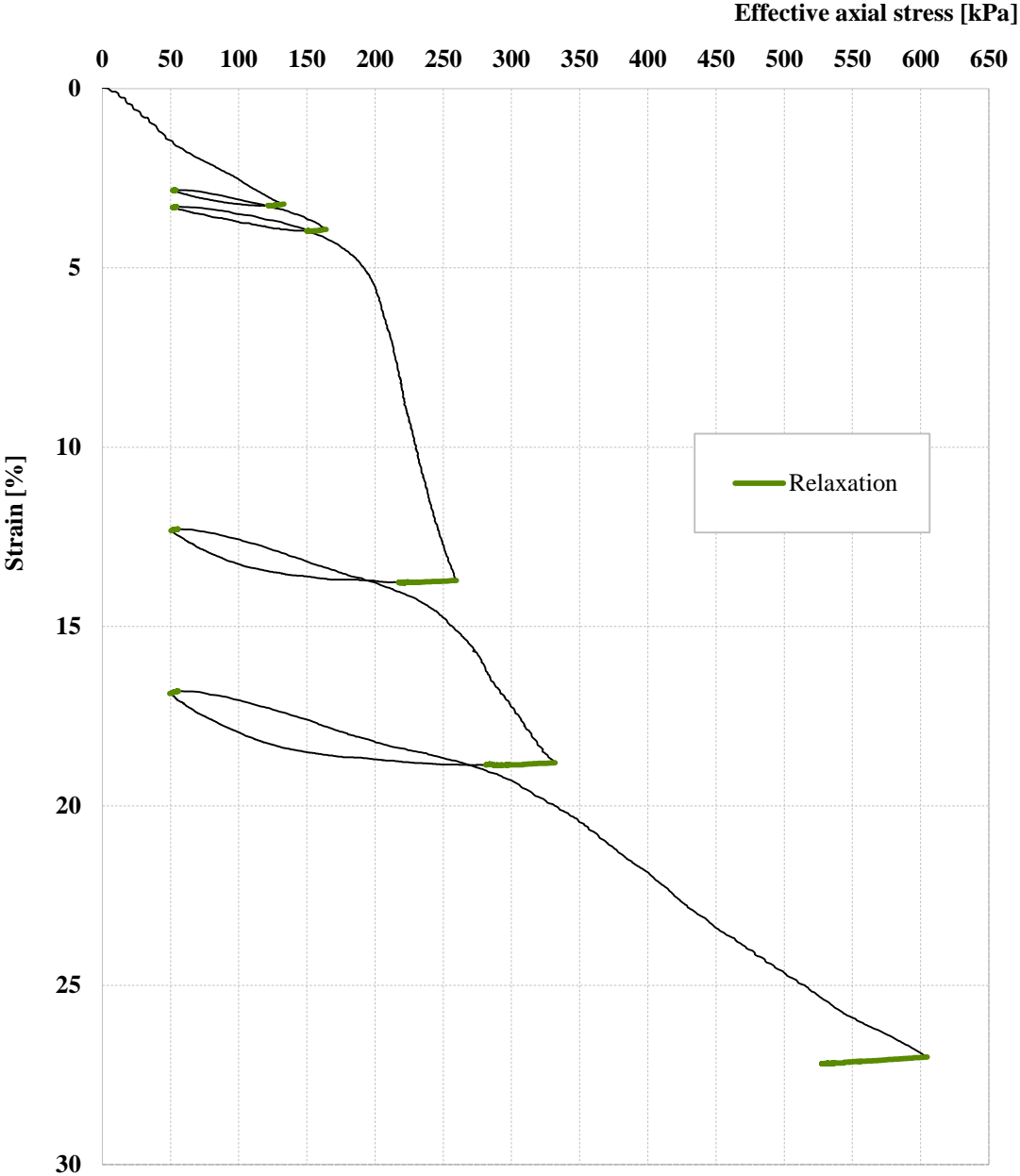


Figure E.3: First unloading series for level 20 m.

### CRS 20 m second unloading series

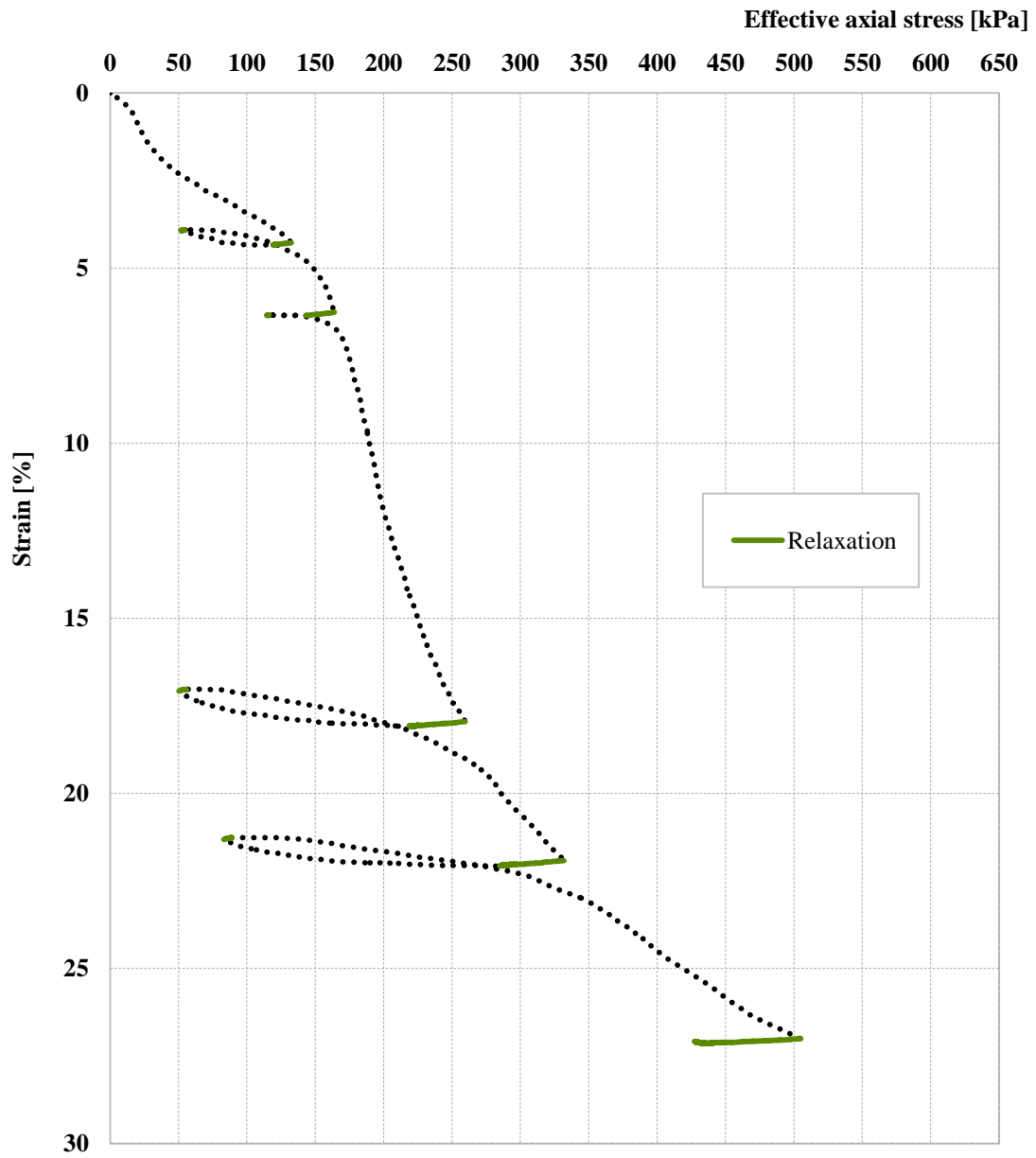


Figure E.4: Second unloading series for level 20 m.

# CRS 25 m first unloading series

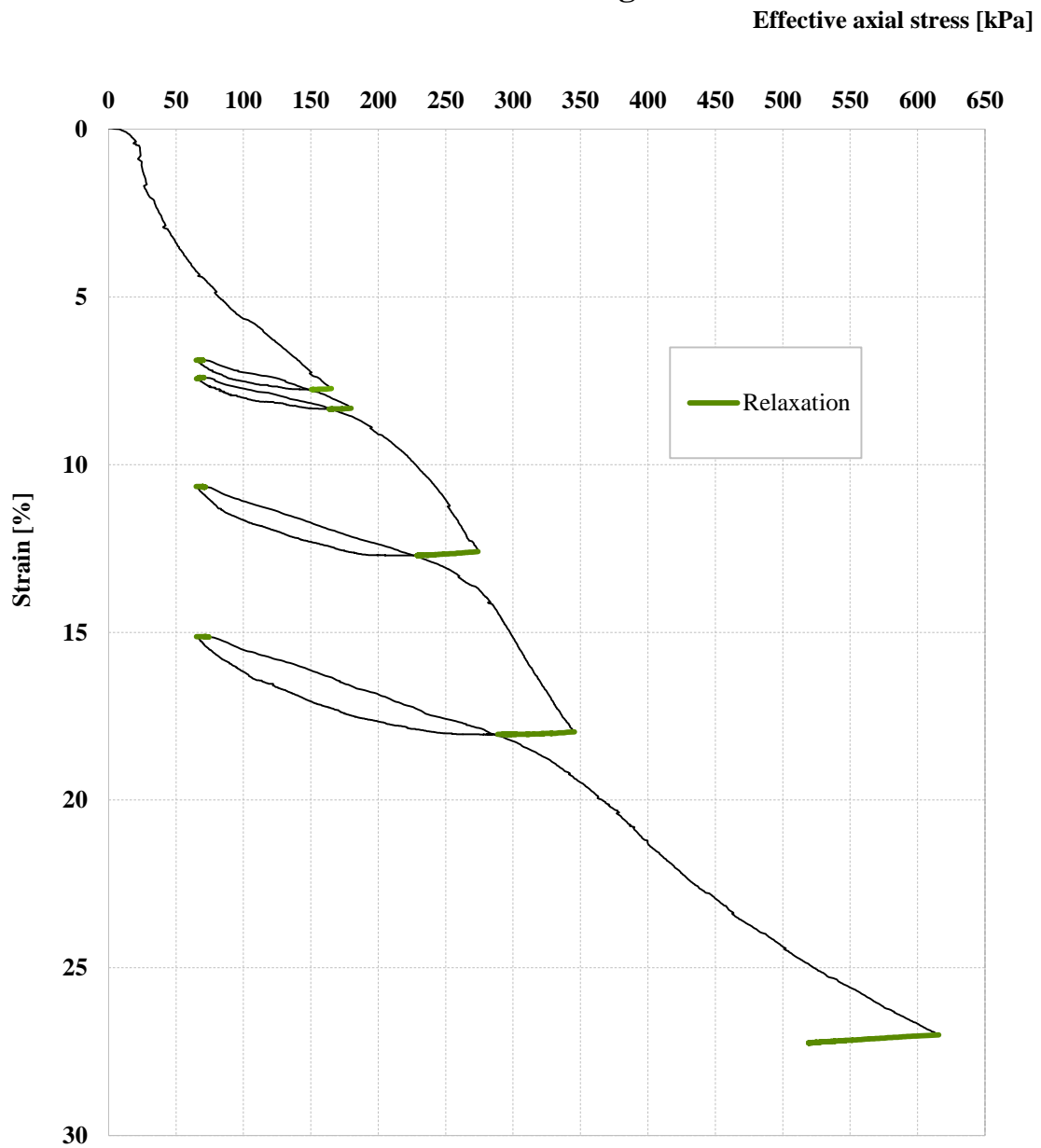


Figure E.5: First unloading series for level 25 m.

# CRS 25 m second unloading series

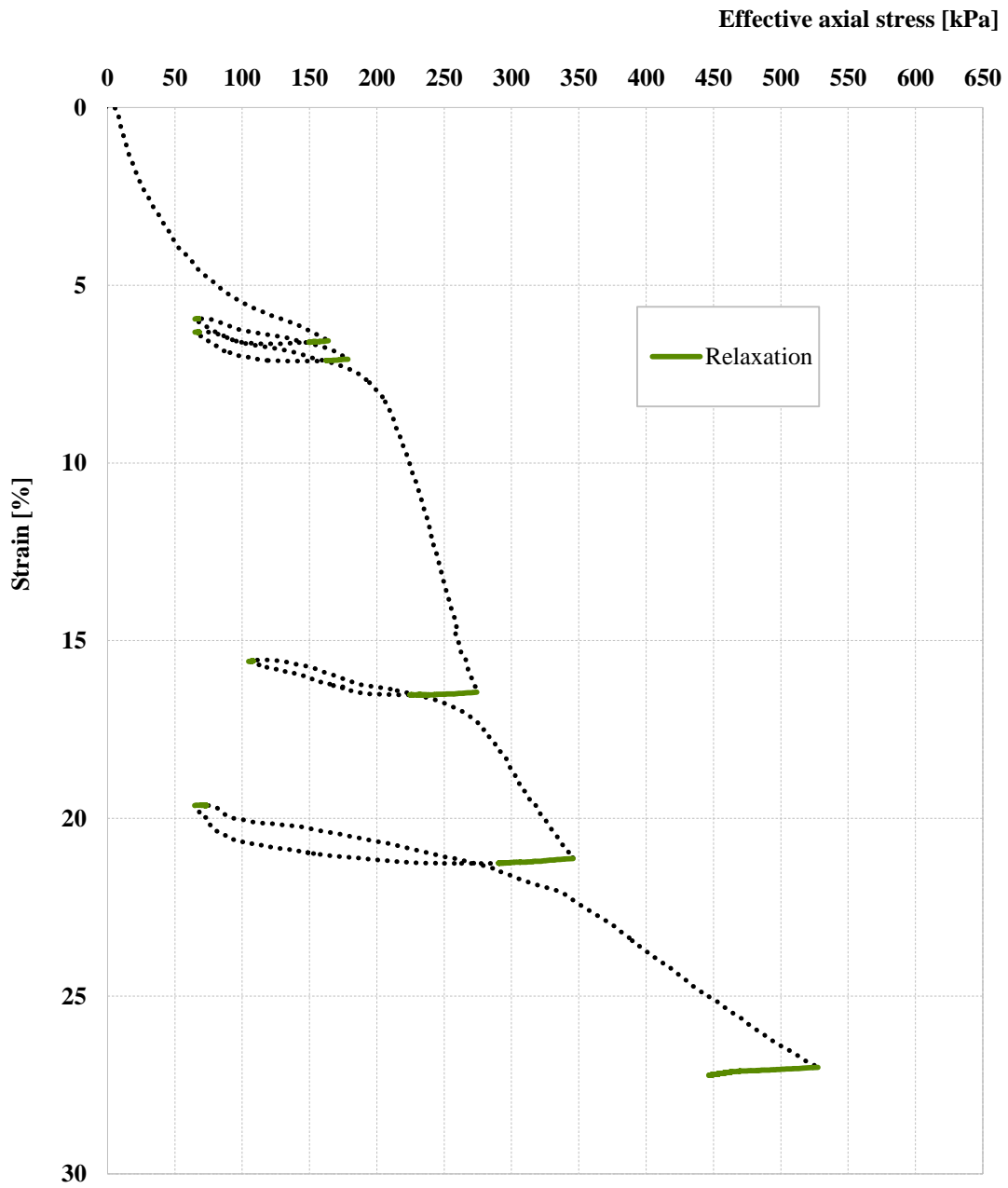


Figure E.6: First unloading series for level 25 m.

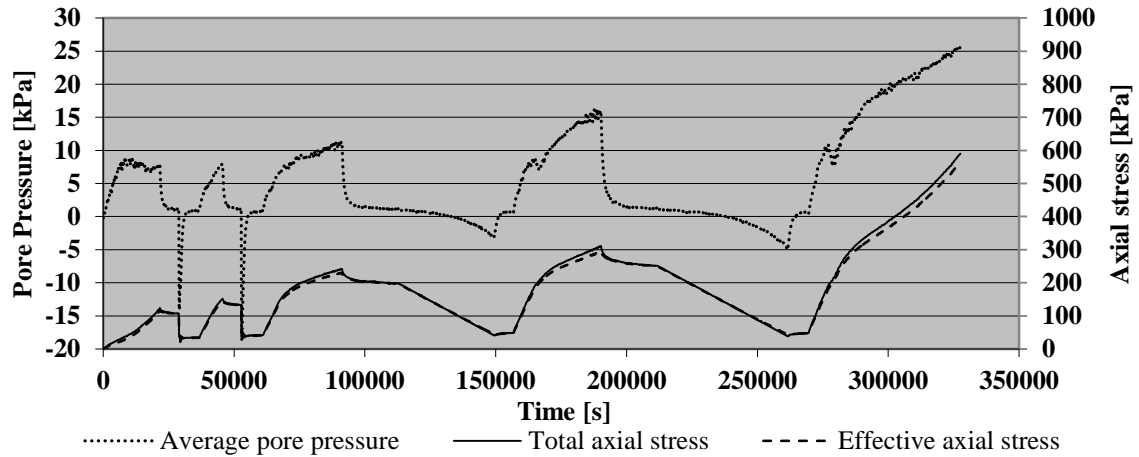


Figure E.7: Pore pressure, total axial stress and effective axial stress versus time for first unloading test series 17 m.

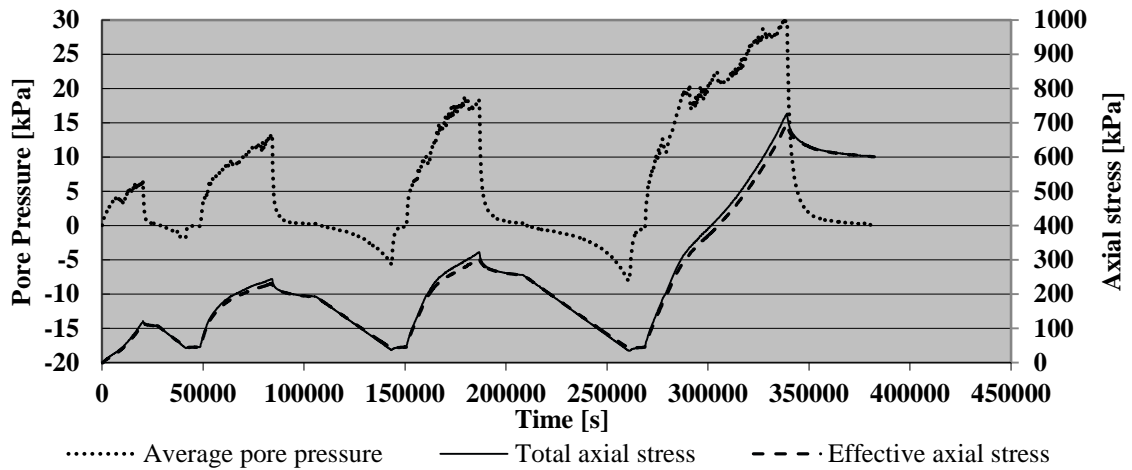


Figure E.8: Pore pressure, total axial stress and effective axial stress versus time for second unloading test series 17 m.

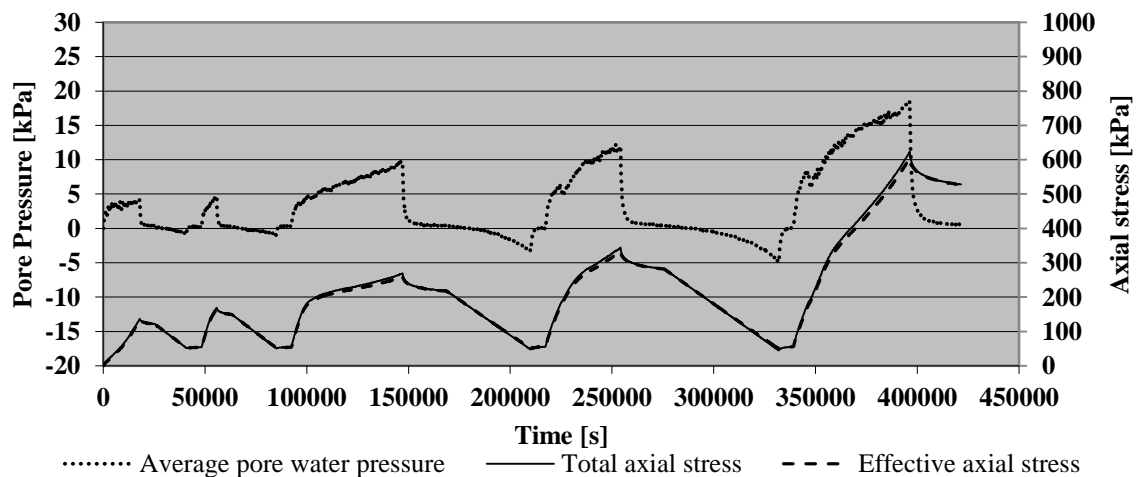


Figure E.9: Pore pressure, total axial stress and effective axial stress versus time for first unloading test series 20 m.



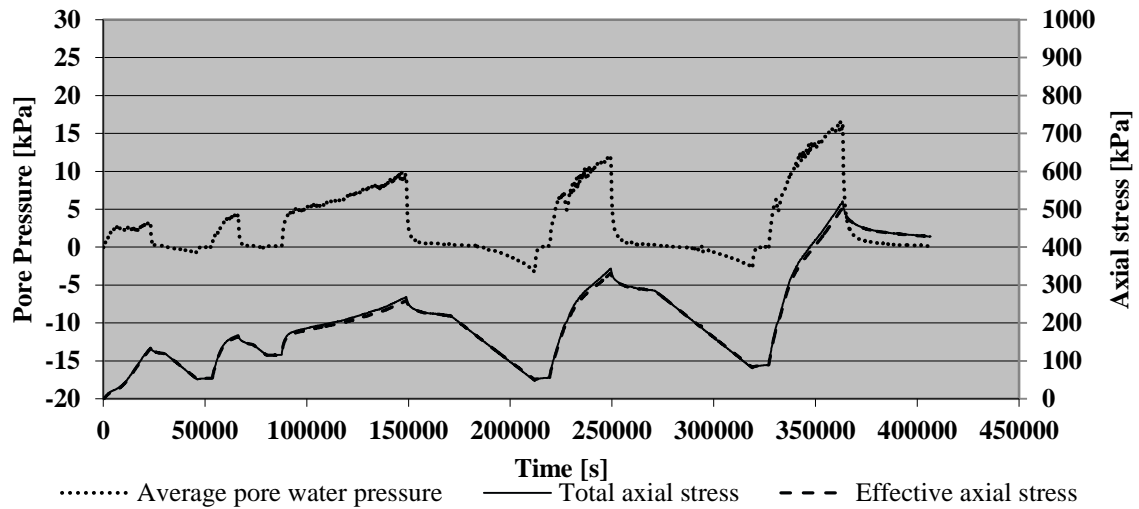


Figure E.10: Pore pressure, total axial stress and effective axial stress versus time for second unloading test series 20 m.

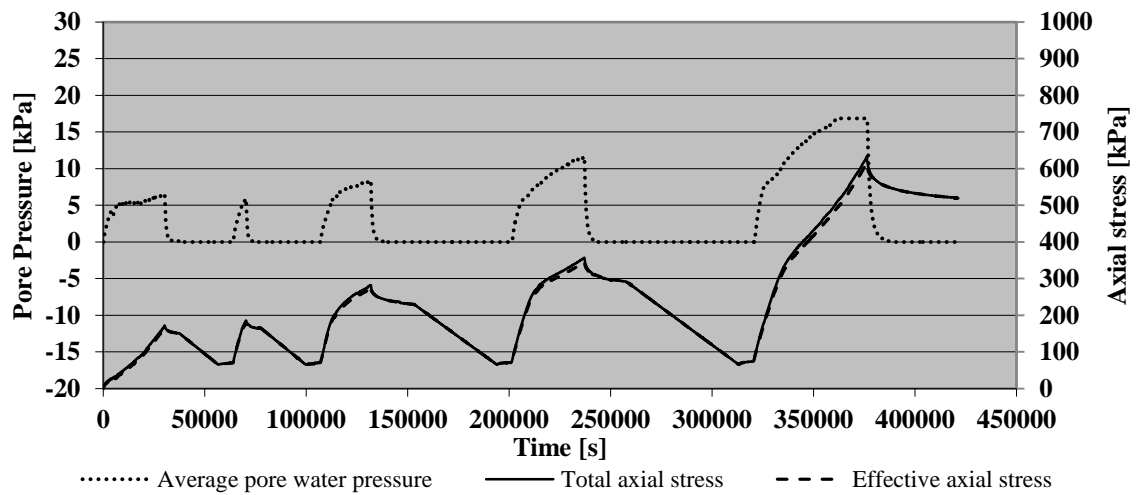


Figure E.11: Pore pressure, total axial stress and effective axial stress versus time for first unloading test series 25 m.

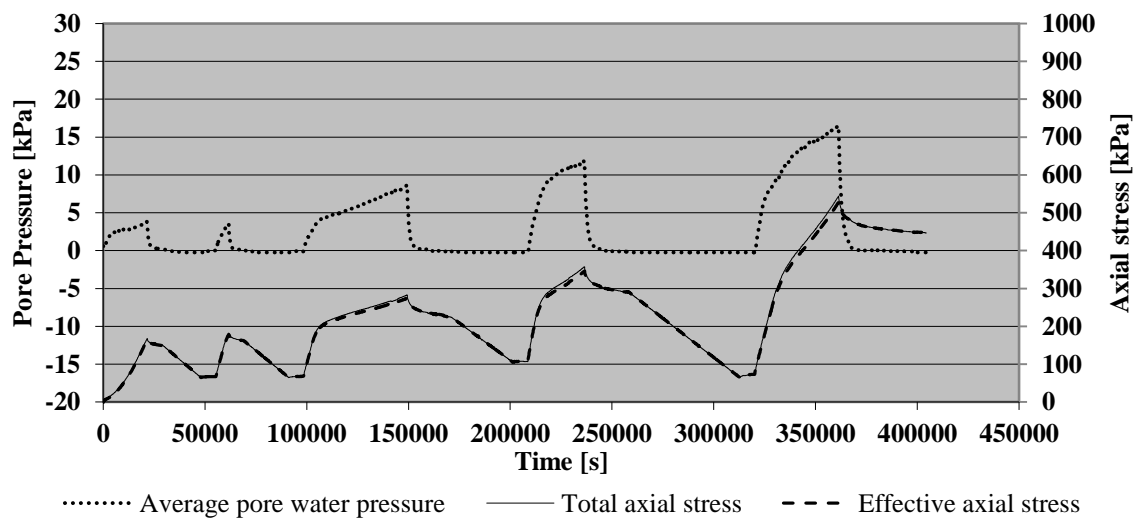


Figure E.12: Pore pressure, total axial stress and effective axial stress versus time for second unloading test series 25 m.

### Rate of axial stress change

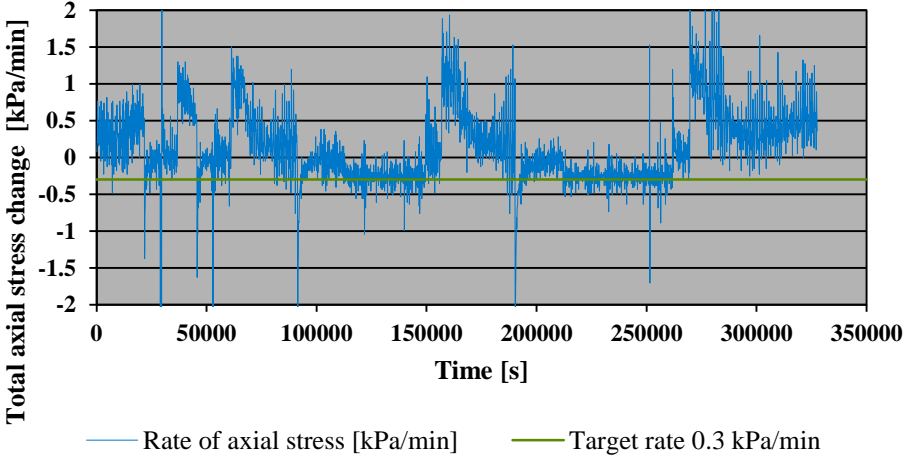


Figure E.13: Rate of axial stress change for first unloading test series 17 m.

### Rate of axial stress change

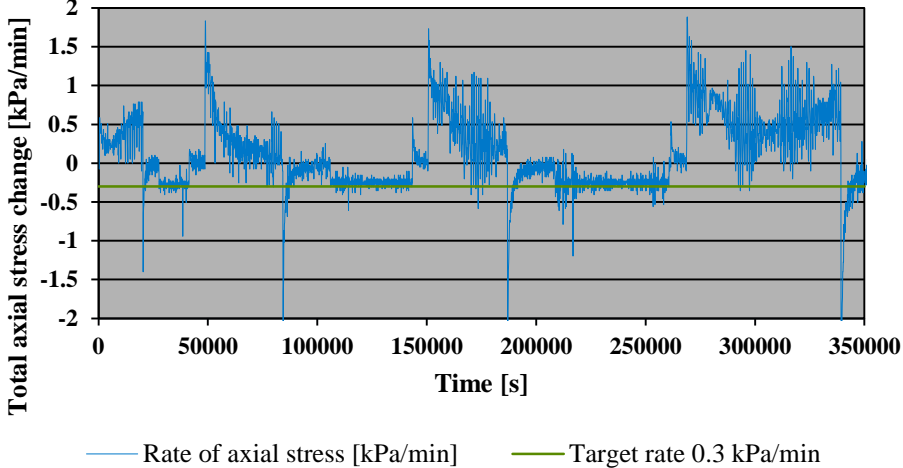


Figure E.14: Rate of axial stress change for second unloading test series 17 m.

### Rate of axial stress change

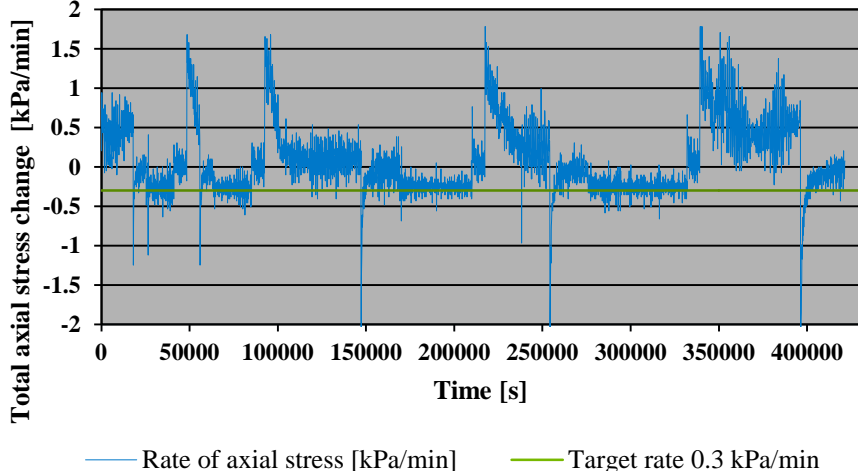


Figure E.15: Rate of axial stress change for first unloading test series 20 m.

### Rate of axial stress change

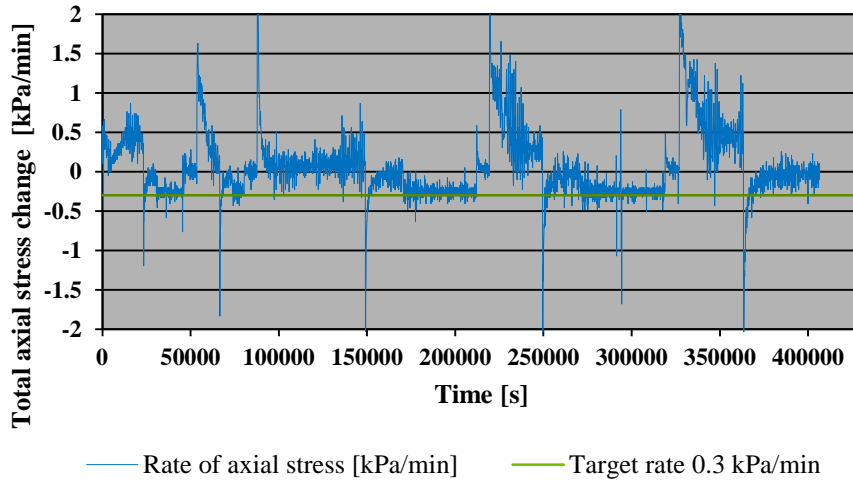


Figure E.16: Rate of axial stress change for second unloading test series 20 m.

### Rate of axial stress change

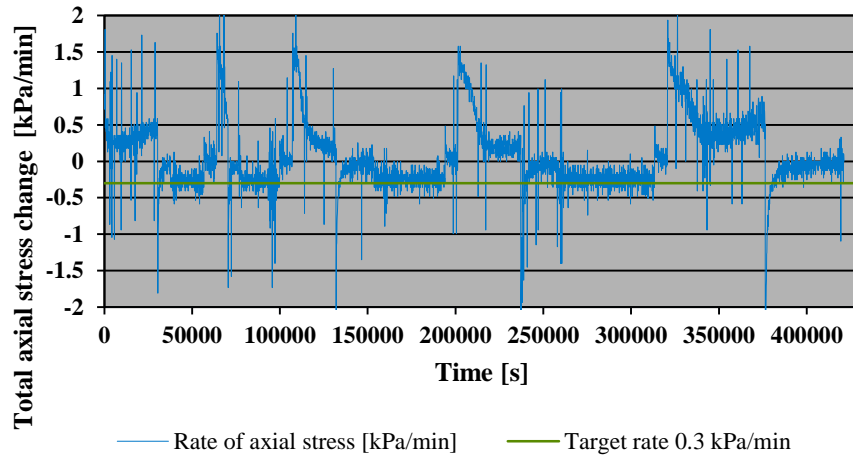


Figure E.17: Rate of axial stress change for first unloading test series 25 m.

### Rate of axial stress change

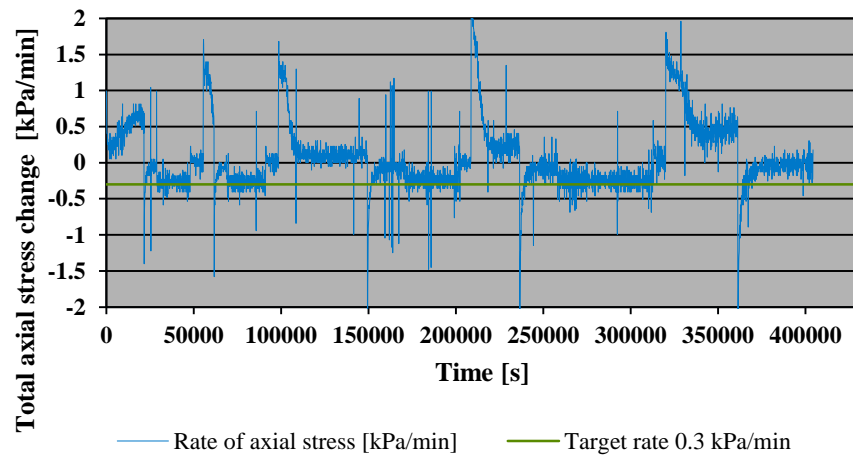


Figure E.18: Rate of axial stress change for second unloading test series 25 m.

### Rate of axial displacement

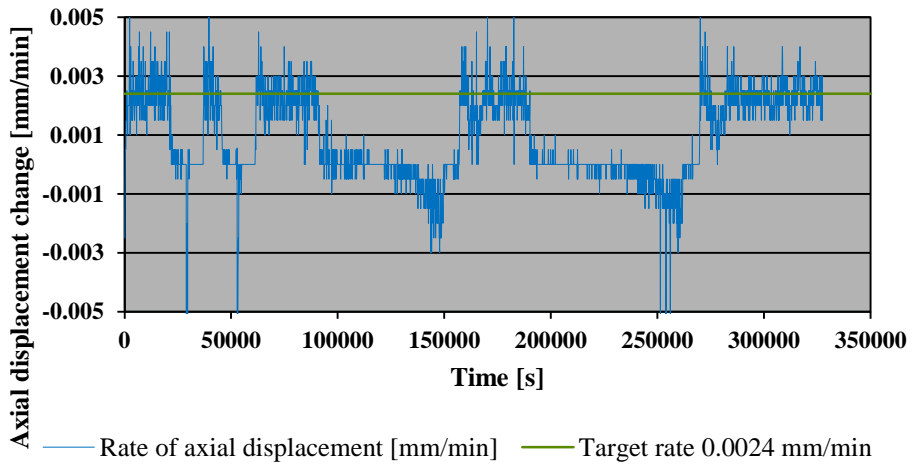


Figure E.19: Rate of axial displacement for first unloading test series 17 m.

### Rate of axial displacement

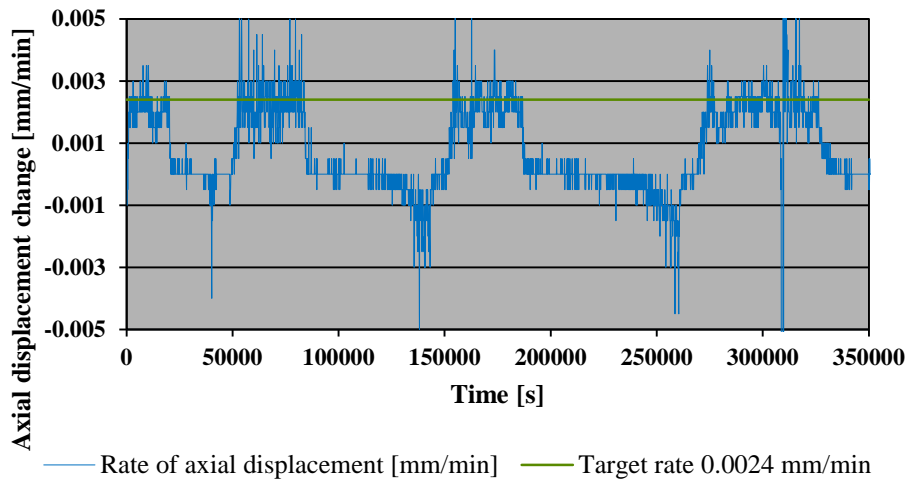


Figure E.20: Rate of axial displacement for second unloading test series 17 m.

### Rate of axial displacement

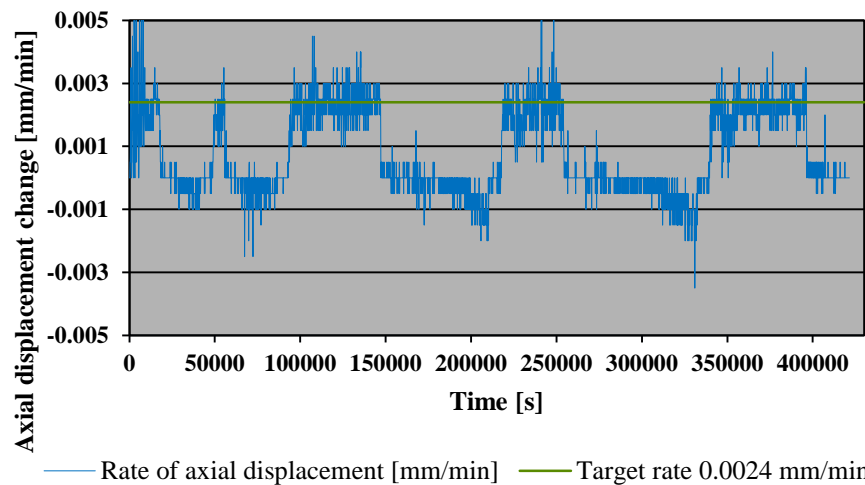


Figure E.21: Rate of axial displacement for first unloading test series 20 m.

### Rate of axial displacement

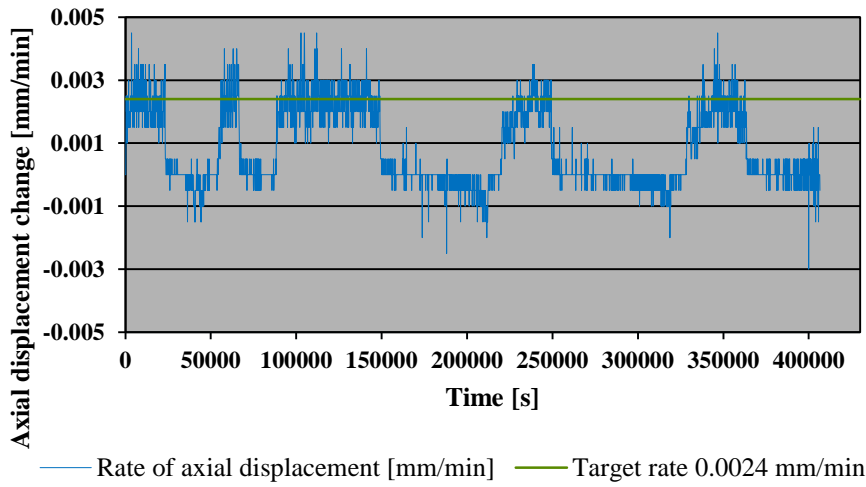


Figure E.22: Rate of axial displacement for second unloading test series 20 m.

### Rate of axial displacement

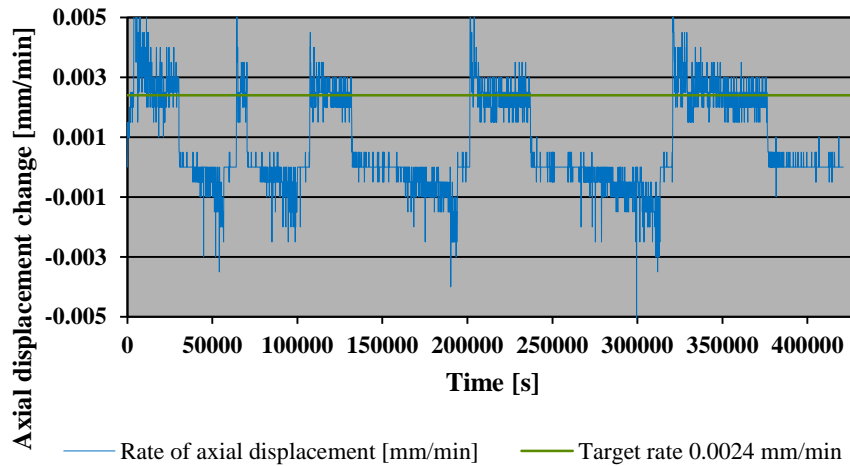


Figure E.23: Rate of axial displacement for first unloading test series 25 m.

### Rate of axial displacement

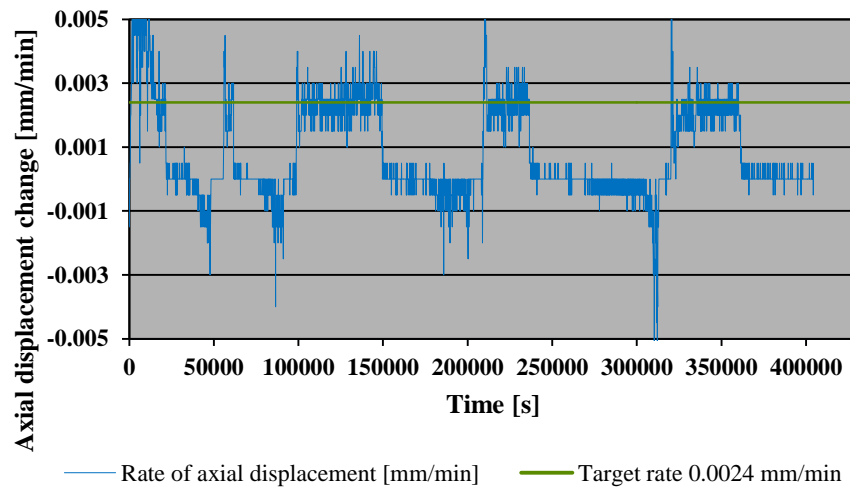


Figure E.24: Rate of axial displacement for second unloading test series 25 m.

## APPENDIX F

### CONDUCTIONG THE IL TESTS WITH UNLOADING STAGES

The test stages for the three conducted IL-tests can be seen in Tabel F.1 – Table F.3. The time for each stage varied due to the feasibility to perform the load increase/unloading of the sample. The stages marked with bold letters were applied for around 10 days due to Tornborg not being at Calmers University of Technology at that time (on parental leave). Due to parallel research activities at Chalmers University of Technology, related to thermal response of clay, the temperature in the laboratory cold room was varied between +5 to +15°C during the time of the IL-tests. The temperature variation is added in Table F.1-Figure F.3.

Stage	Stress increase [kPa]	Total stress [kPa]	Start date	Temperature in lab. room [°C]
1	25	25	2018-02-23	+7
2	50	75	2018-02-24	+7
3	40	115	2018-02-26	+7
4	-30	85	2018-02-27	+7
5	-40	45	2018-02-28(morning)	+7
6	60	105	2018-02-28 (afternoon)	+7
7	60	165	2018-03-01	+7
8	60	225	2018-03-02	+7
9	-60	165	2018-03-03	+7
10	-60	105	2018-03-05	+7
11	-55	50	2018-03-06	+7
<b>12</b>	<b>50</b>	<b>100</b>	<b>2018-03-07</b>	<b>+7</b>
				<b>+15 (2018-03-19)</b>
13	60	160	2018-03-22	+15
14	120	280	2018-03-23	+5
15	-60	220	2018-03-27	+5
16	-80	140	2018-03-28	+5
17	-100	40	2018-03-29	+5
18	100	140	2018-04-01	+5
19	200	340	2018-04-03	+5
20	200	540	2018-04-06	+5

Table F.1: Incremental load test for level 17 m.

Stage	Stress increase [kPa]	Total stress [kPa]	Start date	Temperature in lab. room [°C]
1	25	25	2018-03-02	+7
2	50	75	2018-03-03	+7
3	50	125	2018-03-05	+7
4	-25	100	2018-03-06	+7
<b>5</b>	<b>-50</b>	<b>50</b>	<b>2018-03-07</b>	<b>+7</b>
				<b>+15 (2018-03-19)</b>
6	110	160	2018-03-22	+15
7	-60	100	2018-03-23	+5
8	-50	50	2018-03-27	+5
9	100	150	2018-03-28	+5
10	100	250	2018-03-29	+5
11	-100	150	2018-04-01	+5
12	-50	100	2018-04-03	+5
13	-50	50	2018-04-04	+5
14	100	150	2018-04-06	+5
15	150	300	2018-04-09	+15
16	-100	200	2018-04-11	+15
17	-50	150	2018-04-13	+5
18	-50	100	2018-04-16	+5
19	-50	50	2018-04-18	+5

Table F.2: Incremental load test for level 20 m.

Stage	Stress increase [kPa]	Total stress [kPa]	Start date	Temperature in lab. room [°C]
1	25	25	2018-03-02	+7
2	50	75	2018-03-03	+7
3	75	150	2018-03-05	+7
4	-50	100	2018-03-06	+7
<b>5</b>	<b>-50</b>	<b>50</b>	<b>2018-03-07</b>	<b>+7</b>
				<b>+15 (2018-03-19)</b>
6	120	170	2018-03-22	+15
7	-50	120	2018-03-23	+5
8	-70	50	2018-03-27	+5
9	100	150	2018-03-28	+5
10	100	250	2018-03-29	+5
11	-100	150	2018-04-01	+5
12	-50	100	2018-04-03	+5
13	-50	50	2018-04-04	+5
14	100	150	2018-04-06	+5
15	200	350	2018-04-09	+15
16	-100	250	2018-04-11	+15
17	-100	150	2018-04-13	+5
18	-100	50	2018-04-16	+5

Table F.3: Incremental load test for level 25 m.

## Incremental loaded oedometer test for level 17m

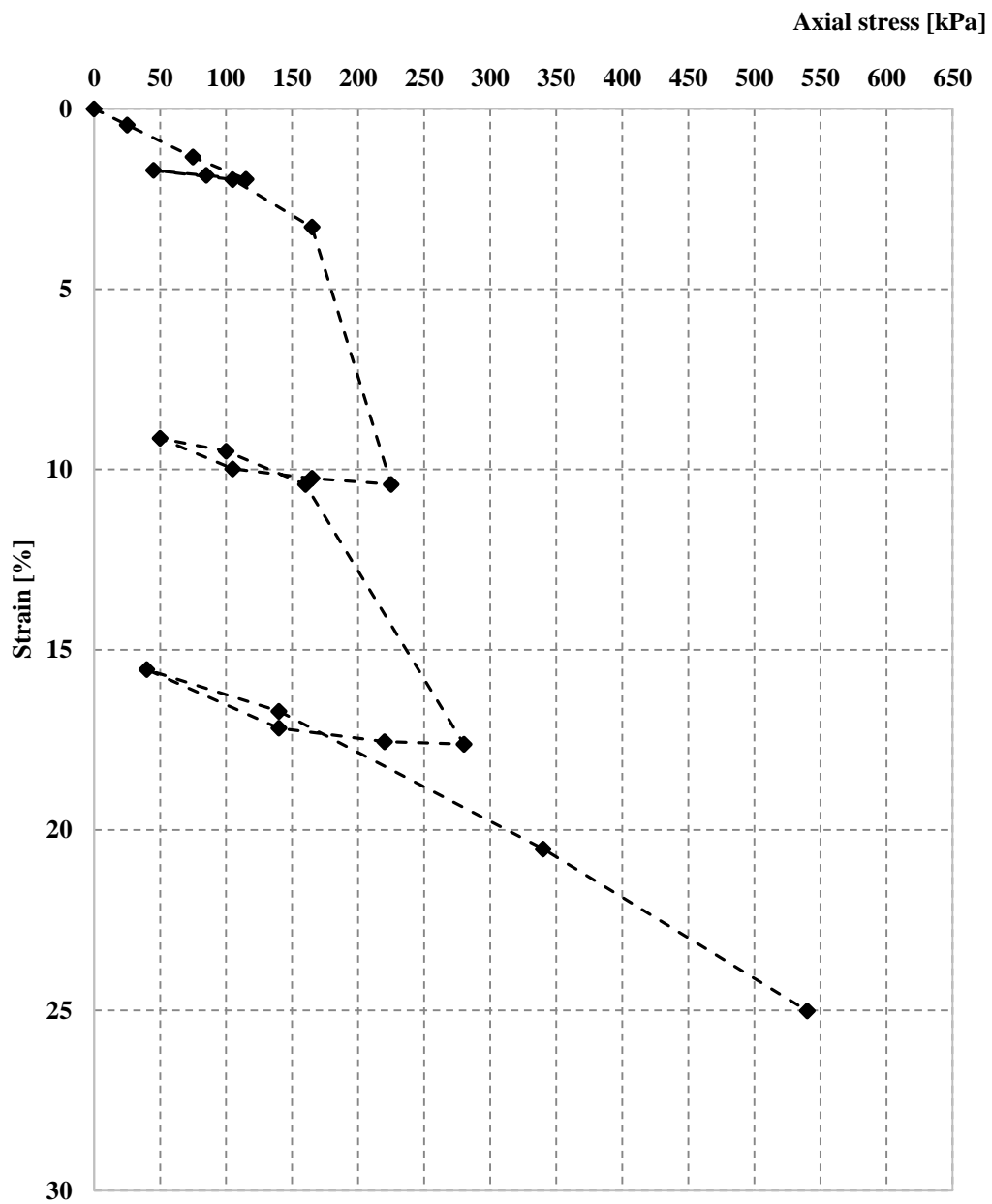


Figure F.1: Incremental loaded oedometer test for level 17 m.



## Incremental loaded oedometer test for level 20 m

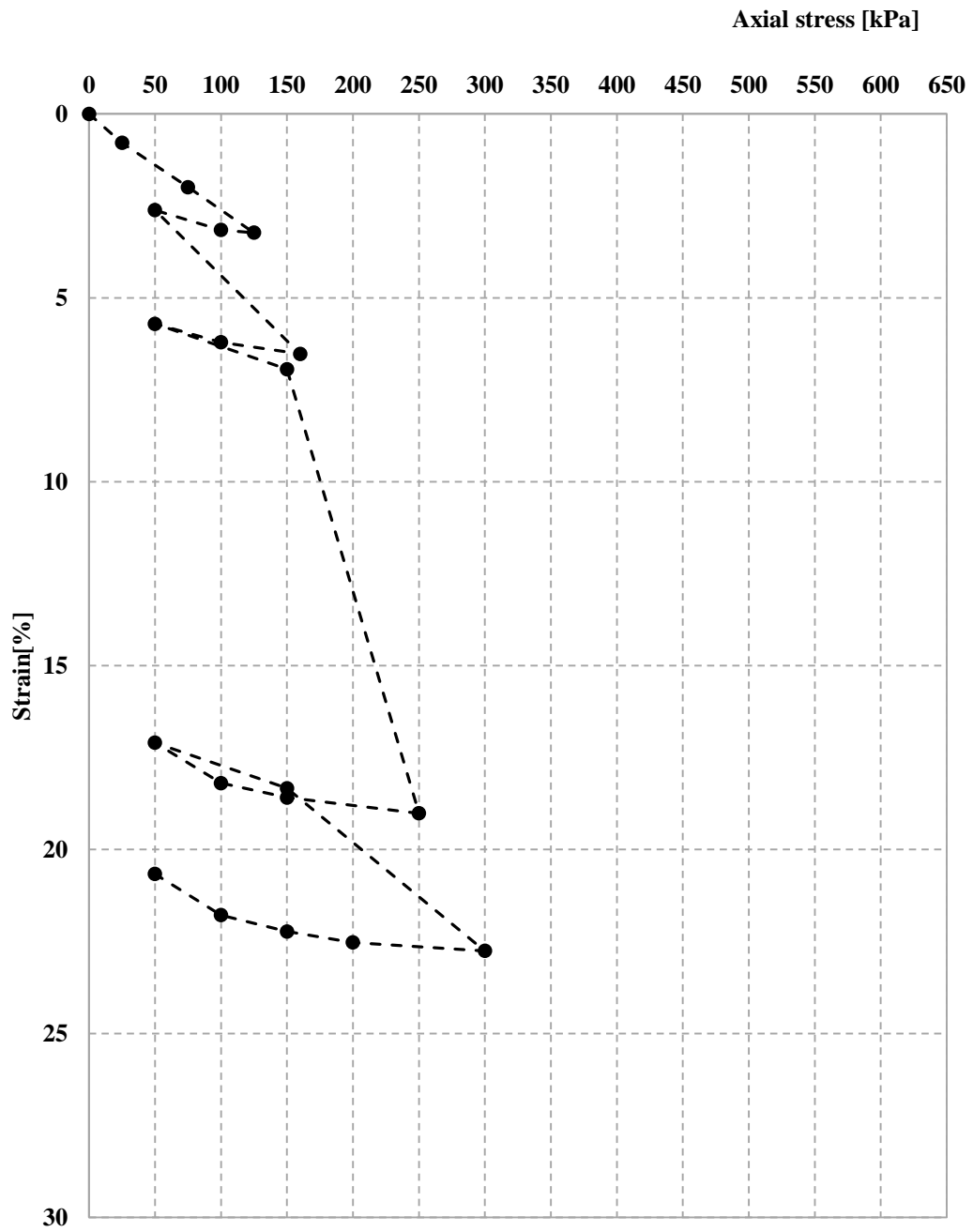


Figure F.2: Incremental loaded oedometer test for level 20 m.

### Incremental loaded oedometer test for level 25 m

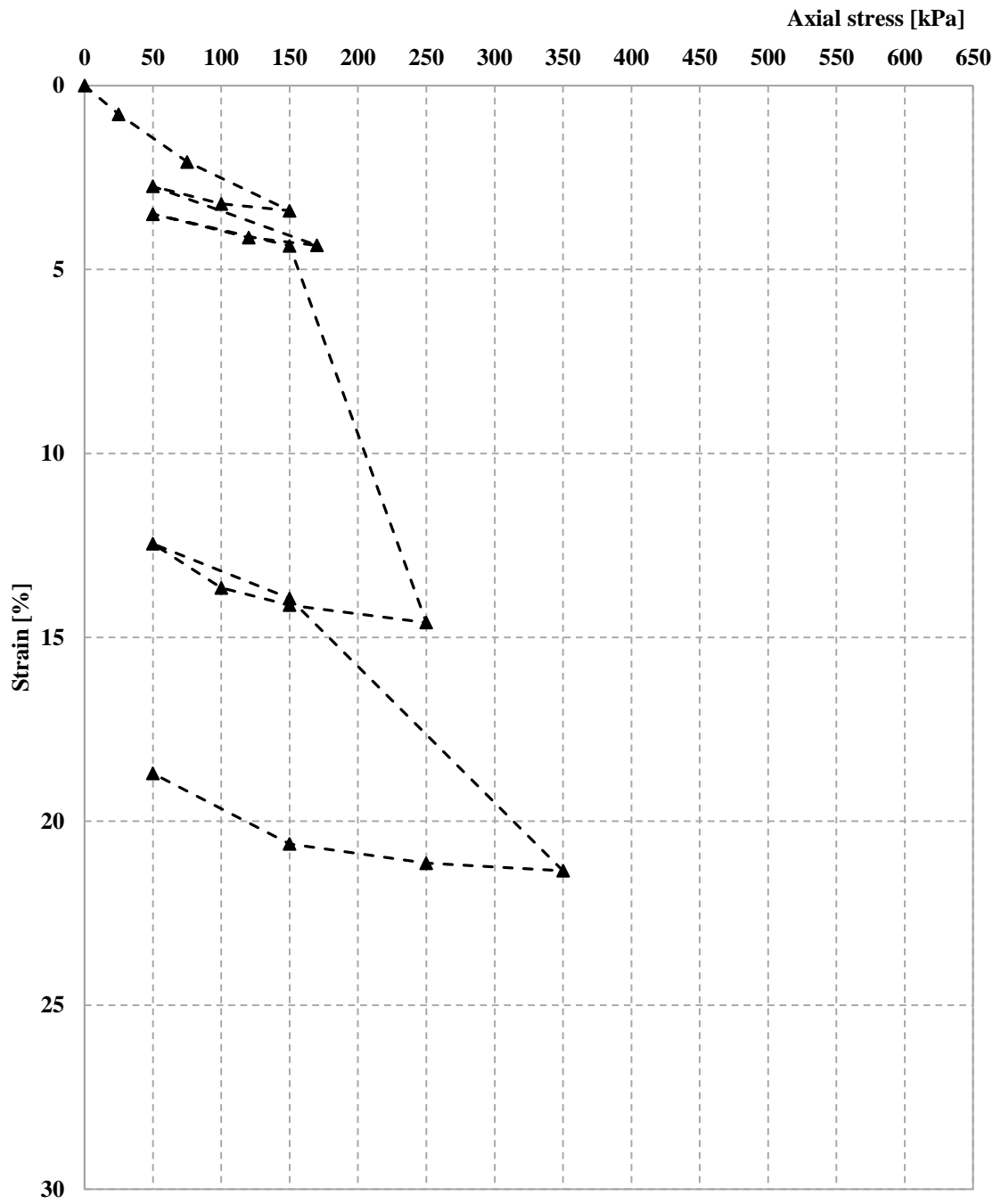


Figure F.3: Incremental loaded oedometer test for level 25 m.

# APPENDIX G

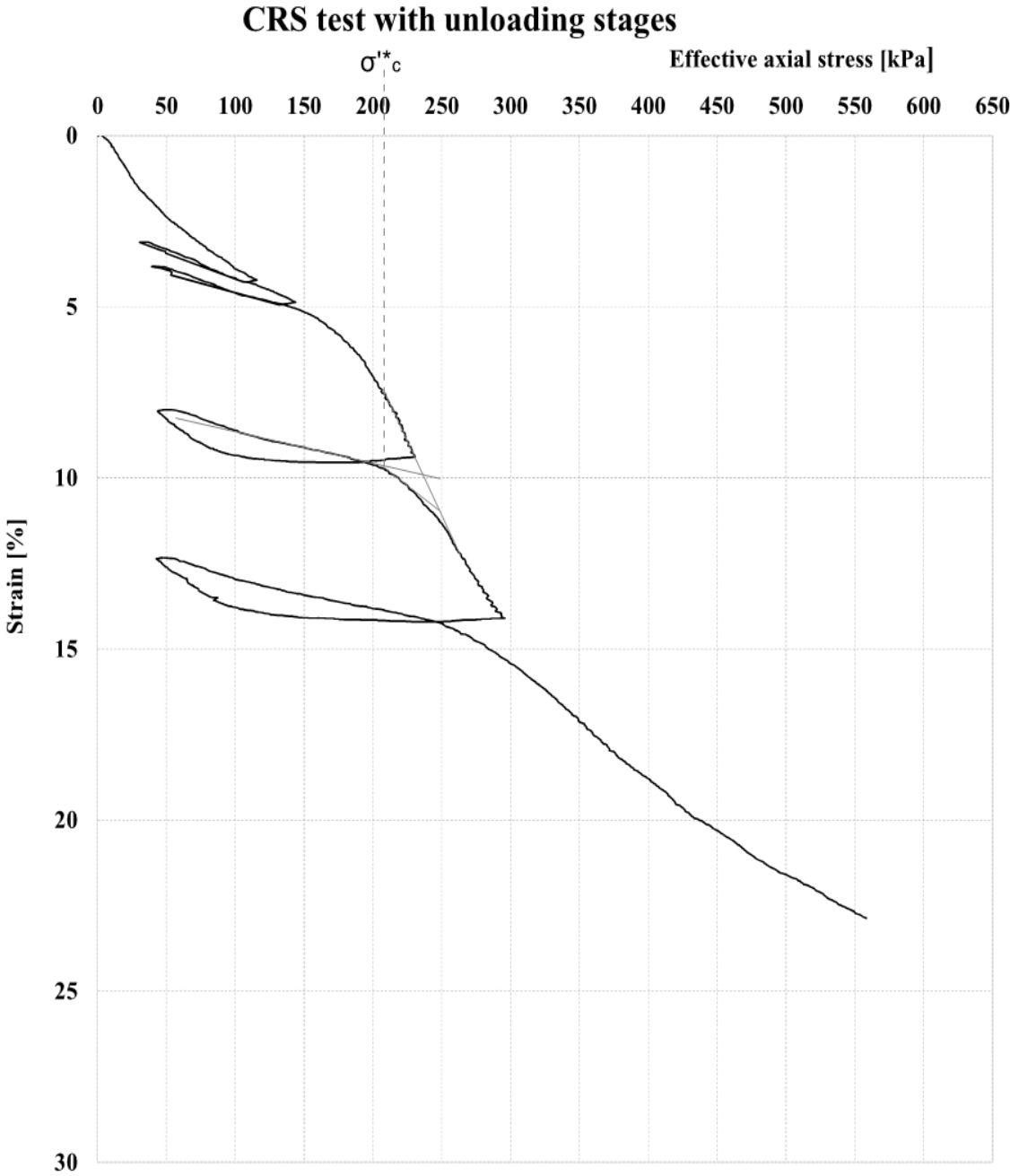


Figure G.1: Method to determine the “new” pre-consolidation pressure  $\sigma_c^{I*}$  for unloaded and reloaded samples.

# APPENDIX H

## 17 m - first unloading test series

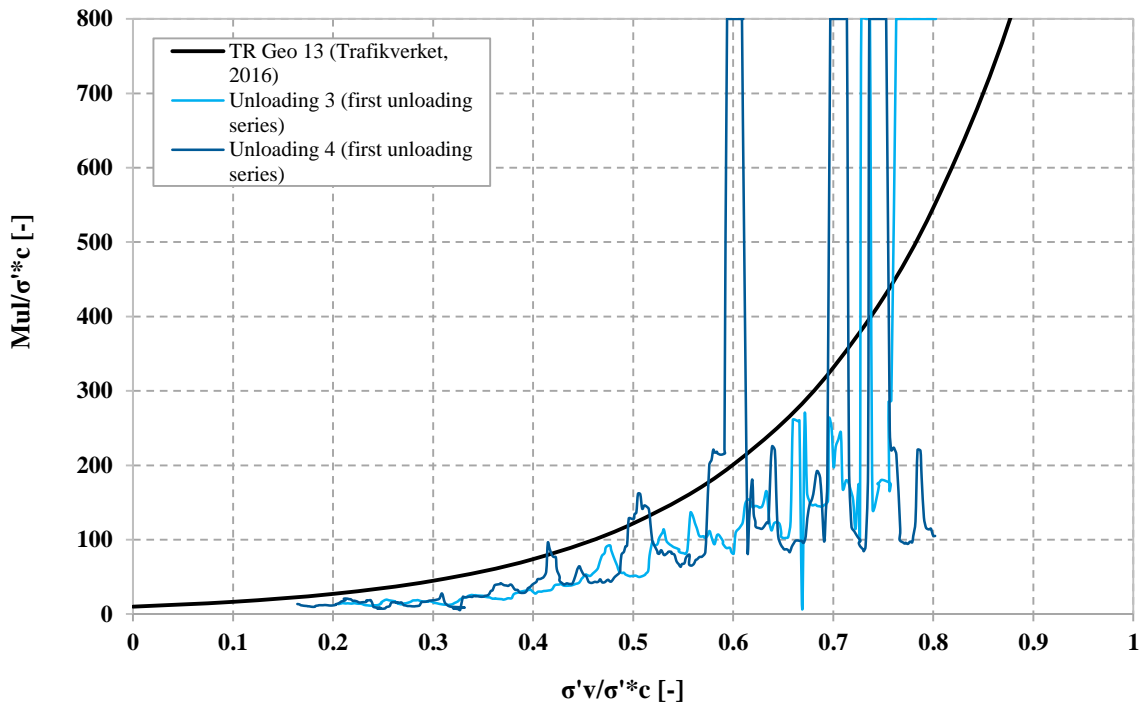


Figure H.1: Unloading modulus for level 17 m, first unloading series.

## 17 m - second unloading test series

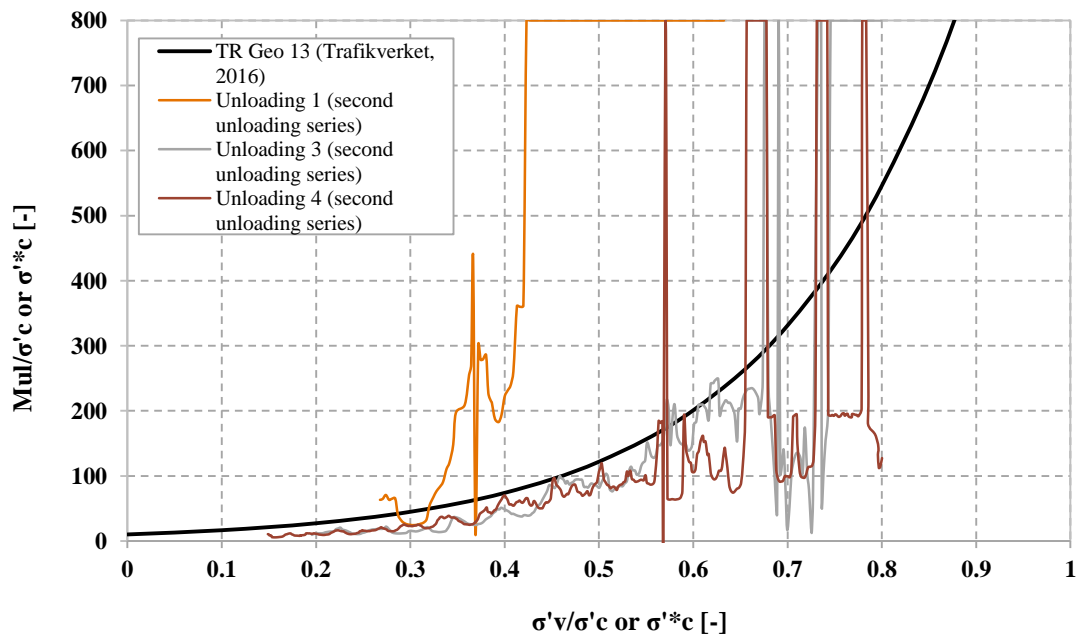


Figure H.2: Unloading modulus for level 17 m, second unloading series.

### 17 m - both unloading test series

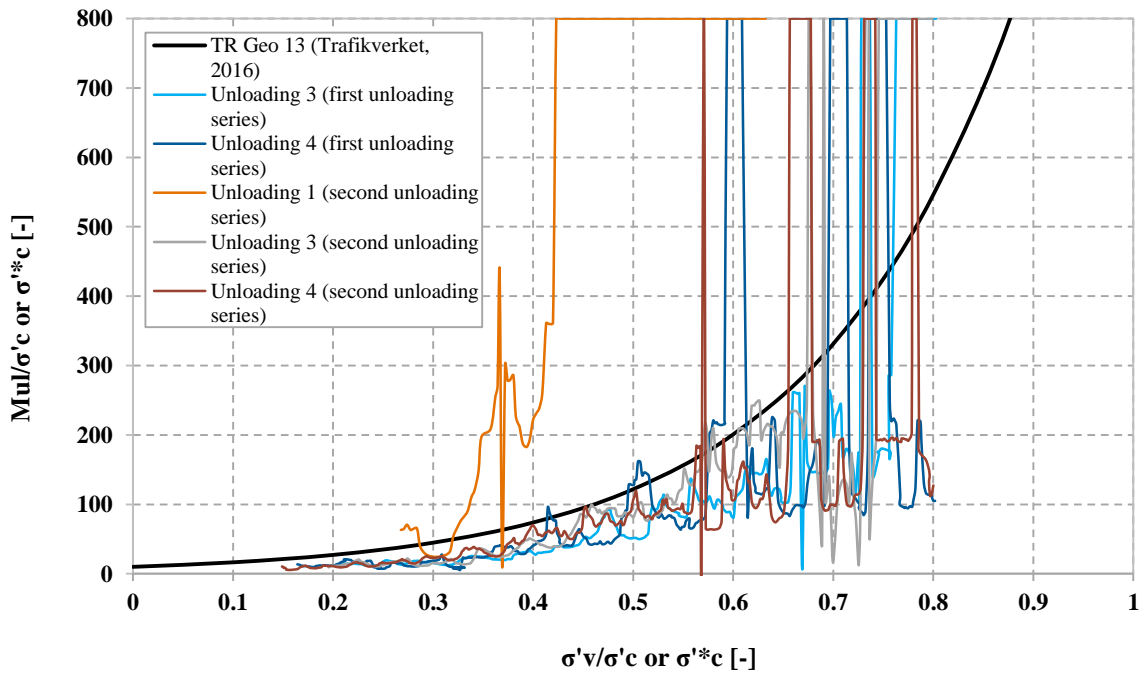


Figure H.3: Unloading modulus for level 17 m, both unloading series.

### 20 m - first unloading test series

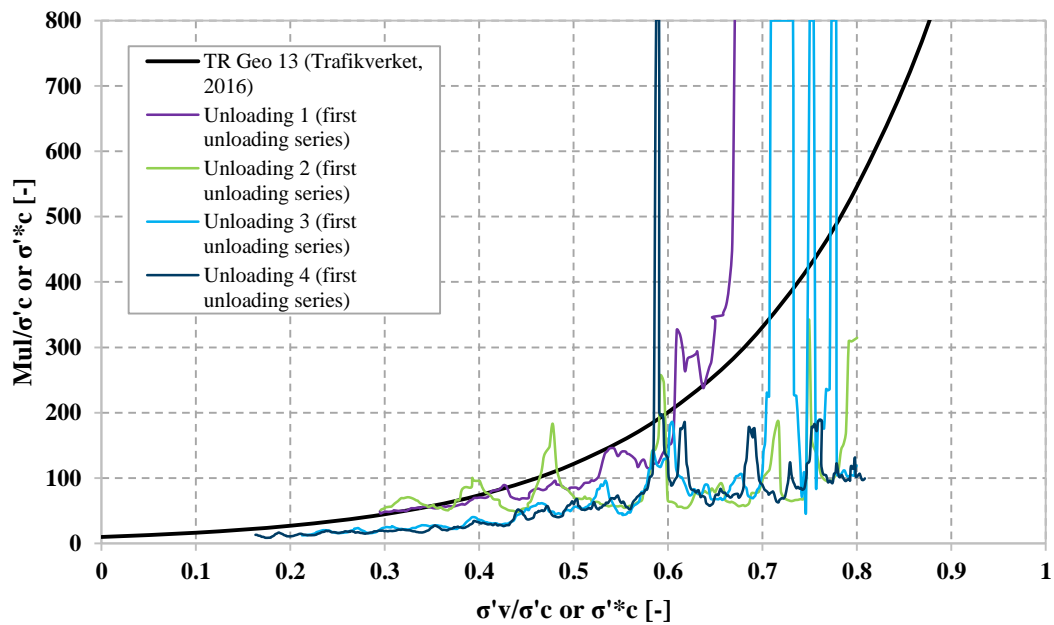


Figure H.4: Unloading modulus for level 20 m, first unloading series.

### 20 m - second unloading test series

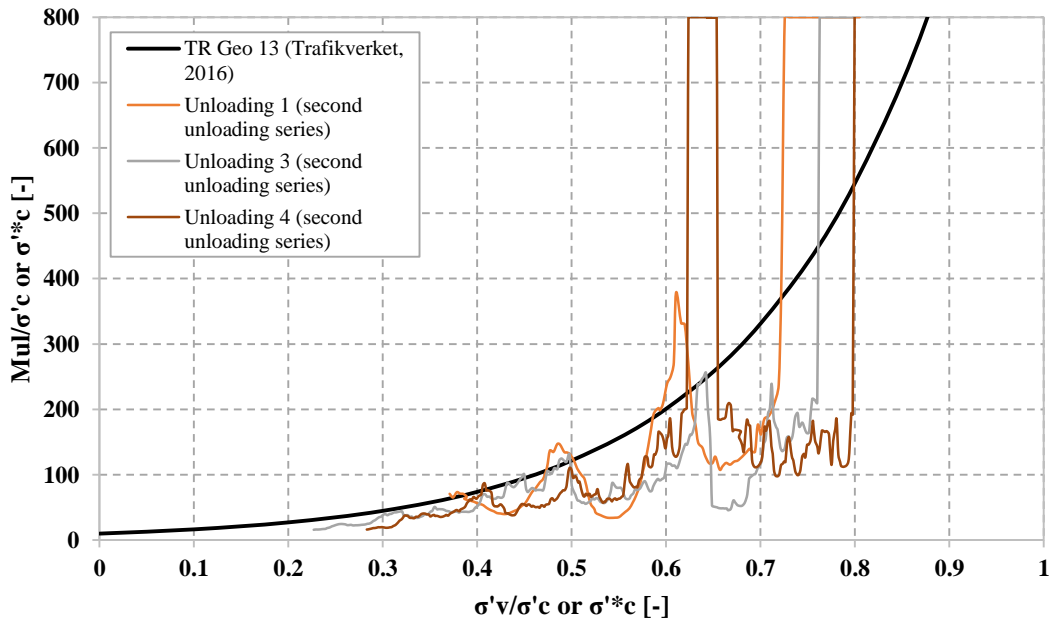


Figure H.5: Unloading modulus for level 20 m, second unloading series.

### 20 m - both unloading test series

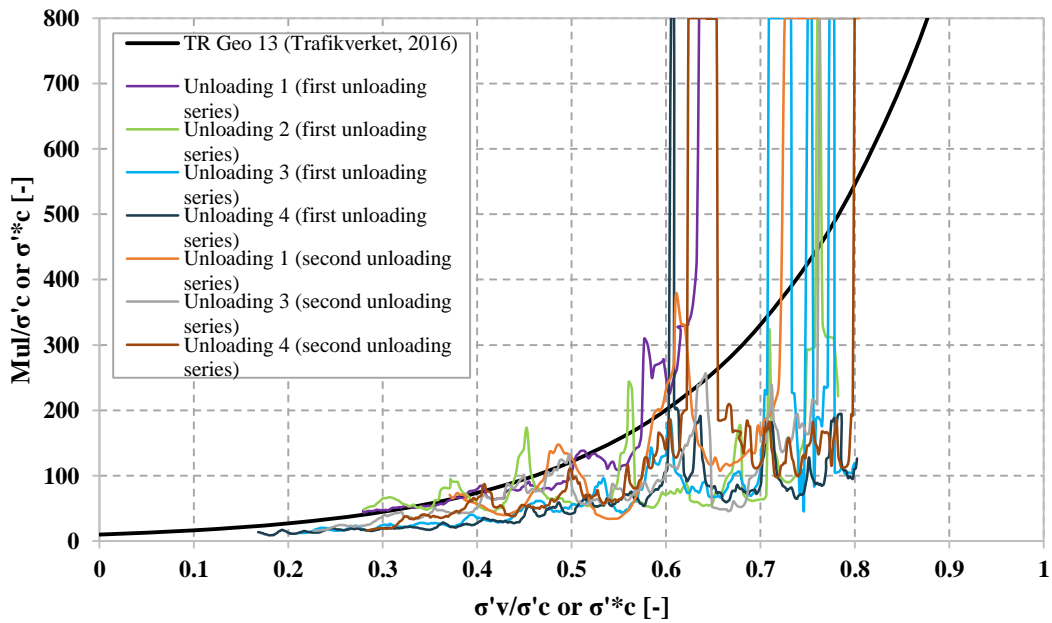


Figure H.6: Unloading modulus for level 20 m, both unloading series.

### 25 m - first unloading test series

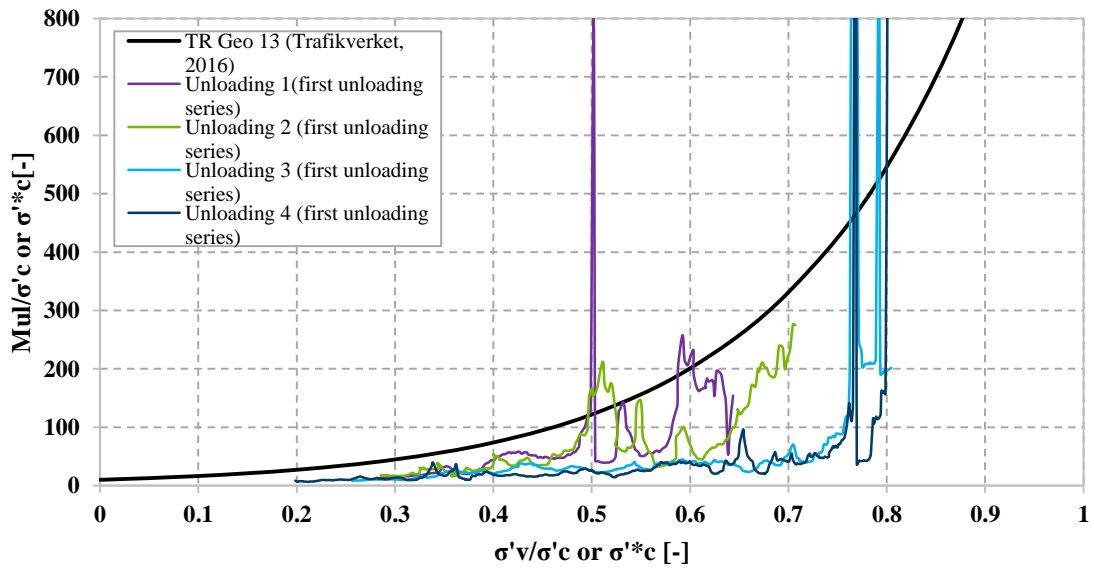


Figure H.7: Unloading modulus for level 25 m, first unloading series.

### 25 m - second unloading test series

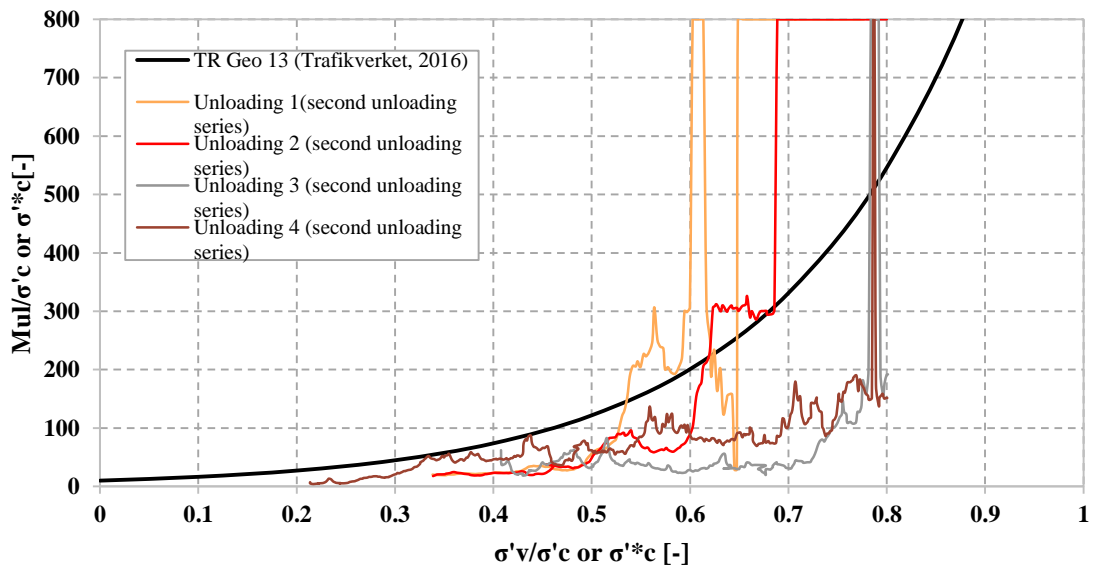


Figure H.8: Unloading modulus for level 25 m, second unloading series.

## 25 m - both unloading test series

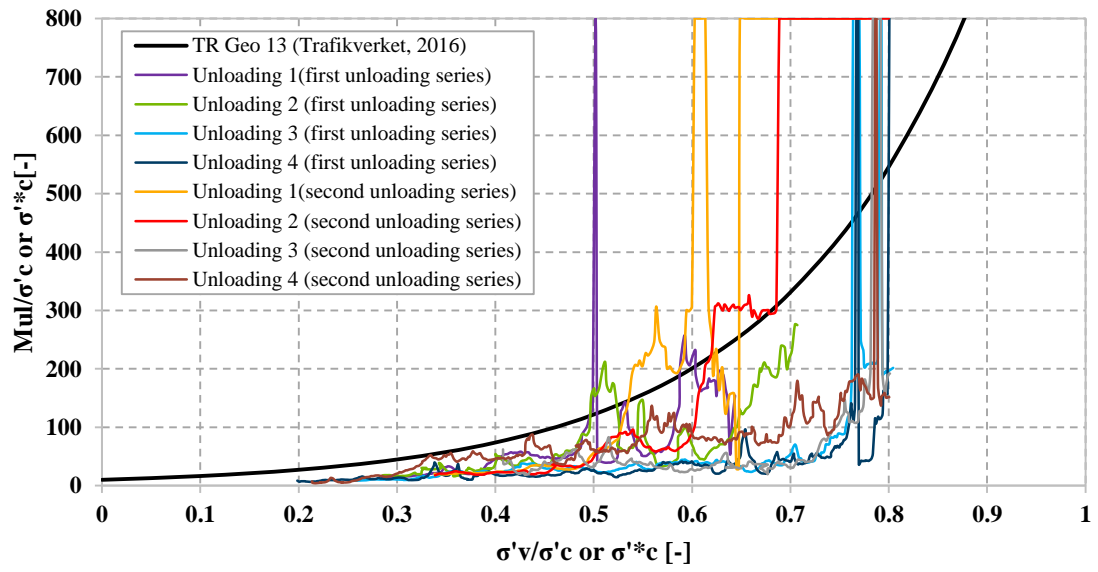


Figure H.9: Unloading modulus for level 25 m, both unloading series.



# APPENDIX I

## CRS curves normalised

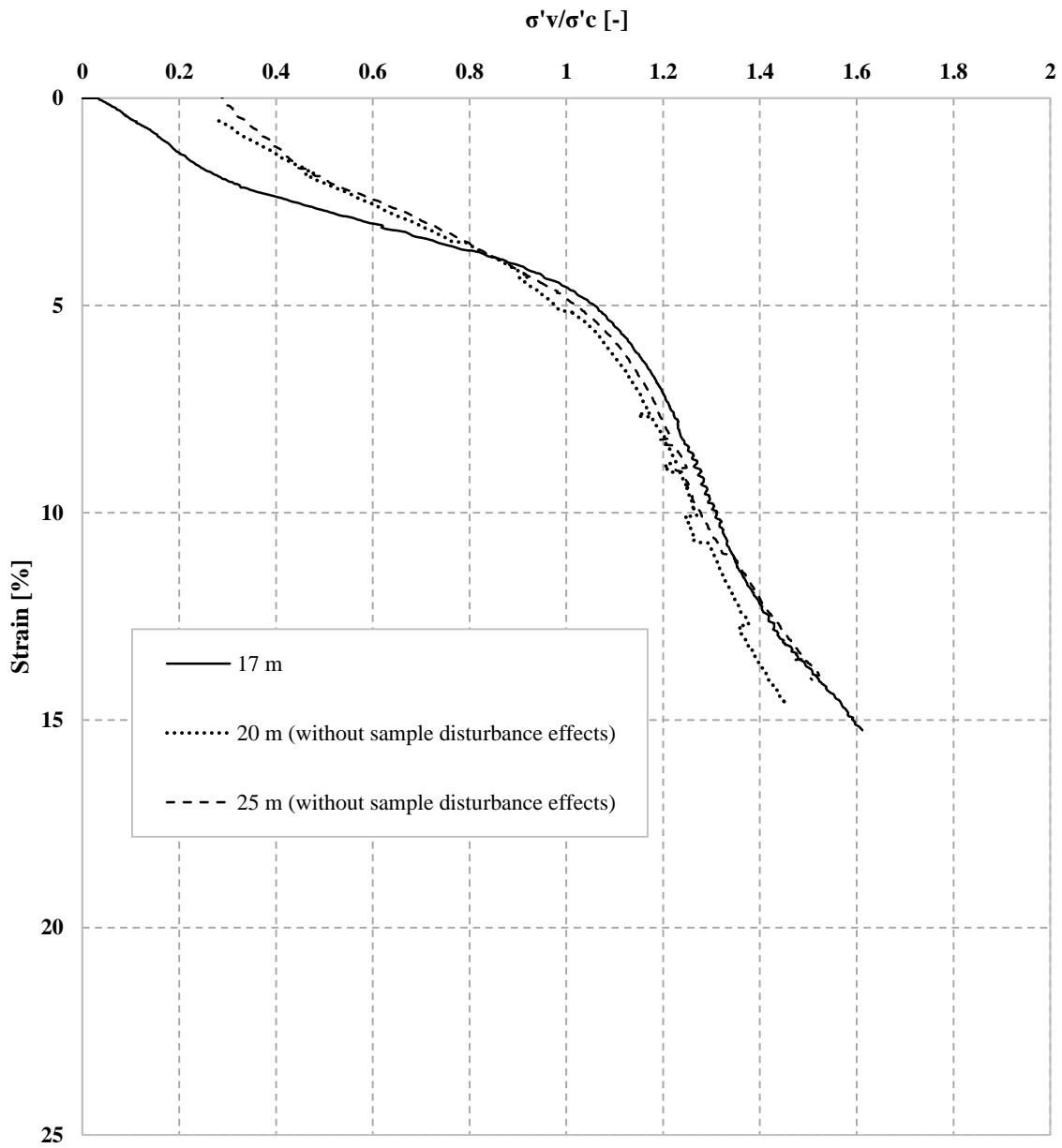


Figure I.1: CRS curves for three levels plotted with normalised stress.

### All unloadings below $\sigma'c$ normalised

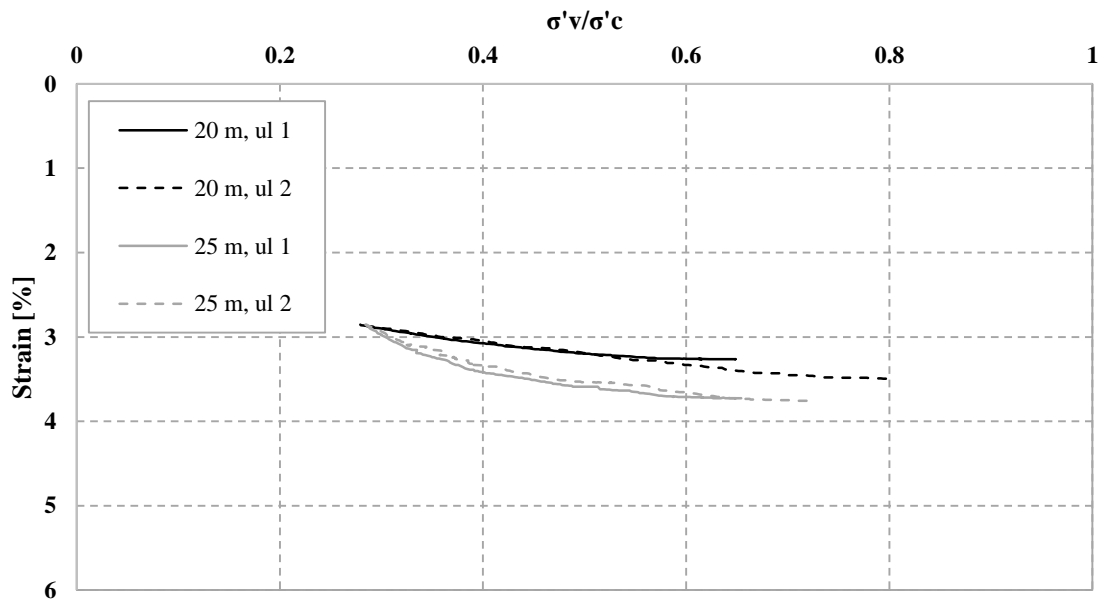


Figure I.2: Unloading sequences for two levels plotted with normalised stress and ending at the same strain.

### All unloadings above $\sigma'c$ normalised

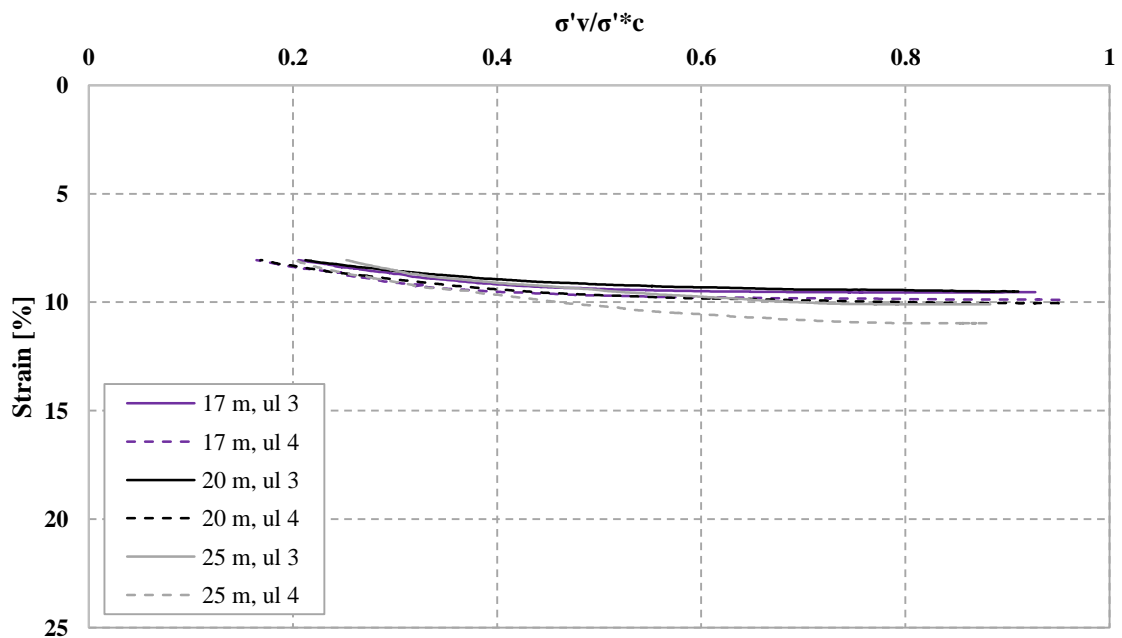


Figure I.3: Unloading sequences for two levels plotted with normalised stress and ending at the same strain.